POLITEKNIK NEGERI BALI

Journal of Engineering Design and Technology

logic

Vol. 23 No. 3, November 2023

LOGIC

Jurnal Rancang Bangun dan Teknologi

p-ISSN. 1412-114X

e-ISSN. 2580-5649

LOGIC

Jurnal Rancang Bangun dan Teknologi

Journal of Engineering Design and Technology

Gedung P3M, lt.1 Politeknik Negeri Bali, Bukit Jimbaran
PO BOX 1064 Kuta Selatan, Badung, Bali - Indonesia
Telp. (+62)361 701981 Fax. (+62)361 701128
Email: logic@pnb.ac.id

LOGIC JOURNAL TEAM

PREFACE

Logic: Jurnal Rancang Bangun dan Teknologi (Journal of Engineering Design and Technology) is a peer-reviewed research journal aiming at promoting and publishing original high quality research in all disciplines of engineering and applied technology. All research articles submitted to Logic should be original in nature, never previously published in any journal or presented in a conference or undergoing such process across the world. All the submissions will be peer-reviewed by the panel of experts associated with particular field. Submitted papers should meet the internationally accepted criteria and manuscripts should follow the style of the journal for the purpose of both reviewing and editing.

Logic is a journal covering articles in the field of civil and mechanical engineering, design, and technology published 3 times a year in March, July, and November. Language used in this journal is English.

LOGIC. P-ISSN 1412-114X
LOGIC. E-ISSN 2580-5649
Indexing : GOOGLE SCHOLAR, DOAJ, EBSCO OPEN SCIENCE DIRECTORY, SINTA, GARUDA

Best Regard,

LOGIC Editorial Team

TABLE OF CONTENTS

LOGIC
Journal of Engineering Design and Technology
Vol. 23 No.3 month November ; p. 156 - 163

p-ISSN : 1412-114X
e-ISSN : 2580-5649
http://ojs2.pnb.ac.id/index.php/LOGIC

STUDY OF IMMERSION BEHAVIOR AND THERMAL STABILITY OF GREEN COMPOSITE PLA/BAMBOO

Komang Widhi Widantha [1], Risa Nurin Baiti[1], Made Widnya Kusuma[1]

[1] Mechanical Engineering Department, Politeknik Negeri Bali, Bukit Jimbaran, Badung, Bali

Correponding email [1)] : komangwidhi@pnb.ac.id

Abstract. One way to address environmental problems caused by the use of synthetic materials is by exploring the potential of new materials that are more environmentally friendly. This research aims to develop PLA/bamboo green composites by investigating the effects of fiber composition and alkali treatment on the thermal stability and immersion behavior of the composites. PLA/bamboo composites were produced using the hot press method with bamboo fibers at 10, 20, and 30 wt.% concentrations. Alkaline treatment was conducted using a 5% NaOH concentration for 24 hours. The tests that have been carried out include TGA analysis, density and immersion test. The PLA/bamboo composite exhibited weight gain due to water absorption during the soaking process. The inclusion of bamboo composition increases the water absorption of the composite, whereas alkali treatment decreases the water absorption of the composite. Furthermore, the introduction of fibers also reduces the degradation temperature of the composite. This research is expected to provide valuable insights for the broader utilization of green composite materials.

Keywords : composite, polylactic acid, bamboo fiber, stability

1. INTRODUCTION

The escalating growth of the global population has led to an increasing demand for food and tableware. Tableware, especially single-use containers that are difficult to recycle, is a major contributor to waste and global warming. Consequently, researchers are increasingly focusing in revealing the environmental effects of various types of materials popularly used as food containers such as aluminum, expanded polystyrene (EPS) and polypropylene (PP) [1]. Due to the huge environmental consequences, an imperative to investigate the creation of eco-friendlier food containers has arisen. The preferred method is to reuse natural materials to replace synthetic materials because they are bio-renewable and environmentally friendly.

Natural fibers, intrinsic components of the human experience, assume a pivotal role. The natural fiber studied in this research is a cellulose-type fiber, specifically bamboo. In terms of its mechanical properties, bamboo exhibits a high level of strength while maintaining a relatively low density of about 640 kg/m^3. In addition, bamboo is one of the fastest-growing renewable plants, which only takes 2-5 years to reach full maturity [2]. One of the drawbacks of natural fibers is that they are susceptible to variations in properties that occur naturally in nature, such as fiber type, fiber length, and fiber chemical composition. This predicament, along with the hydrophilic traits and stability concerns inherent to natural fibers, has spurred investigations into chemical treatments aimed at modifying these attributes.

Mitigation of the limitations inherent to natural fibers finds manifestation in composite materials that amalgamate distinct components to engender novel and enhanced materials. Composites are materials that consist of two components with different properties, so they are combined in such a way as to produce a new and improved

material. Currently, the commonly used matrix is a polymer matrix derived from petroleum processing, which is non-renewable and non-biodegradable.

With the various needs of the properties previously described, he realm of composite materials is currently advancing towards the innovation of materials termed "Green Composites". Green composite is a type of material whose constituents can be naturally found and degraded in nature. Consequently, such composites integrate a matrix fabricated from bio-thermoplastics, encompassing polylactic acid (PLA), polyhydroxy butyrate (PHB) and polysaccharides from plants [3]. PLA is a long chain of lactic acid monomers produced from the fermentation process of corn and potato starch [4].

In the present study, PLA is employed as the matrix, reinforced with bamboo fibers, thereby yielding a "Green Composite" material designated as PLA/bamboo. In general, the composition of natural fibers and matrix greatly affects the mechanical properties of the resulting composite [5]-[7]. Research with bamboo micro-fibrils (BMF) shows that tensile strength and modulus of elasticity are influenced by the composition of reinforcing fibers, where the maximum tensile strength is obtained in specimens with 40% BMF [8]. Other research on polymer composites with bamboo reinforcement shows that 30% fiber composition produces optimum composite mechanical properties [9, 10]. Another facet demanding consideration in the utilization of green composites pertains to their thermal stability and behavior upon immersion. Alkali treatment is one of the methods used to modify the properties of cellulose fibers by dissolving hemicellulose compounds and other impurities in the fiber, to improve the bond between the fiber and the matrix in the composite [11]. Therefore, this research was conducted to study the effect of fiber composition and alkali treatment on the stability and immersion behavior of PLA/bamboo composites. Given its propensity for degradation and water absorption, a comprehensive examination of this trait bears profound relevance in propelling the application of green composite materials [12].

2. METHODS

The research methodology in this study unfolds across three pivotal stages: material preparation, composite manufacturing, and testing. Material preparation begins with selecting and cutting bamboo into short fibers with an average length of 1 cm. The bamboo fibers were then soaked in a 5% NaOH solution for 24 hours. Composites were made by mixing bamboo fibers and PLA matrix with variations in fiber composition of 10%, 20%, and 30%. Composite molding was carried out through a hot press process to form test specimens. This method is relatively cheaper and simpler because it does not use sophisticated control equipment. Initial characterization was carried out to see the effect of variations on the density and mechanical properties of the composite. Immersion testing was carried out in a container of water for 1, 2, 3, and 4 weeks. The thermal stability of the composite was analyzed through Thermal Gravimetry Analysis (TGA) testing.

The materials used in this research include betung bamboo (Dendrocalmus asper), PLA, NaOH and distilled water. Betung bamboo fibers with short size are used as reinforcement in PLA matrix. NaOH powder was used to make a 5% NaOH solution by dissolving it in distilled water. Aquadest was also used in the bamboo rinsing process. The research apparatus encompasses an oven and a hot press instrument. The oven is used in the drying process of raw materials before mixing. Hot press is used in the process of molding bamboo/PLA composites to produce test specimens according to the sample mold.

The bamboo fiber employed originates from betung bamboo (Dendrocalmus asper) sourced from Belega Village, Blahbatuh District, Gianyar Regency. The betung bamboo used has an outer diameter of about 20 cm with a thickness of 1-2 cm. The bamboo used was harvested when it was 3-4 years old. The bamboo obtained is then cut using a wood saw to a size of 20 cm. Then the bamboo is split into bamboo slats with a width of 4 cm to facilitate the soaking process using an alkaline solution. After the solution is homogeneous, the bamboo slats are then soaked with a soaking duration of 24 hours. After the soaking process is complete, the bamboo is then rinsed repeatedly using distilled water. Rinsing is done until all NaOH is completely removed from the bamboo. Then the bamboo is dried in the sun for 3 days until the bamboo is dry. The next process is the collection of bamboo fibers from the two bamboo variations. The collection is done by manual mechanical means, namely by beating the bamboo until it is flat, so that the bamboo fiber will separate by itself. The fibers were then cut with scissors into short fibers measuring 1 cm.

In this study, the variations of bamboo fiber used were 10%, 20% and 30% of the weight of the PLA/bamboo composite. Before the bamboo fiber and PLA were weighed, both materials were preheated in an oven using a stainless steel container at 90˚C for 15 minutes. Heating is done to remove moisture content from both materials which can cause pores in the resulting composite. Both raw materials were then weighed with digital scales with an accuracy of 0.1 gram. In one mixing process, the total weight of the resulting composite is 300 grams, so the weight of bamboo fiber and PLA used can be calculated by multiplying the weight percentage by the total weight of 300 grams. The mixture of the two materials was then put into the oven to be heated at 220˚C for 40 minutes. The heating process will cause the fusion of PLA which acts as a matrix with bamboo fiber as reinforcement. The hot pressing process was then carried out to increase the density and reduce the pores of the composite. Pressing is done at a pressure of 10 KPa at a mold temperature of 120˚C for 10 minutes. The finished composite was then cut to the required specimen size for the testing process.

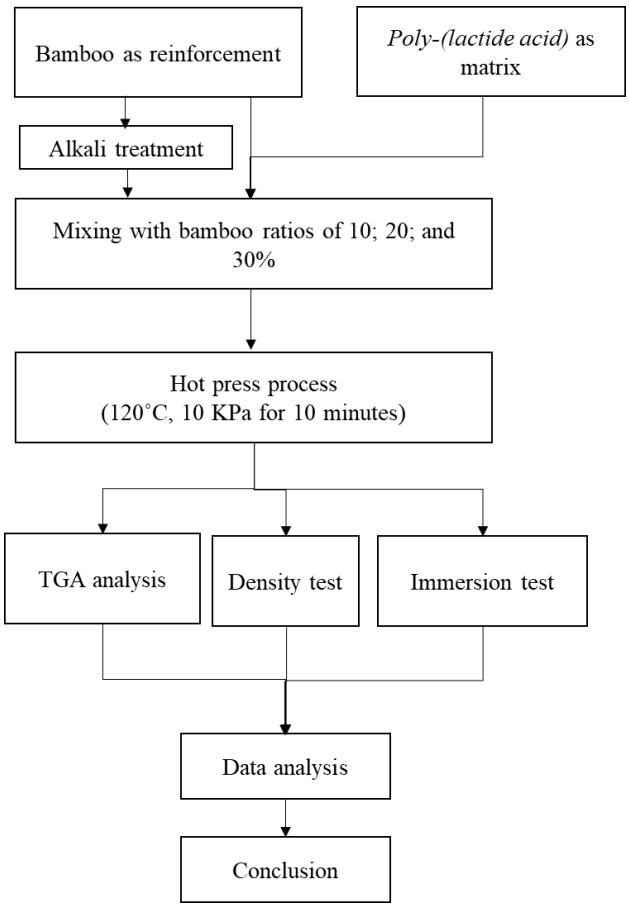

Figure 1. Experimental procedure

The research has been done following Figure 1 and included several characterizations:

a. Density Measurement
One method of measuring density without the need to measure the volume of an object is to compare the weight of an object in air and in a liquid whose density is known, according to the ASTM D792 standard. The weight of the object is measured with an analytical balance with an accuracy of 0.001 g.

b. Immersion Testing
Immersion testing was carried out for 4 weeks in distilled water. The immersion specimens used had an average size of 20x20x5 mm. Before immersion, the composite specimens were dried using an oven at 100˚C for 1 hour. The specimens were then weighed using analytical scales with an accuracy of 0.001 gr.

c. TGA Analysis
Thermal Gravimetry Analysis (TGA) testing is carried out to see the process of changes that occur in the composite when it is heated. TGA testing was conducted at the Material Analysis Laboratory, Department

of Mechanical Engineering, Udayana University. Specimens were prepared weighing approximately 1 gram and then analyzed.

Table 1. Specimen code of PLA/bamboo composite

No	Specimen code	Composition
1	PLA	100% PLA
2	10A	90% PLA + 10% bamboo fiber with alkali treatment
3	20A	80% PLA + 20% bamboo fiber with alkali treatment
4	30A	70% PLA + 30% bamboo fiber with alkali treatment
5	10NA	90% PLA + 10% bamboo fiber without alkali treatment
6	20NA	80% PLA + 20% bamboo fiber without alkali treatment
7	30NA	70% PLA + 30% bamboo fiber without alkali treatment

2. RESULTS AND DISCUSSION

a. Density

Density stands as a pivotal physical parameter influencing the potential applications of materials. Notably, composites, characterized by their light density, emerge as promising candidates for applications prioritizing efficiency, such as transportation. Bamboo fibers are known for their strength and lightweight, so they can be used as an alternative to steel in some applications [13]. Despite its relatively low density of 600-800 kg/m^3, bamboo has a tensile strength of about 200 MPa, with an elongation of 10.2% and a flexural strength of about 230 MPa [14]. The density of the composite material is presented below.

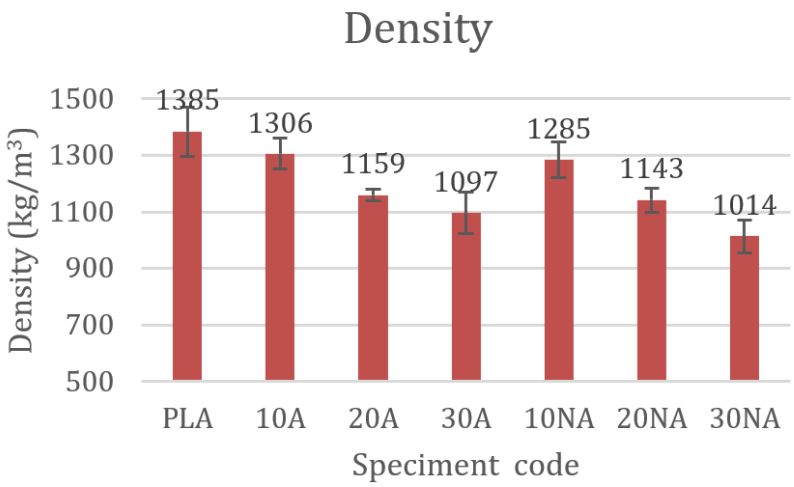

Figure 2. The density of sample composite

Based on the measurements taken, the density of PLA is 1385 kg/m^3. Composite is a type of material with physical properties that are influenced by its constituent materials. Bamboo fiber has a lighter density than PLA, so in theory, mixing PLA with bamboo fiber will produce a material with a lower density. This is consistent with the measurement results, where the higher the fiber composition, the lower the density of the resulting composite. The same trend is obtained for both alkali-treated and untreated fibers. The lower density of alkali-treated specimens is expected because alkali treatment dissolves light components of the fiber such as wax and oil content [15]. The lowest composite density was obtained at 30% fiber composition without alkali treatment, which was 1014 kg/m^3, while the highest density was obtained in the composite with 10% fiber composition with alkali treatment, which was 1306 kg/m^3.

b. Immersion Testing

he escalating interest in PLA arises from its notable biodegradability. One method to explore PLA's biodegradability involves the execution of immersion testing. In this study, the following immersion curve was obtained.

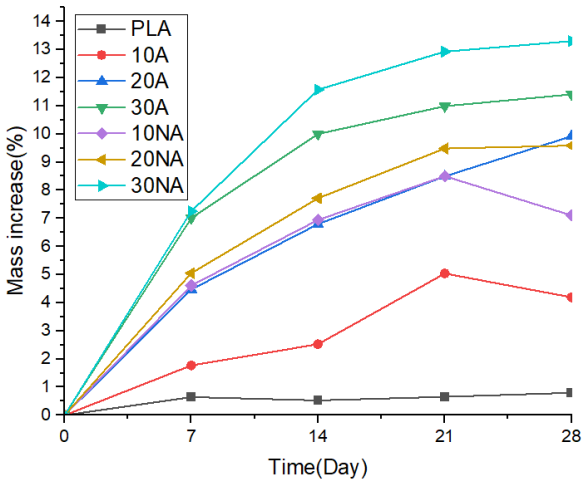

Figure 3. Mass increases of specimens composite

During the immersion test conducted on PLA/bamboo composite specimens, a consistent phenomenon observed across all samples was weight gain. The weight gain exhibited its highest magnitude within the initial 7 days of immersion, after which it gradually subsided over the subsequent weeks, indicative of the composite attaining saturation. Similar results were obtained in another study, where weight loss occurred during the first 7 days of immersion and remained relatively constant until 28 days later [16]. In general, the higher the bamboo fiber composition, the greater the water absorption by the composite. This aligns with the inherent hydrophilicity of natural fibers, rendering them prone to water absorption, a phenomenon evidenced by the observed weight gain. At identical composition, composites with bamboo fibers without alkali treatment experienced a greater increase in weight than those with alkali treatment. These results support previous research where the water absorption content of biocomposites without alkalization is higher than alkalization at 5% NaOH [17]. The largest weight increase occurred in the composite with a composition of 30% bamboo fiber without alkali treatment, which was 13.3%. The composite with the smallest weight increase occurred in the composite with 10% bamboo fiber composition with alkali treatment, which was 4.2%. The pure PLA specimens showed very low water absorption (<1%), so it can be concluded that most of the absorbed water is due to the addition of bamboo fibers. Although PLA is theoretically biodegradable, this immersion test yielded no discernible degradation of the material. This observation implies that the immersion conditions failed to stimulate any degradation process within the material. However, further analysis of the soluble compounds in the immersion solution needs to be done to substantiate this finding. The rate of degradation is influenced by several environmental factors such as water content, type of carbon source, temperature, and pH. The degradation of PLA begins with the hydrolysis of ester groups on its main chain [4].Several factors can cause degradation, such as hydrolysis reaction, thermal activation, photolysis, micro-organism activity and oxidation [18].

c. TGA Analysis

Thermogravimetric Analysis (TGA) stands as a pivotal assessment method for ascertaining the heat stability of materials. TGA curve of the composite specimen is shown as Figure 4. In this study, the composite specimens were heated to temperatures above 900˚C. From several specimens tested, a relatively similar TGA curve was obtained, where there was a decrease in weight up to a temperature of 150˚C, followed by a sloping curve up to temperatures above 250˚C. This weight change occurs due to the evaporation of moisture in the composite specimens. Then there is a drastic decrease until less than 20% of the specimen mass remains at temperatures around 400˚C. In this temperature range, the specimen degradation process occurs. This was attributed to the degradation of the ester linkages involving cyclic oligomers, lactide, and acetaldehyde molecules, along with the emission of gaseous carbon monoxide[19]. The same trend in the composites with fiber addition, which occurs in a single-step process, shows that the degradation of PLA and bamboo fiber occurs simultaneously in the composite.

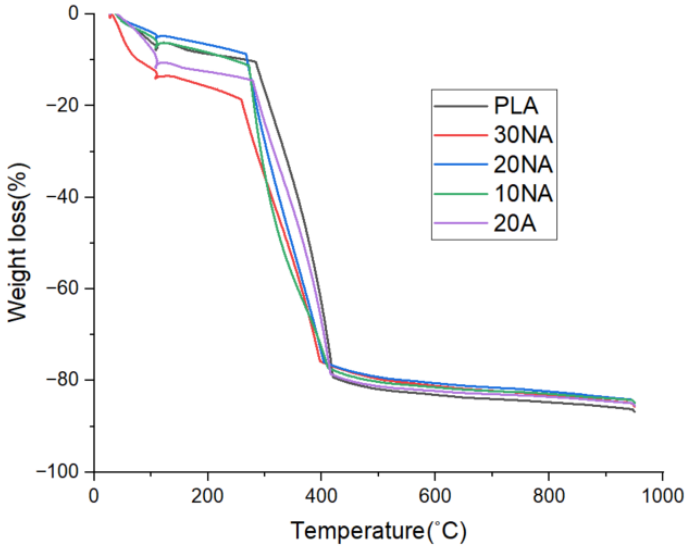

Figure 4. TGA curve of composite specimens

The highest degradation temperature was the pure PLA sample, where the degradation started at 284.1˚C. The addition of bamboo fiber decreased the stability of the composite, where the lowest degradation temperature occurred in the 30% composition of bamboo fiber without alkali treatment, at a temperature of 259.1˚C. This finding contradicts the previous study, which found that the degradation temperature of PLA increased with the addition of coconut fiber [20]. However, other studies show similar results, where the thermal stability of PLA is better than that of its biocomposites [19, 21]. This shows that the thermal stability of PLA biocomposites is influenced by the type of fiber used. In this case, it means that bamboo has a lower thermal stability, causing the PLA/bamboo biocomposite to also have a lower thermal stability. Changes in heat stability are associated with changes in interfacial compatibility and crystal structure of PLA composite [22]. Thus, further explanation of the mechanism of fiber influence on heat stability requires an in-depth analysis of composite crystallinity using X-ray diffraction (XRD).

Table 2. Decomposition temperature of specimens composite

No	Specimen Code	Decomposition temperature (˚C)
1	PLA	284.1
2	20A	278.8
3	10NA	272.2
4	20NA	267.0
5	30NA	259.1

4. CONCLUSION

This research has discussed the development of a bamboo fiber-based "Green Composite" using polylactic acid (PLA) as a matrix. The outcomes of this research underscore that the incorporation of bamboo fiber induces alterations in the properties of composite materials with a PLA matrix. The addition of bamboo fiber reduces the density of the composite because the fiber is lighter. However, the addition of bamboo fibers needs to be controlled due to the hydrophilic nature of the fibers, making the resulting composite more susceptible to changes in properties due to water immersion. The PLA/bamboo composite experienced weight gain due to water absorption in the immersion process. The addition of bamboo composition increases the water absorption of the composite, while the alkali treatment decreases the water absorption of the composite. In addition, the addition of fiber also reduces the degradation temperature of the composite. However, this temperature is still far above the operating temperature of various plastic materials, so this composite still has potential as an alternative material that is more environmentally friendly. Therefore, similar research using natural materials should be further promoted with the help of all stakeholders so that the waste problem can be resolved more quickly.

5. ACKNOWLEDGEMENT
This work was supported by DIPA Politeknik Negeri Bali under contract number (1639/PL8/AL.04/2023).

6. REFERENCES

[1] Gallego-Schmid, *et al.*, "Environmental impacts of takeaway food containers," *J Clean Prod*, vol. 211, pp. 417–427, Feb. 2019, doi: 10.1016/j.jclepro.2018.11.220.
[2] H. I.R, "Bamboo resources, uses and trade: The future," *Journal of Bamboo and Rattan*, vol. 2, pp. 319–326, Mar. 2003, doi: 10.1163/156915903322700368.
[3] N. Naik, *et al.*, "Recent Advances in Green Composites and Their Applications," *Engineered Science*, 2022, doi: 10.30919/es8e779.
[4] R. P. Babu, et al., "Current progress on bio-based polymers and their future trends," Prog Biomater, vol. 2, no. 1, p. 8, 2013, doi: 10.1186/2194-0517-2-8.
[5] R. Gunti, *et al.*, "Mechanical and degradation properties of natural fiber-reinforced PLA composites: Jute, sisal, and elephant grass," *Polym Compos*, vol. 39, no. 4, pp. 1125–1136, Apr. 2018, doi: 10.1002/pc.24041.
[6] R. Sinha, *et al.*, "Density Variation due to Polylactic Acid of Long Bamboo Fibres," 2018, proceedings 2214-7853.
[7] S. G. Nukala, *et al.*, "Development of Biodegradable Composites Using Polycaprolactone and Bamboo Powder," *Polymers (Basel)*, vol. 14, no. 19, Oct. 2022, doi: 10.3390/polym14194169.
[8] D. Puspita, et al., "Fabrication and tensile properties of bamboo micro-fibrils (BMF)/poly-lactic acid (PLA) green composite," in Journal of Physics: Conference Series, Jun. 2019, vol. 1217, no. 1. doi: 10.1088/1742-6596/1217/1/012005.
[9] Nerkar, Kapileshwar, et al., "Effect of Different length fiber on composite Epoxy resin and bamboo," Internation Journal of Creative Research Thoughts, Vol. 9, no 3, 2021.
[10] H. Banga, et al., "Fabrication and Study of Mechanical Properties of Bamboo Fibre Reinforced Bio-Composites," vol. 6, no. 1, 2015.
[11] H. Ma and C. Whan Joo, "Influence of surface treatments on structural and mechanical properties of bamboo fiber-reinforced poly(lactic acid) biocomposites," *J Compos Mater*, vol. 45, no. 23, pp. 2455–2463, Nov. 2011, doi: 10.1177/0021998311401096.
[12] K. G. Satyanarayana, *et al.*, "Biodegradable composites based on lignocellulosic fibers-An overview," *Progress in Polymer Science (Oxford)*, vol. 34, no. 9. pp. 982–1021, Sep. 2009. doi: 10.1016/j.progpolymsci.2008.12.002.
[13] T. V. Popat and A. Y. Patil, "A Review on Bamboo Fiber Composites," " IRE Journals 1, no. 2 2017: 54-72.
[14] S. Jain, *et al.*, "Mechanical behaviour of bamboo and bamboo composite," Journal of materials science 27,1992.: 4598-4604.
[15] Verma, Deepak, and Kheng Lim Goh. "Effect of mercerization/alkali surface treatment of natural fibres and their utilization in polymer composites: Mechanical and morphological studies." Journal of Composites Science 5.7 (2021): 175.
[16] K. E. Mazur et al., "Mechanical, Thermal and Microstructural Characteristic of 3D Printed Polylactide Composites with Natural Fibers: Wood, Bamboo and Cork," J Polym Environ, vol. 30, no. 6, pp. 2341–2354, Jun. 2022, doi: 10.1007/s10924-021-02356-3.
[17] G. Refiadi, et al., "Sifat Komposit Epoksi Berpenguat Serat Bambu Pada Akibat Penyerapan Air," Jurnal Sains Materi Indonesia 19, no. 3, 2018.: 98-104.
[18] L. Wan, et al., "Conceiving a feasible degradation model of polylactic acid-based composites through hydrolysis study to polylactic acid/wood flour/polymethyl methacrylate," Compos Sci Technol, vol. 181, p. 107675, 2019, doi: https://doi.org/10.1016/j.compscitech.2019.06.002.
[19] Kamaludin, Nor Helya Iman, et al. "Thermal behavior and water absorption kinetics of polylactic acid/chitosan biocomposites." Iranian Polymer Journal 30 (2021): 135-147.
[20] Ridwan, Ridwan, et al. "Pengaruh Sifat Material Dan Termal Komposit Pla (Poly Lactid Acid)/Coconut Fiber (Sabut Kelapa) Dengan Modifiksi Perendaman Naoh." Jurnal Sains dan Teknologi Reaksi 20.02 (2022).
[21] Rodríguez-Núñez, Jesús R., et al. "Evaluation of physicochemical and antifungal properties of polylactic acid–thermoplastic starch–chitosan biocomposites." Polymer-Plastics Technology and Engineering 56.1 (2017): 44-54.

[22] Zuo, Yingfeng, et al. "Effect of nano-SiO2 on the compatibility interface and properties of polylactic acid-grafted-bamboo fiber/polylactic acid composite." International journal of biological macromolecules 157 (2020): 177-186.

LOGIC
Journal of Engineering Design and Technology
Vol. 23 No.3 November 2023 ; p. 164 - 168

p-ISSN : 1412-114X
e-ISSN : 2580-5649
http://ojs2.pnb.ac.id/index.php/LOGIC

ULTRASONIC PULSE VELOCITY TEST USING BS METHOD AND T-METHOD TO ESTIMATE CRACK DEPTH OF CONCRETE

Evin Yudhi Setyono

Civil engineering Department,
State Polytechnic of Bali,
Kampus Politeknik Negeri Bali,
Bukit Jimbaran, Kuta Selatan,
Badung - Bali 80361

Correponding email :
yudhisetyono@pnb.ac.id

Abstract. Ultrasonic Pulse Velocity (UPV) as a non-destructive test is commonly used on concrete crack estimation. There are several methods are applied based on the transducer configuration. Among the methods, BS (British Standard) method and T method was used in this study. On this method, transmitter was fixed at certain distance from crack and receiver was moved at several constant intervals, then crack depth was analyze from the relation between the transducer distance and the transit time curve. This research is conducted to study the accuracy of BS method and T-method in estimating the crack depth of concrete using NDT James Instrument V-Meter M-K IV. Concrete beams were made with artificial crack depth 2 cm, and 4 cm. Transducers 54kHz of UPV Mark IV were set at constant interval. Thus, the comparation of actual depth and experimentally result was analyzed. The study concluded that, the accuracy of the BS method has a better estimation result with a relative error of 27,75% and 35,95%, compare to the T-method that has 79,30% and 79,82% error.

Keywords : concrete crack, BS method, T-Method

1. INTRODUCTION

Concrete becomes the second most consumed material in the world, with average per people almost three tonnes per year [1]. Concrete has been proven to be a prior leading construction material. Commonly, it is obtained by mixing cement, water, sand as fine aggregates, coarse aggregates, and sometimes other substances in a certain ratio [2]. The unyielding nature of concrete makes it tough and durable, it can withstand large loads over a long period [3] It also resists many aspects such as fire, rotting, rusting, and requiring minimal maintenance or repair. When the mechanical properties of concrete decrease significantly, cracks will appear on concrete. Besides the poor workmanship factor, concrete cracks are sometimes caused by overloading and corrosion, Specific cracking patterns that appear in concrete, can be led to a specific reason [4]. Cracks often appear as an early warning of the structure; it indicates failure or a problem in it. The first response is to evaluate the structure strength, to determine the suitable repair or reinforcement of the structure [5].

Ultrasonic Pulse Velocity (UPV) test is one non-destructive test that is applied to estimate concrete cracks. There are five common methods, the SDDW method, Tc-To method, delta method, BS Method, and T method, each one has a specific equation for estimating crack depth. The short distance detour wave (SDDW) method is the simplest method, transmission time and wave velocity are measured by arranging the transmitter and receiver at placing near the side of the crack. In the TC-To method, the transmitter and receiver are placed at a certain distance on the health part of the concrete. Next, both transducers are set between the crack as a center, and the transmission time is measured. The Delta method is the same as the Tc-To method, it measures the transmission time by placing the crack and arranging the transmitter and receiver at a non-symmetrical distance.

British Standard (BS) method is a commonly used method that is recommended by BS4408. The transmission time of the transducer at distance 150 mm and 300 mm between the crack is measured to determine the crack depth [6]. The t method that is also studied in this research is a method of requesting discontinuous time

T at the crack position from the curve (relation between the transmission distance and the transmission time). Both methods use the same indirect method, but have transducer arrangement difference. Herlambang[7], studied about the effect of transducer distance and the accuracy of BS method in estimating the depth of the concrete crack, the accuracy was around 83-92% for a transducer distance of 10 cm. Based on this research, we used a transducer interval of 10 cm. Furthermore, data collection in the T-method is more complex than the BS method. Linggasari [8], observed crack in concrete and compared two methods of measurement which was the BS method and T-method. The research used PUNDIT as testing instrument and showed that there was no significant difference (only 1-2%) between both methods.

The information provided in the previous study indicates, that both methods can be used in measurement because there is no significant difference. However, the study has lack information about accuracies. It is also essential to study both accuracies in measuring the concrete crack, to compare which is the best method. This research aims to study and compare the accuracy of the BS method and the T-method in estimating the crack depth of concrete.

2. METHODS

The specimens are beam-shaped non-reinforced concrete with dimensional of 15x15x60 cm. Then, they were given artificial cracks with depth of 2 cm and 4 cm. The NDT James Instrument V-Meter MK IV is used in this study. The depth of concrete crack is estimated by observing transit time between transmitter and receiver using indirect method. the. Estimation of concrete crack depth measurement measured by Indirect transmission. Two different measuring method are used in this study, which are BS Method and T-Method. British Standard (BS) method is a method where transmitter and receiver are placed in certain x distance between the crack, the transit time is measured as T_1, then both transducers are shifted twice in distance, and the transit time is measured as T_2.

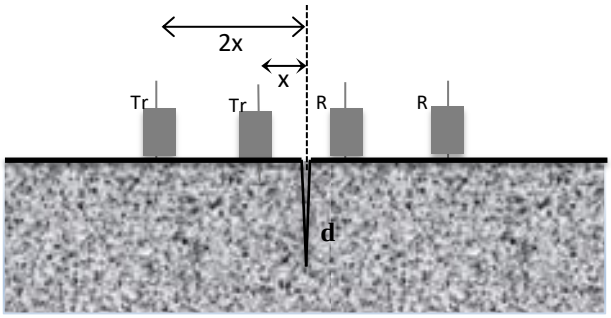

Figure 1. BS method

Depth of crack is calculated from the equation 1 below:

$$d = x\sqrt{\frac{4{T_1}^2 - {T_2}^2}{{T_2}^2 - {T_1}^2}} \quad (1)$$

In this BS method, both transducers are positioned at distance x= 10 cm from the crack then the distance is widened to x= 20 cm (figure 3). Transmission times T_1 and T_2 are then recorded and the depth of crack is calculated refers to Equation 1.

Figure 2. Instrument set up for BS method

The second method is T-method, where transmitter is fixed at a certain distance from the crack as L_1, and receiver is placed and shifted in a constant interval distance of 10 cm (figure 2). Every data of transmission time in each point is collected and plotted, the crack depth is then calculated using equation 2.

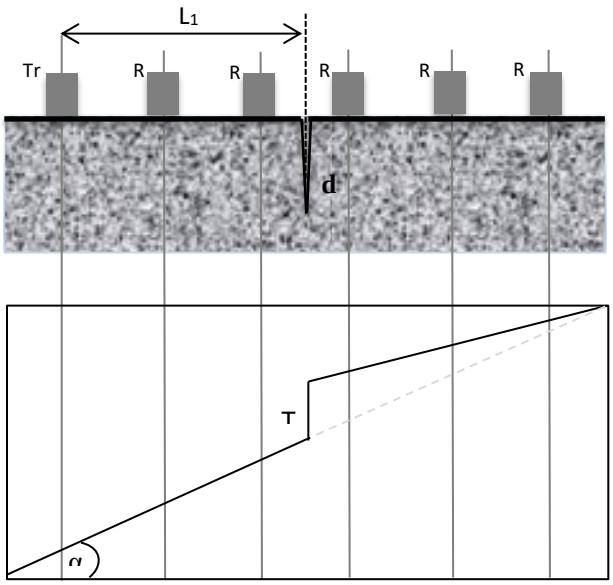

Figure 3. T- method

Depth of crack is calculated from the equation 2 below [9]:

$$d = T.\cot\alpha.\frac{T.\cot\alpha + 2L_1}{2(T.cot\alpha + L_1)} \quad (2)$$

Figure 4. Instrument set up for T-Method

3. RESULTS AND DISCUSSION

The differences between depth crack measured (d-measurement) and actual depth (d-artificial) is stated in error relative. Beam 2 specimen with 40 mm artificial depth has better error relative than beam 1 with 20 mm depth.

Table 1. Summary result of BS-method measurements

Specimen	X (mm)	T_1 (μs)	T_2 (μs)	d-artificial (mm)	d-measurement (mm)	Error relative (%)
Beam 1	10	77,1	150,1	20	27,19	35,95
Beam 2	10	96,1	176,7	40	51,10	27,75

The transmission time and distance data from T-method test are plotted in figure 5 and figure 6. Based on the graph in figure 5, the discontinuous time T for beam 1 is 16,94 μs with the cotangent α of the slope is 2,27. Refer to the equation 2, it is obtained the crack depth is 35,86 mm.

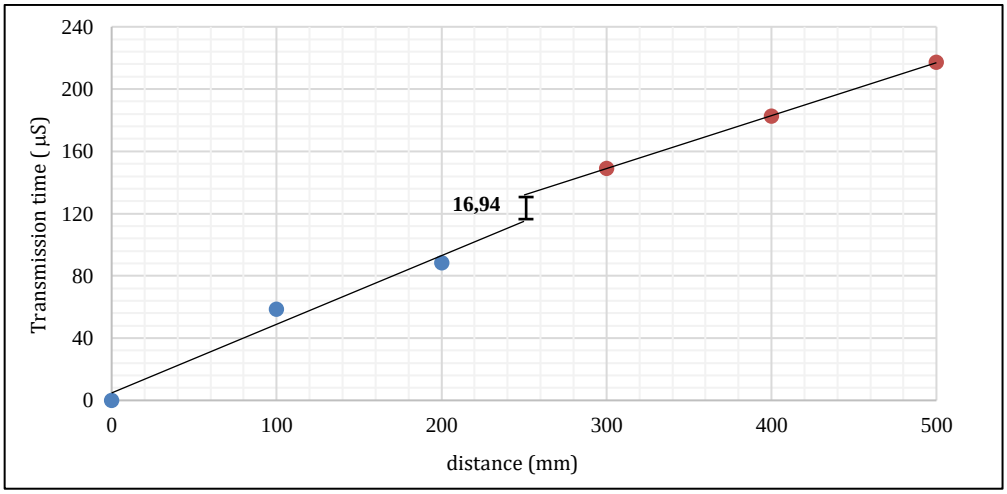

Figure 5. Transmission time of beam 1

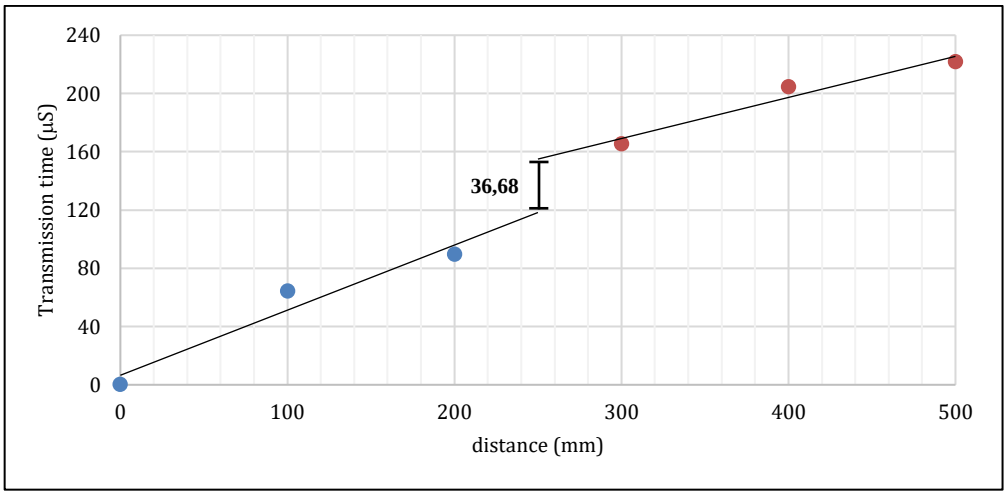

Figure 6. Transmission time of beam 2

Table 2. Summary result of T-method measurements

Specimen	T (μs)	cot α	L_1 (mm)	d-artificial (mm)	d-measurement (mm)	Error relative (%)
Beam 1	16,94	2,27	250	20	35,86	79,30
Beam 2	36,68	2,24	250	40	71,93	79,82

For sample beam 2, from the graphic plot, discontinuous time T is 36,68 μs with the cotangent α of the slope is 2,24. The result of the crack depth is 71,93 mm. Based on the result in table 1 and table 2, it showed that both methods are overestimated the depth of crack. In comparison with Linggasari [8] , the result shows that there is around 27%-33% different from both methods. By using BS method, error relative is 27,75% and 35,95% while by using T-method is 79,30% and 79,82%. The T-method is observed more inaccurate than BS method in estimating depth of the crack. Several possible factors influence this result, besides the lack of the precision of transducer set up. It is also possible due to the wide transducer distance during this measurement. The surface zone concrete predominantly affects the ultrasonic pulse from transmitter to receiver, which may not be represent the the body thus highly subject to errors. The recorded signal probable to fluctuate and gives difficulty during measurements. Thus, it is highly recommended to use an aid tool to assist the transducer during measurements to get the fixed recorded data.

4. CONCLUSION

The research aims to study and compare the accuracy of the BS method dan T-method in estimating the depth of artificial crack concrete beam. The result shows that both methods have different estimation around 27%-33%. The accuracy of the BS method has a better estimation result with a relative error of 27,75% and 35,95%, compared to the T-method which has 79,30% and 79,82% errors. This lack of accuracy is probably caused due to the wider transducer's distance and fluctuation of recorded signals during the measurement. An aid tool as a transducers stabilizer is suggested to be used to obtain better measurement.

5. ACKNOWLEDGEMENT

Thanks were conveyed to the Head of Civil Engineering Materials Laboratory of Bali State Polytechnic for being given permit to access laboratory materials and UPV instruments.

6. REFERENCES

[1] C. R. Gagg, "Cement and concrete as an engineering material: An historic appraisal and case study analysis," *Eng Fail Anal*, vol. 40, 2014, doi: 10.1016/j.engfailanal.2014.02.004.

[2] K. K. Poloju, "Concrete," in *SpringerBriefs in Applied Sciences and Technology*, Springer Science and Business Media Deutschland GmbH, 2022, pp. 1–12. doi: 10.1007/978-981-16-5949-2_1.

[3] H. Wiggenhauser, C. Köpp, J. Timofeev, and H. Azari, "Controlled Creating of Cracks in Concrete for Non-destructive Testing," *J Nondestr Eval*, vol. 37, no. 3, 2018, doi: 10.1007/s10921-018-0517-x.

[4] K. Thulasi, S. Subathra, and T. P. Meikandaan, "AN EXPERIMENTAL STUDY OF CRACK PATTERNS ON REINFORCED CONCRETE BEAM," *International Research Journal of Engineering and Technology*, vol. 05, no. 03, 2018.

[5] Baehaki, M. Andi, and G. R. Yohanes, "Experimental study of crack depth measurement of concrete with ultrasonic pulse velocity (UPV)," in *IOP Conference Series: Materials Science and Engineering*, 2019. doi: 10.1088/1757-899X/673/1/012047.

[6] J.H. Bungey, S.G. Millard, and M.G. Grantham, *Testing of Concrete in Structures, 4th Edition*, 4th ed. London: Taylor & Francis, 2016.

[7] F. S. Herlambang and E. Y. Setyono, "Pengaruh Jarak Transducer dan Tulangan pada Pengukuran Kedalaman Retak Beton Menggunakan Ultrasonic Pulse Velocity (UPV)," *... Nasional Terapan Riset ...*. 2017.

[8] D. Linggasari, "MEMPERKIRAKAN KEDALAM RETAK PADA BETON MENGGUNAKAN GELOMBANG ULTRASONIK," *Jurnal Muara Sains, Teknologi, Kedokteran dan Ilmu Kesehatan*, vol. 3, no. 1, 2019, doi: 10.24912/jmstkik.v3i1.3912.

[9] Ogata, "Method of Measuring Crack Depth of Concrete uses Ultrasonic." Accessed: Jun. 08, 2023. [Online]. Available: http://muses.muses.tottori-u.ac.jp/faculty/ogata/lecture/crack-depth-method.pdf

LOGIC
Journal of Engineering Design and Technology
Vol. 23 No.3 November 2023 ; p. 169 - 174

p-ISSN : 1412-114X
e-ISSN : 2580-5649
http://ojs2.pnb.ac.id/index.php/LOGIC

The Effect of Composition and Type of Metal Filler on Heat Resistance of Silica Rubber Matric Composites

R.N. Akhsanu Takwim [1)], Anggit Murdani [1)], Purwoko [1)], Bayu Pranoto [1)], Naufal Reza Putra [1)]

1) Mechanical Engineering, State Polytechnic of Malang, Jl. Soekarno Hatta 09, Malang, Indonesia

Correponding email : akhsanu.takwim@polinema.ac.id

Abstract. Thermal Tensioning is one of the methods used to minimise the occurrence of residual stress and unwanted distortion during welding. One of the thermal tensioning methods is Static Thermal Tensioning (STT), which involves countering thermal stress during welding. The STT method requires active cooling behind the welding line. Several properties are required for the coolant material, such as thermal conductivity, heat resistance, and good flexibility. To achieve the desired properties, a mixture of different materials was used, commonly called a composite. The purpose of this study is to know the effect of filler metal composition and type on the heat resistance of silica rubber matric composites. This study used 2 independent variables: the filler composition in composites with variations of K1 (60%) and K2 (70%), and the type of filler metal, aluminium and copper powder with variation J1 (100%-0%), J2 (75%-25%), J3 (50%-50%), J4 (25%-75%), and J5 (0-100%). The testing process used Thermogravimetry Analysis (TGA) with replication 2 times. The results of this study showed the specimens with K1;J1 composition,containing 60% pure aluminium filler metal, showed the best heat resistance with a final weight of 88,25%. While specimens with K2;J5 composition, containing 70% pure copper filler metal, showed the worst heat resistance with a final weight of 74,25%.

Keywords : aluminium, composite, copper, heat resistance, silica rubber

1. INTRODUCTION

Welding is one of the manufacturing processes in the industrial world, however this manufacturing process has several weaknesses such as distortion and sensitization during welding. Welding can also be defined as the process of joining two metals to the point of recrystallisation of the metal with or without the use of additional materials and to perform this welding the presence of heat energy is required [1]. Inconsistent heating and cooling during welding can result in thermal expansion and contraction, causing residual stress and desirable deformation [2]. Residual stress and distortion that occur can be reduced by using the thermal tensioning method, which is welding by adding active cooling behind the welding line and heating beside the welding line. One of the thermal tensioning methods is Static Thermal Tensioning (STT), the working principle is thermal tensioning to fight thermal stress during welding [3].

[3] has researched the effect of the temperature variation of static thermal tensioning on angular distortion and microstructure behaviour of gmaw welded sus 304 stainless steel plate where GMAW welding with the most optimal STT method is at a temperature of 250C, namely with an angular distortion value of 2° 78'.To be an active cooling must have several properties such as good thermal conductivity, heat resistance, and flexibility. To get all those properties it is needed to combine several materials that have those properties. This mixture commonly called a composite, causes the formation of a new structure that has the combined properties and characteristics of the forming materials [4].

The reinforcing phase used in this research is particles, which are aluminium and copper powder. This is

because aluminium is easily found in the market. In addition, aluminium is a good conductor of electricity and heat, has a low melting point, and has good corrosion resistance [5]. Copper was also chosen as the reinforcing phase because copper with high purity is also good for conducting electricity and heat, also has a high melting point [6]. While the matrix used is elastomer or rubber because it can be elastically deformed very high [7]. However, chemical and physical modifications to rubber is needed so that it can be utilised in another sector. This is needed to overcome the limitation of rubber properties [8]. Rubber compound fillers such as Carbon Black (CB) and silica are often used to improve the mechanical properties of the rubber [9]. Silica rubber is an example of a product derived from rubber. The addition of silica to rubber has benefits compared to organic rubber such as being able to be used over a wide temperature range (-100 °C to 250 °C) [10]. [11] has conducted research effect of silica and silicone oil on the mechanical and thermal properties of silicone rubber, It was found that the fumed silica-filled sample had a higher tanδ than the precipitated silica.

The composite will be tested for heat resistance or thermal resistance. The higher the resistance of a material, the lower heat loss [12]. This heat resistance test will use the thermogravimetric analysis method, which studies mass reduction against temperature increase. The matrix and filler bonds will be released as the temperature increases causing the material to degrade [13]. Therefore, further research is needed to determine the material that has the best heat resistance to become a substitute material for active cooling in the welding process with STT method..

2. METHODS

2.1 Research Methods

The method used to find the scientific truth in this research is the experimental method. Experimental research method is a research method that investigates causes and effects by adding control variables.

2.2 Specimen and Equipment Preparation

The specimen made from composites with filler containing aluminium and copper powder and matrix containing silica rubber with dimensions of 96 mm in length, 13 mm in width, and 4 mm in thickness. Specimen made using acrylic mould as shown in Fig 1.

Figure 1. Acrylic mould

The specimens used for testing are 20 samples with a variation of 10 types and 2 replications. The specimen that has been made is clamped on an electric heater as shown in Fig 2.

Figure 2. Clamping the specimen

After the specimen is clamped, the next step is to switch on the thermocontrol and set it at room temperature as shown in Figure 3.

Figure 3. Set the Thermo control at room temperature

2.3 Research Variable

The independent variables in this study are the composition of filler metal in the composite and the type of filler metal. The composition of filler metal in the composite used in this research is as follows:

a. 60% filler metal and 40% matrix (K1)
b. 70% filler metal and 30% matrix (K2)

The type of filler metal used is aluminium and copper powder with variation:

a. 100% aluminium-0% copper (J1)
b. 75% aluminium-25% copper (J2)
c. 50% aluminium-50% copper (J3)
d. 25% aluminium-75% copper (J4)
e. 0% aluminium-100% copper (J5)

The dependent variable in this study is heat resistance, the good and bad heat resistance of a specimen is determined by the percentage of the remaining weight of the specimen after testing by giving a pressing load from the clamp. the sample used has a size of 96×13×4mm.

The controlled variable used in this study is testing temperature, the peak temperature for this research is 500 °C

2.4 Method of Collecting Data

The testing process is performed on specimens with two replications for each variation. Before testing it is necessary to weigh the initial weight of the specimen. After that do the testing process and record the weight change of the specimen at each temperature. After the testing process is complete weigh the specimen again and compare it with the records.

3. RESULTS AND DISCUSSION

3.1 Microstructure

To strengthen the discussion of this research, micro photos are also used to determine the bonding structure of the specimen.

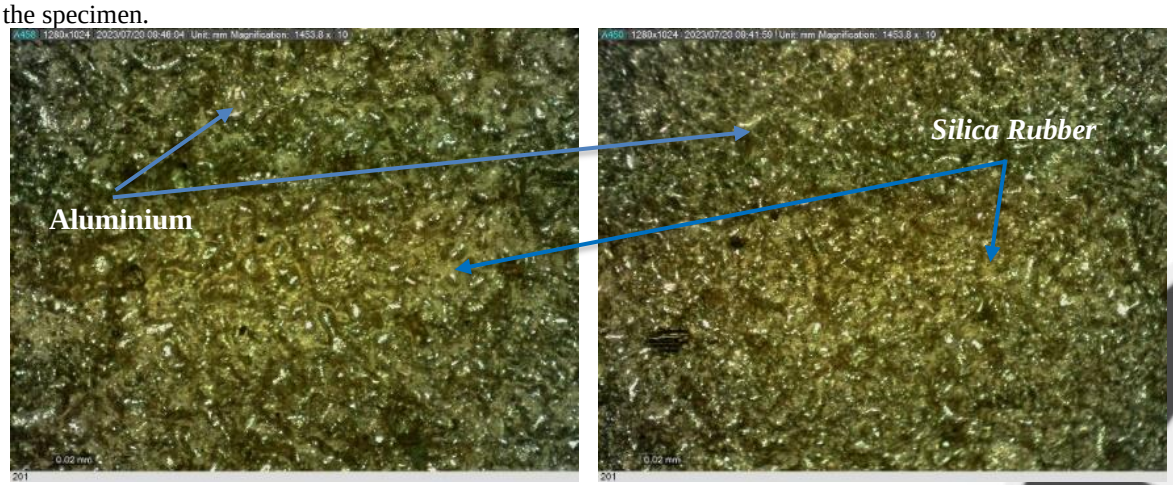

(a) (b)

Figure 4. Micro photo specimen K1;J1 (a) and K2;J1 (b)

In Figure 4 which shows a micro photo of specimen J1, it is shown that the filler metal and matrix attach nicely. This causes no air trapped inside and the specimen has a smooth surface.

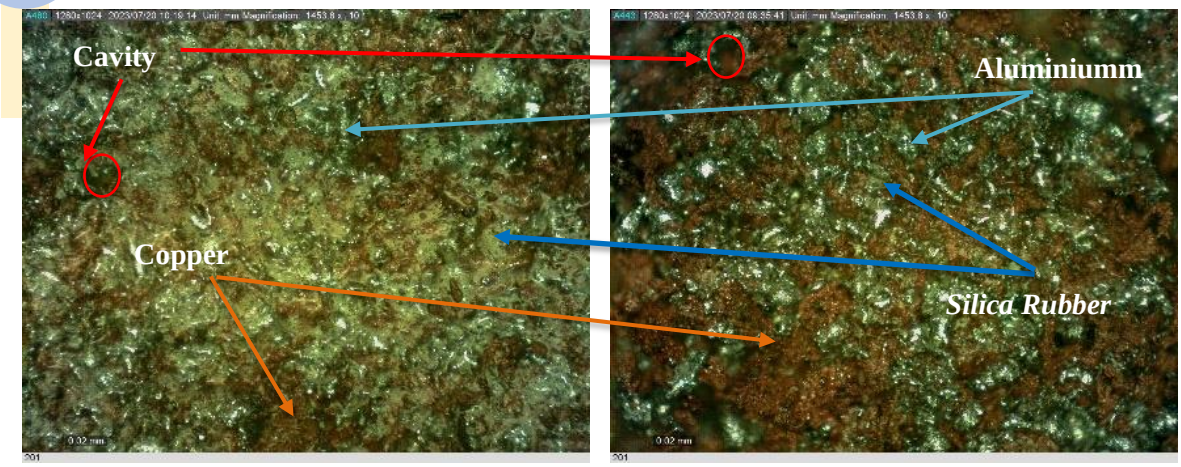

(a) (b)

Figure 5. Micro photo specimen K1;J3 (a) and K2;J3 (b)

A micro photo of specimen J3 is shown in Figure 5. It can be seen that the filler metal is attached to the matrix, but the aluminium and copper powder cannot be merged. In specimens K2;J3 some parts are slightly blurred, this indicates there are differences in height or cavity in the specimen. Air will enter the cavity in the specimen.

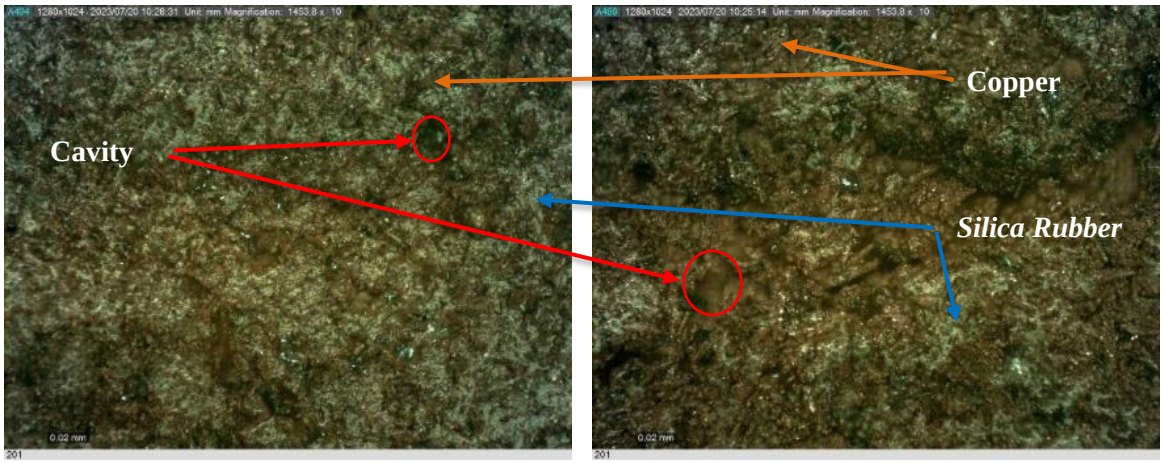

(a) (b)

Figure 6. Micro photo specimen K1;J5 (a) and K2;J5 (b)

Specimen J5 is the most brittle specimen, it can be seen in Figure 6 that the copper powder is grouped and difficult to attach to the matrix. This causes the specimen to be brittle and easily broken. In specimen K2;J5 it can be seen there are more cavities when compared to specimen K1;J5. These cavities will be entered by air which makes the specimen combustion process faster.

3.2 Discussion

Figure 7 shows the weight change of all types of specimens. It can be seen the K1;J1 specimen has the most residual weight. This is because aluminium has a smaller thermal conductivity than copper and also the filler used in the specimen is only 60%. In addition, the structure of this specimen shown in Figure 5 (a) shows that air is difficult to enter the bond between filler and matrix, which causes the combustion process to occur only at high temperatures. This causes the specimen to still have a residual weight of 88,25%. The K2;J5 specimen has the smallest residual weight percentage which means this specimen has the worst heat resistance. This is because copper has a bigger thermal conductivity than aluminium, it is also supported by the large use of filler in the specimen which reaches 70%. In addition the structure of the specimen shown in Figure 7 (b) shows the copper is difficult to attach with the matrix which causes many cavities in the specimen. This cavity will be filled with oxygen which can accelerate the combustion process. These factors make the matrix in the specimen burn faster and reduce, this causes the specimen to only have residual weight of 74,25%.

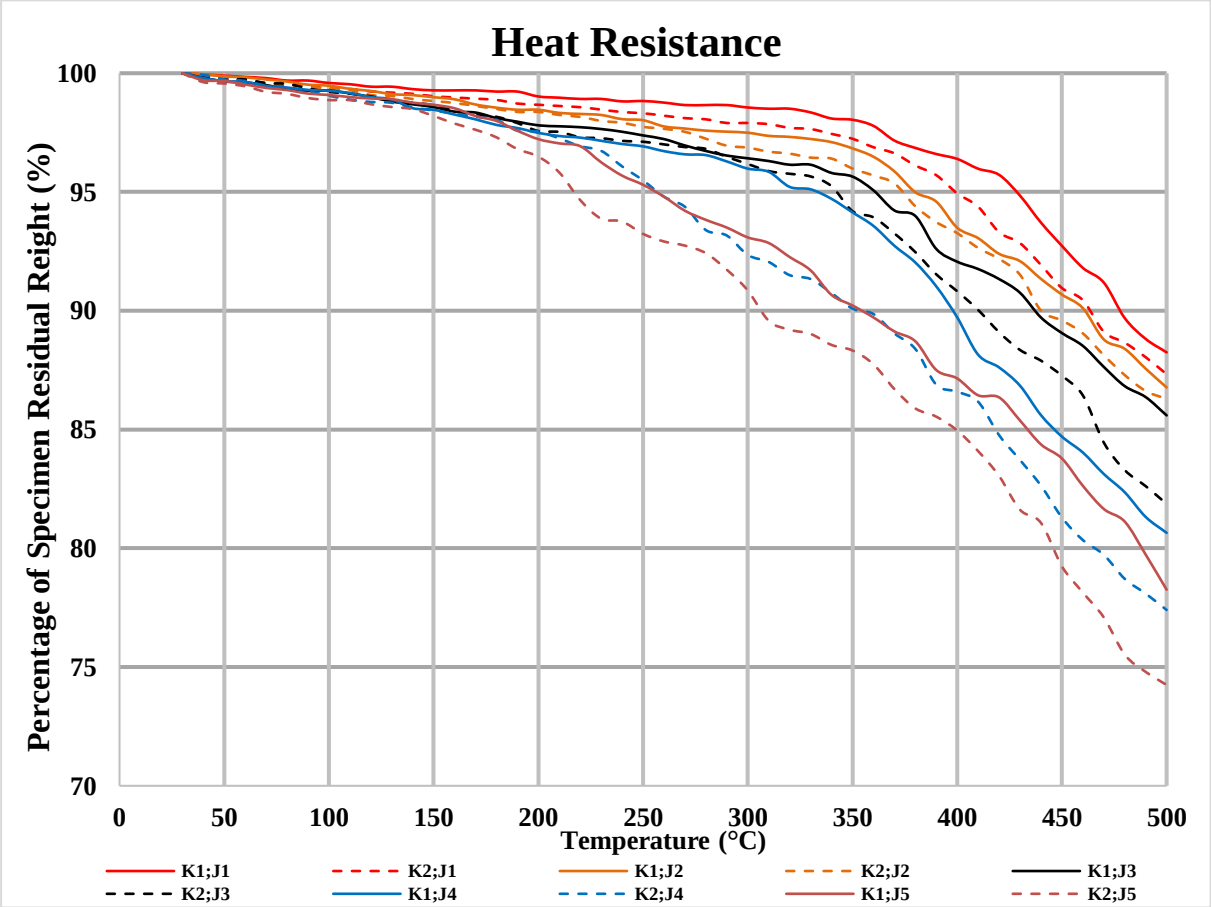

Figure 7. Heat resistance test result data

4. CONCLUSION

Based on research on the effect of composition and type of filler metal on the heat resistance of silica rubber matric composite, the conclusions obtained are as follows:

1. The composition of filler metal in the composite affects the heat resistance of the composite with silica rubber matrix. The less filler metal composition used in the composite, the better the heat resistance. The best heat resistance is in specimen K1; J1 where the composite contains 60% filler metal and the type of filler metal used is pure aluminium which has a final weight of 88.25%. Specimen K2;J5 is the specimen with the worst heat resistance where the composite contains 70% filler metal and the type of filler metal used is pure copper with a final weight of 74.25%.
2. The type of filler metal affects the heat resistance of silica rubber-matric composites. The best heat resistance is possessed by specimen K1;J1, which is a specimen containing 60% filler in the form of 100% aluminium metal with an average final weight of 88.25%. The poorest heat resistance belongs to specimen K2;J5, which is the specimen containing 70% filler in the form of 100% copper metal with an average final weight of 74.25%.
3. The interaction of metal composition and metal type has a significant effect on the heat resistance of silica rubber-matched composites. The decrease of filler metal composition in the composite and the more use of aluminium as filler metal will increase the heat resistance of silica rubber matched composite. The best heat resistance is obtained in specimens K1; J1, namely specimens with a filler metal composition of 60% in the form of 100% aluminium with an average final weight of 88.25%. The worst heat resistance was obtained in specimens K2; and J5 with 70% filler metal composition in the form of 100% copper with an average final weight of 74.25%.

5. REFERENCES

[1] R. Yudistira Pratama, M. Basuki, dan P. Erifive, "Pengaruh Variasi Arus Pengelasan SMAW Untuk Posisi Pengelasan 1G Pada Material Baja Kapal Ss 400 Terhadap Cacat Pengelasan," *Semin. Teknol. Kebumian dan Kelaut.*, vol. 2, pp. 1–7, 2020.

[2] M. Seyyedian Choobi, M. Haghpanahi, dan M. Sedighi, "Investigation of the effect of clamping on residual

stresses and distortions in butt-welded plates," *Sci. Iran.*, vol. 17, no. 5 B, pp. 387–394, 2010.
[3] R. N. A. Takwim, P. Purwoko, dan B. Pranoto, "Effect of Temperature Variation of Static Thermal Tensioning on Angular Distortion and Sensitization behaviour of GMAW Welded SUS 304 Stainless Steel Plate," *J. Ranc. Bangun dan Teknol.*, vol. 21, no. 3, pp. 218–224, 2021.
[4] Sutrisno, Y. H. Sularso, dan Mustafa, "Pengaruh Serbuk Geomaterial Pada Komposit Polyester Terhadap Ketahanan Panas," *Semin. Nas. Sains dan Teknol. Terap. IV 2016*, pp. 117–122, 2016.
[5] S. Mizhar, Suherman, dan R. Fauzi, "Pengaruh Penambahan Magnesium Terhadap Kekerasan , Kekuatan Impak Dan Struktur Mikro," *Mek. Tek. Mesin*, vol. 2, no. 2, pp. 77–84, 2016.
[6] Muhammad dan R. Putra, *Bahan Ajar Bahan Teknik*, vol. 21, no. 1. Aceh Utara: Fakultas Teknik Universitas Malikussaleh, 2014.
[7] R. D. Wibowo, "Analisis Pemodelan Konstitutif Hiperelastis Biderman dan Neo-Hookean Pada Karet Industri PT.Cipta Daya Mandiriinsani Indonesia dan Literatur Jorgen Bergstrom," *Science (80-.).*, vol. 1, no. 1, p. 2514922, 2009.
[8] J. Saelao dan P. Phinyocheep, "Influence of styrene on grafting efficiency of maleic anhydride onto natural rubber," *J. Appl. Polym. Sci.*, vol. 95, no. 1, pp. 28–38, 2005.
[9] A. Cifriadi, P. Sugita, T. Kemala, dan S. Nikmatin, "Kajian Penggunaan Carbon Black N990 sebagai Bahan Pengisi Kompon Karet Alam : Sifat Dinamik , Kestabilan Termal , dan Ketahanan Panas," *J. Ris. Kim.*, vol. 14, pp. 24–34, 2023.
[10] W. Sujana dan W. I Komang Astana, "Pemanfaatan Silicon Rubber Untuk Meningkatkan Ketangguhan Produk Otomotif Buatan Lokal," *J. Energi dan Manufaktur*, vol. 6, no. 1, pp. 37–42, 2013.
[11] C. Zhang, L. Liu, Z. Zhang, K. Pal, dan J. K. Kim, "Effect of silica and silicone oil on the mechanical and thermal properties of silicone rubber," *J. Macromol. Sci. Part B Phys.*, vol. 50, no. 6, pp. 1144–1153, 2011.
[12] R. Mishra, J. Militky, dan M. Venkataraman, *Nanoporous materials*. Elsevier Ltd., 2018.
[13] H. E. Mayasari dan N. M. Setyadewi, "Ketahanan Termal dan Ketahanan Perendaman Komposit NBR/EPDM dengan Berbagai Kompatibiliser," *J. Teknol. Proses dan Inov. Ind.*, vol. 5, no. 1, p. 11, 2020.

LOGIC
Journal of Engineering Design and Technology
Vol. 23 No.3 November 2023 ; p. 175 - 181

p-ISSN : 1412-114X
e-ISSN : 2580-5649
http://ojs2.pnb.ac.id/index.php/LOGIC

EVALUATION OF FLOOD HANDLING AT SEMINYAK WAY II, IN THE TUKAD MATI DRAINAGE SUB-SYSTEM

I Gusti Ngurah Kerta Arsana [1], Mawiti Infantri Yekti [2], Dewa Ayu Utari Winandari [2]

1) Environmental Engineering, Faculty of Engineering, Udayana University, Badung Regency
2) Civil Engineering, Faculty of Engineering, Udayana University, Badung Regency

Correponding email [1] : kertaarsana64@gmail.com

Abstract. Flood is a natural phenomenon that often occurs in several areas of Badung Regency. Losses result in damage to buildings, roads, and other public facilities. Floods are caused by a more sloping land topography, changes in land use to dense settlements, and soil conditions. This study aims to deal with flooding by evaluating the existing canal on Jalan Kunti II Seminyak. The method used for testing data consistency is the RAPS (Rescaled Adjusted Partial Sums) method. The distribution used is Log Person Type III. Testing of frequency distribution used the Smirnov – Kolmogorov Test and the Chi-Square Test. Analysis of rainfall intensity using the Mononobe formula. Calculation of planned flood discharge (Q) uses the Rational method, Nakayasu method, and theoretical discharge control for 2, 5, 10, and 25-year return periods with the existing channel capacity. The result of the analysis shows that the theoretical discharge with a return period has met of planned flood discharge so that the drainage on Jalan Kunti can accommodate the planned flood with a return period of 10 years. Where the drainage capacity of Jalan Kunti is 0,412 m^3/second & 0,461 m^3/second. The drainage ditch with a capacity of 200 m^3/second to Tukad Mati has not been able to accommodate the planned flood discharge for the 25-year return period of 242.33 m^3/second. The Tukad Mati channel for the existing Q 675,825 m^3/second has been able to accommodate the flood discharge Q at the 25-year return period of 314.49 m^3/second.

Keywords: Channel Capacity, Channel Dimensions, Flood

1. INTRODUCTION

Floods require attention and handling from both the government and the community. According to [1], Floods are events where river flow overflows as a result of water that is above its storage capacity so that it overflows and forms puddles on the plains or lower surrounding areas. Floods occur due to rising water levels due to rainfall exceeding its normal limits, changing temperatures, dams or embankments breaking, fast melting of snow, or obstructed water flow in other places [2]. Besides that, the causes of flooding are also due to other factors such as the condition of the rain catchment area, the duration of rain entities, and the land cover of certain areas. Broadly speaking, flooding occurs due to the contribution of the physical conditions of certain areas, including land topography which is more sloping compared to other land areas. Another cause was put forward by [3] that one of the reasons for flooding was the siltation of the canal due to garbage and sedimentation. In addition, changes in land use are also related to a decrease in the ability of the soil to absorb water, so it also has an impact on increasing runoff to the surface. Sedimentation/siltation at the mouth of the river is also one of the causes of flooding.

Drainage has the meaning of draining, draining, removing, or diverting water. In general, drainage has a definition, namely a series of water structures with the function of reducing or removing excess water from a certain area or land, so that the land can function properly and optimally. Drainage also means an attempt to control

the quality of groundwater salinity [4]

The existence of drainage becomes very important in life. Drainage has the function of reducing the amount of excess water in certain areas so that the area or land can function optimally, controlling soil erosion, and damage to buildings and roads, controlling water to the surface to improve flood areas, and controlling excess rainwater so that no flood disaster occurs. However, the reality on the ground is that several drainages have failed to function so water that cannot be accommodated by the drainage itself causes overflow to inundate residential areas and roads [5]. Various factors are the cause of the failure of the drainage function, such as landfills, silt or sediment deposits, urban growth, industrial development, and others. When the drainage is no longer able to accommodate discharge when it floods, it can be said that the drainage has a problem. Drainage failure causes flooding which greatly affects human activities [6].

Badung Regency is located at 08º14'01" - 08º50'52" South Latitude and 115º05'03" -115º26'51" East Longitude, has several areas that are prone to flooding and inundation, especially in Kuta District which has an area of 17.52 km^2. One of the causes of flooding in Kuta District is the condition of Tukad Mati whose watershed passes through most of the Kuta District area. In January 2018, Jl. However, in observations made in 2020-2021 during the rainy season between December-January, based on a field survey the depth of inundation on Kunti II Street during the rainy season is approximately 20-30 cm or an adult's calf with an inundation duration of 2-3 hours. This stagnant water occurs because the flow of water from the sewer is blocked from flowing into Tukad Mati.

The lack of arrangement in the Tukad Mati sub-drainage greatly affects runoff in the surrounding area as happened on Kunti II Street. In addition, the elevation of the tertiary channel with the Tukad Mati sub-drainage is very small. As well as Kunti II Street which was flooded, it is a basin area, so when the intensity of rainfall is high enough, runoff will occur on the road. As well as the lack of public awareness in maintaining cleanliness also had a major impact on the inundation that occurred on Kunti II Street. In addition, even though there have been countermeasures from the government by increasing the capacity and quality of drainage downstream of the Tukad Mati sub-system drainage channel, inundation still occurs on Kunti II Street.

This study aims to evaluate the extent to which the ability of the existing drainage sections on Kunti II Street, the sewer and Tukad Mati to cope with annual flooding and to calculate the dimensions of the drainage containers on Kunti II Street, the sewer, and Tukad Mati so that they can accommodate the planned flood discharge so that it can provide solutions/input to overcome the flood and can be used as a reference in planning drainage channels.

2. METHODS

The research method carried out uses a quantitative method or the method used in the description of the actual phenomenon according to the conditions in the field with the stages of data collection, data analysis, and interpretation of the results of the analysis [7]. In addition, to test the power consistency using the RAPS (Rescaled Adjusted Partial Sums) method. For distribution using Log Person Type III. Frequency distribution testing uses the Smirnov-Kolmogorov Test and Chi-Square. For analysis of rainfall intensity using the Mononobe formula. Calculation of the planned flood discharge or Q using the Rational method, the Nakayasu method, and evaluation of the total capacity of the existing canal with its theoretical discharge control lies in the return periods of 2, 5, 20, and 25 years with the existing canal capacity.

3. RESULTS AND DISCUSSION

In determining the amount of planned flood discharge, what must be done first is to analyze data from rainfall obtained from the nearest station around Seminyak. These stations are Sanglah Station and Ngurah Rai Station. Rainfall analysis data is a daily maximum span of 19 years, namely from 2001 to 2019 which was obtained through the Meteorology, Climatology and Geophysics Center for Region III Denpasar. Considering that the number of rain stations is limited to the scope of the study, the calculation of the average rainfall for the area is carried out using the Algebraic average method. This method is carried out using measurements at several stations at the same time and can only be used if the rainfall occurs in a homogeneous watershed and the yearly variation is not large enough. In calculating the average maximum daily rainfall, a total of 2468.35 mm was obtained.

In addition, a test was carried out on the consistency of rain data using RAPS (Rescaled Adjusted Partial Sums) which was applied to the calculated results at Sanglah Station and Ngurah Rai Station. The results of calculations at the Sanglah station are that the Q/√n value is smaller than the critical Q/√n value with a significant level of 90% (0.40 <1.10) and the R/√n value is smaller than the critical R/√n value (0.85 < 1.34) and the results of calculations at Ngurah Rai Station, namely the Q/√n value is smaller than the critical Q/√n value with a significant level of 90% (0.40 <1.10) and the R/√n value smaller than the critical R/√n value (0.99 < 1.34). Based on these calculations, the data shows that it is consistent.

Next, the selection of the frequency distribution is carried out based on the results of calculating the sloping coefficient (Cs) and peaking coefficient (Ck). Based on the selection conditions for the appropriate type

of distribution or frequency distribution, where (Cs) = 0.53 and (Ck) = 5.50, so that no distribution complies with the applicable frequency distribution requirements, the conclusion uses the Log Person Type III method. Use of the Log Person Type III method to analyze planned rainfall by taking 2,5,10,25 return period. The calculation results are described according to the following table:

Table 1. Calculation Results of Log Person Type III

T (Return Period)	Frequency (K)	Log Xt	X design rain (mm/day)	Rounding off
2	0.000	2.099	125.621	126
5	0.842	2.196	157.215	157
10	1.270	2.246	176.206	176
25	1.751	2.302	200.300	200

To prove whether the results calculated using the Log Person Type III method can be used or not, a test must be carried out with the Smirnov – Kolmogorov test which shows that the distribution distribution using the Log Person Type III method is acceptable or not. This can be proven by the magnitude of the value greater than (0.3075 > 0.29) which has a degree of confidence of 5%.

In addition, in determining the equation for the probability distribution it has been chosen so that it can represent a statistical distribution for the analysis of sample data. The formula used is the formula cited by [8] in his book. The results of testing the value of the Log Person Type III distribution using Chi-Square can be described in Table 2 below.

Table 2. Testing the value of Log Person Type III distribution using Chi-Square

Probability	Expected Frequency	*Observed Frequency*	(Ef-Of)	$(Ef-Of)^2$
P≤1.99	3,8	2	1,8	3,24
1.99<P≤2.07	3.8	4	-0.2	0.04
2.07<P≤2.15	3.8	2	1.8	3.24
2.15<P≤2.23	3.8	8	-4.2	17.64
2.23<P≤2.311	3.8	3	0.8	0.64
Total	19	19		24.8

Based on the results of the tabulation above, the calculated X^2 is 24.8 / 19 = 1.305 with X^2hit < X^2cr (1.305 < 5.991) meaning that the distribution using Log Person Type III is acceptable. After the tabulation results are obtained, a rainfall analysis is determined with the results of the design rain calculations at various return periods as shown in table 3 below.

Table 3. Design Rain for Various Return Periods

No	Return Period (T)	Rain Plan (mm)
1	2	126
2	5	157
3	10	176
4	15	200

The calculation of rainfall intensity uses the mononobe formula proposed by Ishiguro [9] with the following calculation results:

Table 4. Calculation of Rainfall Intensity (mononobe)

	R24			
t	R2	R5	R10	R25
(hour)	75.373	94.329	105.724	120.180
1	44.078	55.164	61.828	70.282
2	11.457	14.338	16.070	18.268
3	8.037	10.058	11.273	12.814
4	6.398	8.007	8.974	10.201
5	5.403	6.762	7.579	8.615
6	4.723	5.911	6.624	7.530
7	4.223	5.285	5.924	6.734
8	3.838	4.803	5.383	6.119
9	3.530	4.418	4.951	5.628
10	3.277	4.101	4.597	5.225
11	3.065	3.836	4.300	4.888
12	2.885	3.610	4.047	4.600
13	2.729	3.415	3.828	4.351
14	2.592	3.244	3.636	4.133
15	2.471	3.093	3.467	3.941
16	2.364	2.958	3.316	3.769
17	2.267	2.838	3.180	3.615
18	2.180	2.728	3.058	3.476
19	2.101	2.629	2.947	3.350
20	2.028	2.538	2.845	3.234
21	1.962	2.455	2.752	3.128
22	1.900	2.378	2.666	3.030
23	1.844	2.307	2.586	2.940
24	1.791	2.241	2.512	2.856

Apart from being in table form, a curve depicting the IDF graph with various return periods 2,5,10,20 is displayed below:

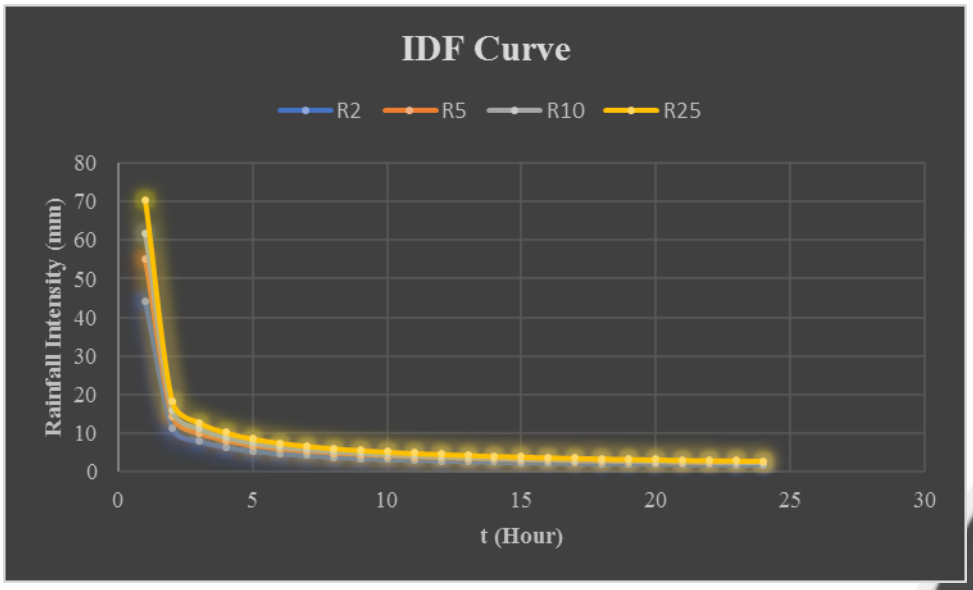

Figure 1. DF Graph with Various Return Periods

After knowing the value of the intensity of rainfall, the drainage calculation is carried out on Jalan Kunti II by determining the area of the drainage area, the length of the channel, the difference in height, and the slope of the channel is calculated according to the conditions in the field. Based on the existing conditions of the drainage canal on Jalan Kunti II Seminyak, the method used in estimating concentration time is the formula from Kirpich [10]. This formula is used because there is no watershed above the surface of the land that enters the end of the Jalan Kunti II drainage canal.

$$tc = \left(\frac{0.87 x L^2}{1000 x S} \right)^{0.385} \quad (1)$$

Information :
tc = concentration time (hours)
L = length of main channel from upstream to channel (m)
S = Average main channel slope (%)

The capacity of the existing canal is calculated based on the dimensions of the existing canal obtained from field survey results by dividing the canal into field segments with the channel code SKT, SKB where the canal is used to mark the canal on Jalan Kunti. Then proceed with calculating the discharge (Q) of the sewer (sub-drainage of Tukad Mati), and the discharge (Q) of Tukad Mati. For these drainage channels use a return period of 5 and 10 years, while the Tukad Mati sub-drainage uses a return period of 5 and 10 years, and the Tukad Mati channel uses a return period of 10 and 20 years. Here the author describes in tabular form contained in the table below:

Table 5. Existing Channel Dimensions

Channel Code	B	H	A
SKT	0.7	0.8	0.56
SKB	0.7	0.9	9.63

Table 6. Calculation of Channel Length, Channel Slope, Time of Concentration, and Rain Intensity Return Period 5 Years

Channel Code	L (m)	S	Tc (Hour)	I (5 years)
SKT	166	0.00060	0.984	55.057
SKB	176	0.00057	1.052	52.630

Table 7. Calculation of Channel Length, Channel Slope, Time of Concentration, and Rain Intensity Return Period of 10 Years

Channel Code	L (m)	S	Tc (Hour)	I (10 years)
SKT	166	0.000602	0.984	70.277
SKB	176	0.0005681	1.052	67.179

In addition, calculations are made on the design flood discharge (Q) using the Rational Method. For a watershed consisting of the same land use, the value of C (coefficient of runoff) is chosen to be 0.8. This means that 80% of rain runoff enters the drainage canal and only 20% seeps into the ground. In other words, most types of ground cover use concrete and asphalt pavements. The description, the author presents in table form is as follows:

Table 8. Calculation of Theoretical Water Discharge Return Period 5 Years

Channel Code	I (5 years)	A (km^2)	C	Qt 5 years (m^3/s)
SKT	55.057	0.0027	0.8	0.033
SKB	52.630	0.0181	0.8	0.212

Table 9. Calculation of Theoretical Water Discharge Return Period 10 Years

Channel Code	I (5 years)	A (km^2)	C	Qt 10 years (m^3/s)
SKT	70.277	0.0027	0.8	0.042
SKB	67.179	0.018098	0.8	0.040

The capacity of the existing canal is calculated based on the dimensions of the existing canal obtained from field survey results, by dividing the canal into field segments with the channel code SKT, SKB where the canal is to mark the canal on Jalan Kunti. Where the existing Q of SKT and SKB is 0.421 m^3/sec and 0.461 m^3/sec which is greater than the Q of 5-year and 10-year plan floods (OK). The results of the largest design flood Q analysis in the sewer channel with the Nakayasu method are at t = 3.131 and Q25 Year is 242.33 m^3/second. The

results of the design flood analysis in the sewer channel using the Nakayasu method obtained results with Q2 Years = 151.98 m^3/sec, Q5 Years = 190.20 m^3/sec, Q10 Years = 256.08 m^3/sec and Q25 Years = 242.33 m^3/sec. The results of the Planned Flood Discharge in the sewer with the Nakayasu Method are described more clearly in the following table:

Table 10. Planned Flood Discharge of the Nakayasu Method

Return Period	Water Discharge Plan (m^3/s)
T = 2 years	151.98
T = 5 years	190.20
T = 10 years	209.03
T = 25 years	242.33

In analyzing flood control, the planned flood discharge in the sewer to deal with T = 25-year floods is the planned flood discharge calculated using the Nakayasu method of 242.33 m^3/s. So the discharge capacity (Q) that can be flowed by the studied exhaust channel is 200.598 m^3/second < 242.33 m^2/second from Q25 Years (NOT OK).

Distinguish between river floods and floods in drainage channels in flood analysis. For floods in the drainage canal, the analysis process uses the ratio formula, while for floods in the river use the Nakayasu unit hydrograph analysis. The results of the largest design flood Q analysis in Tukad Mati with the Nakayasu method are at t = 3 and Q25 Year is 314.49 m^3/second. The results of the design flood analysis in the Tukad Mati Nakayasu Method obtained results with Q2 Years = 197.24 m^3/second, Q5 Years = 246.84 m^3/second, Q10 Years = 276.66 m3/second and Q25 Years = 314.49 m^3 /second.

The analysis for controlling the Tukad Mati flood uses the planned flood discharge to overcome the T = 25-year flood using the Nakayasu method of 314.49 m^3/s. The complete results are listed in table 10 below:

Table 11. Planned Flood Discharge of the Nakayasu Method

Return Period	Water Discharge Plan (m^3/s)
T = 2 years	197.24
T = 5 years	246.84
T = 10 years	276.66
T = 25 years	314.49

So the discharge capacity (Q) that can be flowed by the Tukad Mati canal under study is 675.825 m^3/second > 314.49 m^3/second from Q25 Years (OK).

4. CONCLUSION

Based on the results of the discussion above, it is concluded that:

1. The results of the analysis show that the drainage channel on Jalan Kunti II with a theoretical discharge with a return period has fulfilled the flood discharge requirements for the planned return period of 10 years where the drainage capacity on Jalan Kunti is SKT 0.412 m^3/s & SKB 0.461 m^3/s, drainage ditches with a capacity 200.598 m^3/sec to Tukad Mati has not been able to accommodate the planned flood discharge for the 25 year return period of 242.33 m^3/sec. In the Tukad Mati channel for the existing Q 675.825 m^3/sec, it has been able to accommodate the flood discharge Q for the 25th year return period of 314.49 m^3/sec.
2. On the drainage on Jalan Kunti II, Tukad Mati. Theoretical discharge with a return period is sufficient. In the Sewer Channel, the existing cross-sectional capacity is not sufficient for the Q plan. The solution that can be implemented is the need to increase flood control in the upstream part of the Tukad Mati watershed. As well as the need for public awareness in maintaining cleanliness is expected to overcome flooding on Jalan Kunti II.

5. REFERENCES

[1] I. P. N. Hartawiguna, I. K. Soriarta, and I. M. Sudarma, "Analisis Banjir Wilayah, Desa Baktiseraga Kecamatan Buleleng dan Desa Sambangan Kecamatan Sukasada, Kabupaten Buleleng," *J. Tek. Gradien*, vol. 12, no. 2, pp. 25–39, 2020.
[2] L. Sebastian, "Pendekatan pencegahan dan penanggulangan banjir," 2008.
[3] I. G. N. O. Suputra, I. N. Norken, and I. G. A. A. Putera, "Identifikasi Risiko pada Pelaksanaan Pembangunan Denpasar Sewerage Development Project (DSDP) di Denpasar," *J. Ilm. Tek. Sipil Vol*, vol. 9, no. 02, 2005.

[4] Suripin, *Sistem Drainase Perkotaan Yang Berkelanjutan*. Yogyakarta: ANDI OFFSET, 2004.
[5] P. E. Sanggor, J. E. Waani, and L. G. J. Lalamentik, "Studi Pengaruh Beban Gandar Dan Drainase Terhadap Indeks Kondisi Perkerasan Jalan Pada Ruas Jalan Manado-Amurang," *TEKNO*, vol. 16, no. 70, 2018.
[6] Y. Andika, I. T. Saputro, and Y. F. Bonai, "TINJAUAN DIMENSI SALURAN DRAINASE PADA RUAS JALAN FRANS KAISEPO KOTA SORONG," *J. Karkasa*, vol. 4, no. 2, pp. 76–83, 2018.
[7] P. D. Sugiyono, *metode penelitian kuantitatif, kualitatif,dan R&D*. 2016.
[8] Bambang Triatmodjo, *Hidrologi Terapan*. Yogyakarta: Beta Offset Yogyakarta, 2013.
[9] S. Asbintari, "Komparasi Metode Formulasi Intensitas Hujan Di Kawasan Hulu Daerah Aliran Sungai (DAS) Batang Lubuh Kota Pasir Pengaraian." Universitas Pasir Pengaraian, 2016.
[10] D. Listyarini, Y. Hidayat, and B. Tjahjono, "Mitigasi Banjir Das Citarum Hulu Berbasis Model Hec-Hms," *J. Tanah dan Lingkung.*, vol. 20, no. 1, pp. 40–48, 2018.

LOGIC
Journal of Engineering Design and Technology
Vol. 23 No.3 November 2023 ; p. 182 - 187

p-ISSN : 1412-114X
e-ISSN : 2580-5649
http://ojs2.pnb.ac.id/index.php/LOGIC

INNOVATION DESIGN THE TEXT TO BRAILLE BASED TECHNOLOGY IN COMPUTER VISION

Adi Pratama Putra [1)], Muhamad Khoirul Anam [1)], Muhammad Zainal Roisul Amin [2)], Rezki Nalandari [2)], Adi Mulyadi [2)], Harwanti Noviandari [3)]

1) Mechanical Engineering, PGRI University of Banyuwangi, Banyuwangi, Indonesia
2) Electrical Engineering, PGRI University of Banyuwangi, Banyuwangi, Indonesia
3) Counseling Guidance, PGRI University of Banyuwangi, Banyuwangi, Indonesia

Correponding email [1)]: tama.adie@yahoo.com

Abstract. This paper discusses the design of assistive technological innovations for writing text on books onto braille boards and computer vision-based sound. So far, programs for converting writing into braille are still very difficult to find, changing from written form to sound. The design for the development of assistive technology that will be produced refers to an analysis of the current needs for blind students, where these students can only read Braille, not Latin. Broadly speaking, this research is image processing of Latin letters with board braille output and sound using a camera scanner with an algorithm processing on the Raspberry Pi system, so that scripts with Latin characters can be enjoyed by the blind. The result of the testing method in this program is to use a trial and errors system method with debugging that focuses on image processing, one of the reasons for this focus is because the image source has a big influence on the physical environment around the image source area.

Keywords : Blind Student, Braille, Raspberry Pi, Computer Vision, Image Processing

1. INTRODUCTION

Having a physical condition with a disability is not what every individual wants because they have to live life with physical limitations, so that it can hinder some of the activities that must be carried out like individuals in normal conditions. According to Law no. 4/1997 concerning Persons with Disabilities, Article 1 states that persons with disabilities are any person who has physical and/or mental disabilities, which may interfere with or constitute an obstacle for him to carry out activities properly, consisting of persons with physical disabilities, persons with mental disabilities, and persons with disabilities. physical and mental disabilities [1],[2],[3]. The types of disabilities can be divided into seven types, namely blind, deaf, speech impaired, physically impaired, moderately impaired, mentally impaired, and double impaired. [4]. Persons with physical disabilities, one of which is the blind, blindness is a person's loss of sight or the function of his sight that disappears even though he is still able to see light rays or unable to see completely [5],[6],[7]. According to the Indonesian Association of the Blind (IAB) / PATUNI in Indonesian language, the blind are those who are unable to see completely until those who are able to see the rest of their sight, but they are unable to use that vision to read writing with a size of 12 points with normal light even though they have been assisted by using glasses. [8],[9].

Blind people are individuals who do not function perfectly in their sense of sight (both) as channels for receiving information in daily activities, just like sighted people [10]. Even so, the blind only experience visual impairment. The intelligence of blind children is not disturbed. Blind people are just like any other normal child. It's just that they experience differences in receiving information and in their perception that there are special schools, especially schools for blind children, in lower grades they will be given material to recognize the Braille alphabet. Braille letters, embossed letters created by Louis Braille [11]. Braille letters are formed from a combination of six dots that form alert letter symbols so that they can be read by the blind [12]. Braille letters

consist of two rows of three dots, Louis [13]. So that the braille letters are arranged based on six raised dots with dot positions 1, 2, 3 (vertical), 1, 4 (horizontally), 4, 5, 6 (vertical). So that the pattern forms like a domino and the dots are named 1, 2, 3, 4, 5, and 6. In mastering braille, there are several things that must be considered, including: Understanding the location of the dots, Sensitivity to touch, understanding the position of the lines.

This ability is difficult to know. For this reason, special media are needed for learning so that they can meet the needs of teaching and learning in schools. Writing and printing system (based on the Latin alphabet) for the blind in the form of a code consisting of six dots of various combinations highlighted on paper so that they can be touched, Tumirah [14]. In mastering braille, there are several things that must be considered, including: understanding the position of the point, tactile sensitivity, understanding of 2 line positions. This ability is difficult to know. For this reason, special media are needed for learning so that they can meet the needs of teaching and learning in schools [15]. From observations that have been made in special schools and on campuses that have blind students, currently the technology for converting Latin writing from books to braille is not much of a technology that underlies it, that's why we want students with special needs, especially blind people, to be able to read all of the writing the one in the Latin book that will be converted to a braille board, the board will display up and down the braille code according to what is in the book using the camera and converted to raspberry pi with image recognition. It is hoped that with this technology blind students will have no more obstacles to reading Latin textbooks.

2. METHODS

The method applied in this study is the process design of the application of assistive text to braille technology with image processing input on the camera, the camera results are processed into braille and sound with a Raspberry Pi to send data up and down braille using a push pull solenoid. Computer Vision processes data in the form of text fed back to the domain via the internet network to correct words that are inappropriate or illegible on the camera.

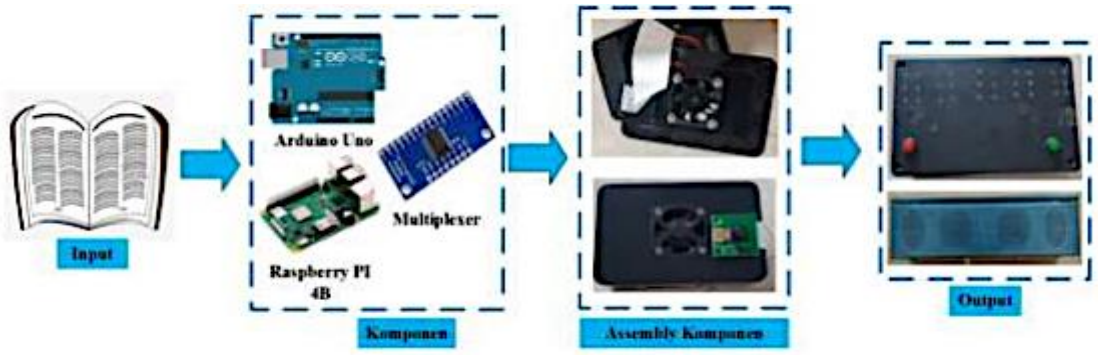

Figure 1. Process Design for Implementing Text to Braille

2.1 Development Plan of the Text to Braille Technology

The text to braille development plan that will be produced refers to the analysis of current needs for blind students, where these students can only read braille but not Latin writing, therefore this research designed an application system for identifying Latin letters using computer vision. The Latin letter conversion system uses the Artificial Neural Network (ANN) method. Broadly speaking, this research is image processing of Latin letters with board braille output and sound using a camera scanner processed on the Raspberry Pi system, so that scripts with Latin character characters can be enjoyed by the blind.

This system was built using an 8MP (Megapixel) resolution camera as a source for capturing text images on objects with the Raspberry Pi Microcomputer as an image processor, image processing on this tool was built using the OpenCv open source library and several other open source libraries as support. The conversion from image to text which is still in the form of const char* data is then fed to Arduino Uno using USART (Universal Synchronous Asynchronous Receiver Transmitter) communication which is then converted into a binary value which is used to drive the selenoid actuator according to the received binary value.

3. RESULTS AND DISCUSSION

3.1 Figure And Desain

Images and designs of text to braille can be seen as follows.

1. The name of Technology Innovation

The product name of the assistive device for students with special needs with visual impairments is image processing-based text to braille assistive technology for the blind.

Figure 2. Display Braille Design

2. Text to Braille Product Specifications

It has a camera with 8MP Raspberry Pi resolution which allows it to be used to read text on paper very quickly. The braille field is built using a mini selenoid which allows the system to switch from 1 braille text to another braille text quickly. For processing the system uses the Raspberry Pi 4B, which is a very fast processing system.

Figure 3. Text To Braille Component

Raspberry Pi 4b Rear View

Raspberry Pi 4b Front View
And 8MP Camera

Figure 4. Assembly Text to Braille

3. Program Flow

In this program, a text to braille assistive technology system for students with special needs based on image processing was built using the Open Cv open source library and several other open source libraries for modeling and implementing analog image processing algorithms into digital form. The source of image capture in this program uses an OV model camera with a 5MP resolution. Arduino Uno acts as a receiver of const char* data from the Raspberry Pi microcomputer and converts text data into binary form using USART (Universal Synchronous Asynchronous Receiver Transmitter) communication to trigger the work of the selenoid actuator drive found on the braille board assisted by a digital multiplexer with 16-bit resolution.

In general, the hardware design and system flowchart can be seen in the following figure:

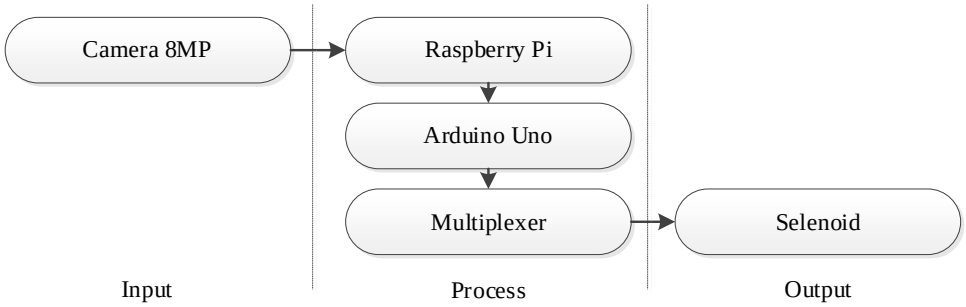

Figure 5. Hardware Block Diagram

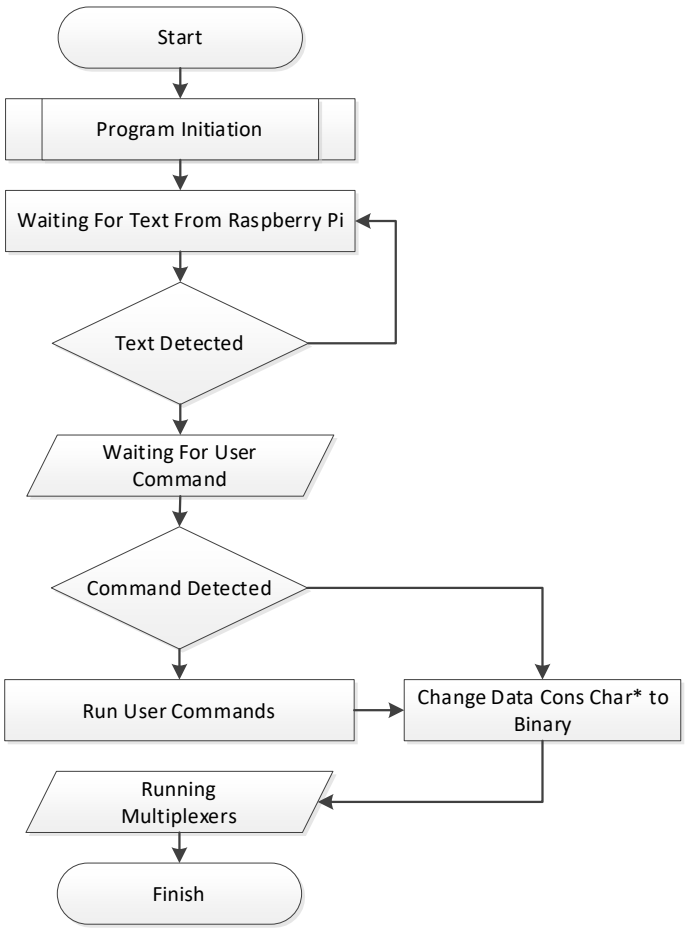

Figure 6. Flowchart *Raspberry Pi*

3.2. Results of Application of Assistive Technology Innovations

For the results of the application of text to braille assistive technology innovation for the blind, it has been tested and is running well and is able to convert text to braille, although there are still problems that not all text can be read, some tests still have to change the position of the textbook that will be converted to the blackboard. braille.

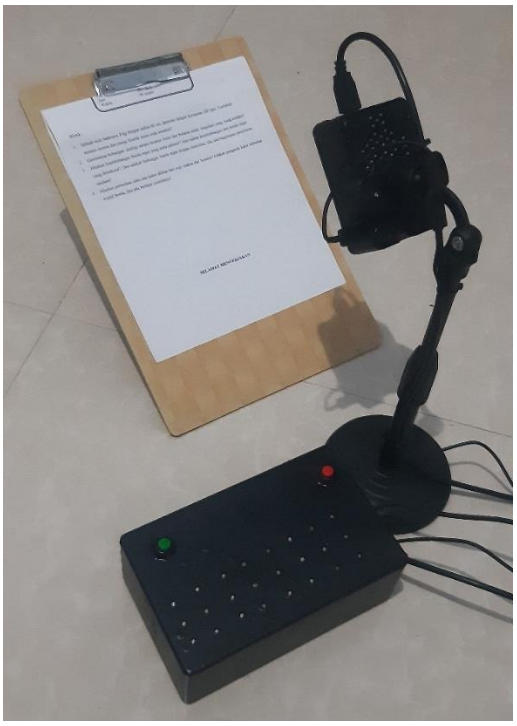

Figure 7. Created Products

4. CONCLUSION

The result of the testing method in this program is to use a trial and errors system method with debugging that focuses on image processing, one of the reasons for this focus is because the image source has a big influence on the physical environment around the image source area. The system testing process in this program uses an analog source in the form of text printed on paper in a horizontal position using external lighting from the camera and shows an error rate of 70%. The results of the design of a prototype tool for reading text books onto a braille board can provide opportunities for the blind to actualize their potential according to the abilities and differences that exist in each person.

5. ACKNOWLEDGEMENT

We express our deepest gratitude to the Directorate of Learning and Student Affairs, Directorate General of Higher Education, Ministry of Education, Culture, Research and Technology in 2022 which has provided Technology Assistance Funds for Learning in Higher Education. The Chancellor and Chair of LPPM and all parties who have assisted in this research.

6. REFERENCES

[1] S. Millati, “Social-Relational Model Dalam Undang-Undang Penyandang Disabilitas,” *INKLUSI J. Disabil. Stud.*, vol. 3, no. 2, pp. 285–304, 2016, doi: 10.14421/ijds.030207.

[2] B. Penelitian, S. Kesehatan, and A. Paramita, “Mental Health Services Disability and Life Style of Indonesian Analisis Pola dan Faktor Lama Ppemberian Air Susu Ibu (ASI) Tahun 2013 View project Yurika Wardhani,” 2016, doi: 10.22435/hsr.v19i1.4994.99-107.

[3] A. Maftuhin *et al.*, “Aksesibilitas Ibadah bagi Difabel: Studi atas Empat Masjid di Yogyakarta,” *INKLUSI*, vol. 1, no. 2, pp. 249–268, Dec. 2014, doi: 10.14421/IJDS.010207.

[4] E. S. Sari, “Implementasi pembelajaran pendidikan agama islam bagi anak berkebutuhan khusus: studi kasus di Sekolah Luar Biasa (SLB) Negeri Kota Mataram,” Jan. 2023.

[5] S. Mambela, “Tinjauan Umum Masalah Psikologis Dan Masalah Sosial Individu Penyandang Tunanetra,” *Buana Pendidik. J. Fak. Kegur. dan Ilmu Pendidik. Unipa Surabaya*, vol. 14, no. 25, pp. 65–73, Mar. 2018,

doi: 10.36456/bp.vol14.no25.a1465.

[6] O. : Intan and M. Mir, "Resiliensi Mahasiswa Tunanetra (Studi Kasus Terhadap Mahasiswa Tunanetra Tidak Dari Lahir Di Fakultas Ilmu Pendidikan Universitas Negeri Yogyakarta)," *J. Ris. Mhs. Bimbing. Dan Konseling*, vol. 3, no. 3, pp. 309–325, Mar. 2017, Accessed: May 09, 2023. [Online]. Available: https://journal.student.uny.ac.id/index.php/fipbk/article/view/6553

[7] 152020073 Muhamad Gumeular, "Hubungan Antara Persepsi Penyandang Disabilitas Netra Tentang Program Resosialisasi Dengan Kemandirian Di Balai Rehabilitasi Sosial Penyandang Disabilitas Sensorik Netra (Brspdsn) Wyata Guna Bandung," Oct. 2019.

[8] M. Braille Kesehatan Reproduksi Remaja Tunanetra and C. Author, "Pengembangan Modul Braille Pendidikan Kesehatan Reproduksi Bagi Remaja Tunanetra," *Al-Ittizaan J. Bimbing. Konseling Islam*, vol. 3, no. 2, pp. 49–55, Oct. 2020, doi: 10.24014/ITTIZAAN.V3I2.12109.

[9] M. Rachmawati, "Interaksi Sosial Tunanetra Dalam Proses Adaptasi Di Tengah Masyarakat (Studi Kasus : Balai Rehabilitas Sosial Penyandang Disabilitas Sensorik Netra Tan Miyat, Bekasi)," Jul. 2021, Accessed: May 09, 2023. [Online]. Available: https://repository.uinjkt.ac.id/dspace/handle/123456789/58088

[10] H. Sundari and R. Aulia, "Apakah Penyandang Tunanetra Bisa Berbahagia? Gambaran Kebahagiaan Pada Penyandang Tunanetra," *Al-Qalb J. Psikol. Islam*, vol. 10, no. 1, pp. 42–51, Oct. 2019, doi: 10.15548/ALQALB.V10I1.827.

[11] E. Harista IAIN Syaikh Abdurrahman Siddik Bangka Belitung Jalan Raya Mentok Km, D. Petaling, M. Barat, and B. Kepulauan Bangka Belitung, "Penggunaan Media Pembelajaran Bahasa Indonesia Untuk Anak Berkebutuhan Khusus Di Sekolah Menengah Pertama Luar Biasa (Smplb) Negeri Sepulau Bangka (Using Media in Learning Indonesian Subject for Children with Special Needs at SMPLB in Bangka Regency)," *Sirok Bastra*, vol. 9, no. 1, pp. 1–14, Aug. 2021, doi: 10.37671/SB.V9I1.271.

[12] M. I. Fauzi, "Model tablig mubalig tunanetra : Studi kasus pada kegiatan tablig Ustaz Sumardi," Jun. 2021.

[13] S. Pebriandi, "Penggunaan Al-Qur'an Braille Digital Oleh Jamaah Tunanetra Di Yayasan Raudlatul Makfufin Serpong," Jul. 2021, Accessed: May 09, 2023. [Online]. Available: https://repository.uinjkt.ac.id/dspace/handle/123456789/57149

[14] M. K. Dzunurain[1] and J. Wasisto, "Pemanfaatan Koleksi Buku Braille Sebagai Sumber Informasi Siswa Penyandang Tunanetra di Sekolah Luar Biasa Bagian A Negeri Semarang," *Anuva J. Kaji. Budaya, Perpustakaan, dan Inf.*, vol. 6, no. 1, pp. 57–68, Apr. 2022, doi: 10.14710/ANUVA.6.1.57-68.

[15] F. Inayahtur Rahma Sekolah Tinggi Agama Islam Pancawahana Bangil, "Media Pembelajaran (kajian terhadap Langkah-langkah Pemilihan Media dan Implementasinya dalam Pembelajaran bagi Anak Sekolah Dasar):," *Pancawahana J. Stud. Islam*, vol. 14, no. 2, pp. 87–99, 2019, Accessed: May 09, 2023. [Online]. Available: http://ejournal.kopertais4.or.id/tapalkuda/index.php/pwahana/article/view/3608

LOGIC
Journal of Engineering Design and Technology
Vol. 23 No.3 November 2023 ; p. 188 - 193

p-ISSN : 1412-114X
e-ISSN : 2580-5649
http://ojs2.pnb.ac.id/index.php/LOGIC

PUBLIC TRANSPORTATION LINE PASSENGER PREDICTION USING MAMDANI METHOD OF FUZZY LOGIC TO FORESEE HOLIDAY PASSENGER SURGE

Elfira Makmur [1)], Dessy Ana Laila Sari [1)]

1) Departmen of Electrical Engineering Education, Universitas Negeri Makassar, Jln. Daeng Tata Raya Parangtambung, Mannuruki, Kecamatan Tamalate, Makassar, Sulawesi Selatan, Indonesia 90224

Correponding email [1)] : dessynaa@unm.ac.id

Abstract. This study aims to predict the number of passengers on the Mall Pannakkukang-Galesong Harbor route on the "Teman Bus" fast transit transportation system in Makassar City. Public transportation modes often face the problem of an imbalance between the number of buses and the number of passengers, which can reduce the comfort and efficiency of passenger mobility. To overcome this problem, this study uses a fuzzy logic approach, specifically the Mamdani fuzzy method, to predict the number of passengers who will take the bus based on input variable data that has been collected, such as day temperature and weather, as well as the output variable, namely the number of passengers. The results obtained in this study are based on the inputs given, namely the day with a value of 0.5 and the weather temperature with a value of 30. The number of passengers is 1500, which means the number of passengers is included in the quiet category.

Keywords : Fuzzy Logic, Mamdani Method, Prediction, Bus Passenger

1. INTRODUCTION

Buses are one of the most common types of public transportation that are used by many people and play an essential role in urban mobility. The Buy the Service action for “Teman Bus” was put in place by the Ministry of Transportation of the Republic of Indonesia to improve non-cash public transportation in urban regions [1]. Teman Bus is an Indonesian quick transit system that runs in several locations, including Makassar on line 1, which covers the Pannakkukang Mall route to Galesong Harbor.

The imbalance between the number of buses and the number of passengers is a common issue in mass transit modes of transportation. This also occurred on Makassar City buses covering from Pannakkukang Mall to Galesong Harbor. Passenger density is significant on specific days or under particular weather conditions. This means that "Teman Bus" customers have to decide between cramming in the bus or waiting for the next bus, which is likely to take a long time, lowering the comfort of passenger mobility. As a result, it is necessary to anticipate the number of passengers who are expected to board the bus on the Pannakkukang Mall-Galesong Harbor route so that the number of buses arriving is equal to the number of passengers.

The authors of the research "*Implementation of Mamdani fuzzy implication in predicting traffic volume and duration of green lights on an intersection*" [2] used the Mamdani fuzzy logic approach to predict the number of positive COVID-19 in Java West. The descriptive method was utilized for the research, and the data collecting method was an observation on the Pikobar website. Researchers utilized variable data in the form of rises of ODP, PDP, and positive for COVID-19, with three predetermined categories for all variables, namely low, medium, and high. The output variable, on the other hand, is the result of a positive prediction 14 days later. A linear curve is employed for fuzzification needs. The MAX function was used to compile the rules, while Centroid was utilized for defuzzification.

Fuzzy logic can be utilized to predict the number of passengers. Fuzzy logic is a branch of mathematics that analyzes uncertainty. The Mamdani approach [3] is one of the fuzzy system principles utilized in the procedure of predicting the number of bus passengers. The Mamdani fuzzy technique is based on a mathematical idea that allows for very flexible fuzzy reasoning while also supporting imperfect data. Based on the computed research

results, the Mamdani fuzzy approach has a lower error rate compared to other fuzzy methods [4]. Mamdani's fuzzy logic implementation is expected to provide a more accurate prediction of the number of passengers based on relevant input variables like the time of day and conditions temperature, as well as the output variable, namely the quantity of passengers, so that "Teman Bus" companies can be more alert when there is a surge in passengers.

2. METHODS

A quantitative method is implemented in this research. Data collecting, creating fuzzy sets, implication function application, assertion (defuzzy), and deriving conclusions are the stages used in this research. **Figure 1** illustrates this issue.

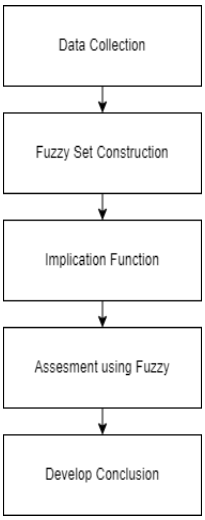

Figure 1. Research Process

This study's data collecting stage relied on primary data gathered through interviews and direct surveys of passengers and transportation system operators. Other data is secondary data, which contains historical data and records provided by PT Borlindo Mandiri Jaya in the form of number of passengers, what day, and the weather in March 2023. Table 1 shows the data.

Table 1. Bus Passenger Dataset in March

Date	Day (work day/holiday)	Temperature (celcius)	Number of Passengers (n)
01/03/2023	1	27	2019
02/03/2023	1	29	2117
03/03/2023	1	30	2071
04/03/2023	1	30	1936
05/03/2023	0	29	1600
06/03/2023	1	28	1997
07/03/2023	1	29	2079
08/03/2023	1	31	1965
09/03/2023	1	31	2246
		…..	
		…..	
31/03/2023	1	30	1684

Following the collection of data, the prediction process begins, which in this case utilizes the fuzzy logic of the Mamdani method. Fuzzy logic is logic with a fuzziness value between true and false [5]. A fuzzy system is a system that is constructed on clear definitions, functioning procedures, and descriptions that are based on fuzzy logic. The Fuzzy Inference System (FIS) employs fuzzy logic to map the input space into the output space using the IF_THEN rule[15][16]. FIS is based on linguistic concepts and employs fuzzy algorithms to provide a mathematically studied method. In this case, the fuzzy logic used is Mamdani fuzzy logic. Ebrahim Mamdani developed the Mamdani method as the MAX-MIN method in 1975. The steps of fuzzy mamdani are fuzzy set construction (fuzzification), inference, and defuzzification [6], [7]. The fuzzification stage is the process of

converting numeric input into a linguistic value that the system can accept. The inference phase is concerned with the linguistic rules that are employed to generate uncertain output values. Defuzzification is the process of converting ambiguous output data into numerical values that humans comprehend [8].

The Mamdani fuzzy method has been widely used in a variety of research fields[14], including previous studies with a similar theme, specifically predicting the number of positive COVID-19 with the Mamdani fuzzy system [9], and Renaldi Primaswaraa Prasetya with the subject of determining the duration of traffic lights with the Mamdani fuzzy logic system [10]. In the case of this research, the data utilized is imprecise and ambiguous. Mamdani's fuzzy logic makes it achievable to represent uncertain human thinking using linguistic variables and fuzzy rules. Mamdani's fuzzy logic can overcome this uncertainty and deliver more accurate results by employing the concept of fuzzy membership. This indicates that Mamdani's fuzzy logic was effective in forecasting the number of passengers on the Pannakkukang Mall line to Galesong Port.

3. RESULTS AND DISCUSSION

This study utilizes input variable data, namely day and weather temperature, to forecast the number of bus passengers on the Pannakkukang Mall-Galesong Harbor using Mamdani fuzzy logic, while the output variable is the number of passengers. Table 2 shows the variables that were used.

Table 2. Input and Output Variable

Function	Variable	Environment of Topic
Input	Days	[0-1]
	Temperature	[20-40]
Output	Number of Passengers	[0-2800]

The variables that are gathered are used to create fuzzy sets. The fuzzy sets for the input variable days are divided into two categories, whereas the fuzzy sets for the input variables weather temperature and output are divided into three groups. Table 3 shows these variables and sets.

Table 3. Variable of Fuzzy Set

Variable	Fuzzy Set	Domain
Days	Holiday	[0, 0.3, 0.6]
	Working Day	[0.5, 0.8, 1]
Temperature	Low	[20, 25, 30]
	Middle	[25, 30, 35]
	High	[30, 35, 40]
Number of Passengers	Quite	[0, 0, 800, 1500]
	Normal	[800, 1500, 2200]
	Crowded	[1500, 2200, 2800, 2800]

According to **Table 3**, the fuzzy set can be represented by the variables of the day, weather temperature, and passenger number as follows:

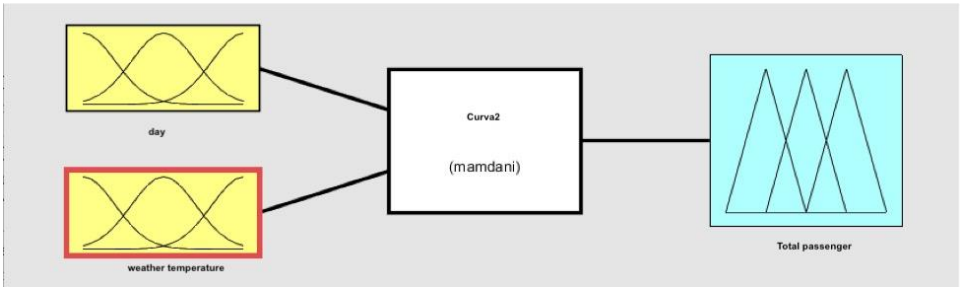

Figure 2. Membership function of Input and Output Variable

3.1 Fuzzy Sets of Inputs

In this study, the input variables were divided into two categories: days and temperature. As shown in Table 3, we separated each group into various classifications ranging from low to high. Figures 3(a) and 3(b) depict each set of input.

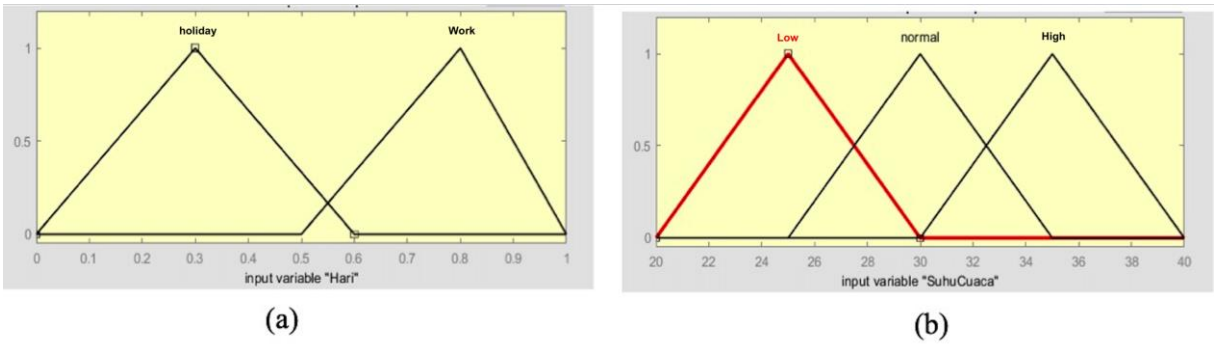

Figure 3. Fuzzy sets representation of input variables (a) Days (b) Temperature

3.2 Fuzzy Set of Output

This Fuzzy System's output is the number of passengers. Output is classified into three categories based on its prospective range, namely quiet, normal, and crowded. The output grouping is used as an indicator for the company to determine whether or not it should increase or decrease the quantity of buses operating at the time. Figure 4 displays a fuzzy set graph for the number of bus passengers.

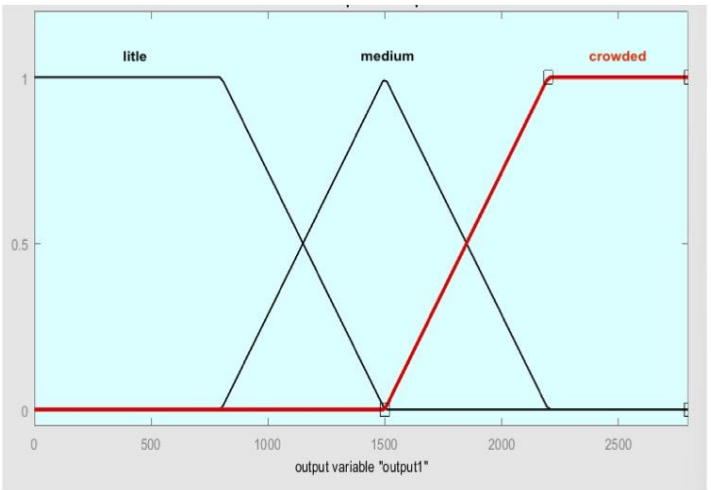

Figure 4. Fuzzy set of output variable

3.3 Fuzzy Rules

The relationship between the conditions on the input variables and the fuzzy sets on the output variables is described by fuzzy rules. Each fuzzy logic rule has an implication [11][13]. The AND operator is used for coordinating the fuzzy sets between the two input variables in the form of fuzzy rules. The IF-THEN operator, on the other hand, is used to map between fuzzy sets on input and output variables. **Figure 5** shows fuzzy rules set on the Matlab program.

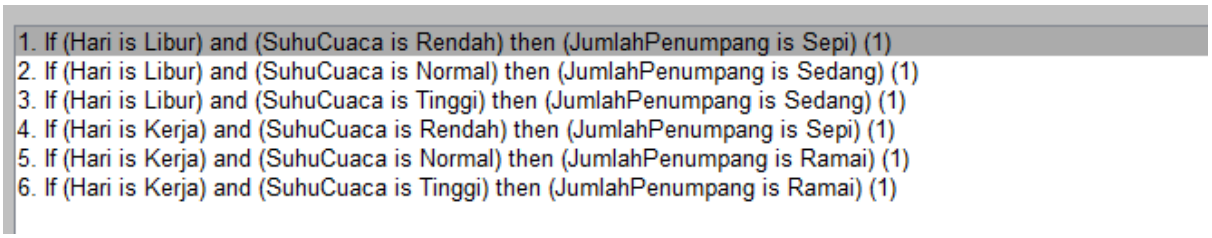

Figure 5. Fuzzy rules sets in Matlab Program

3.4 Defuzzification

The centroid (composite moment) method was utilized in this study's Mamdani fuzzy logic defuzzification method t generate cisp values by taking the center point (z*) in the fuzzy area. In general, centroid determination can be formulated by. $z^* = \frac{\int z\mu(z)dz}{\int \mu(z_j)}$

Where: (Equation 1.1)[12]

z = domain valuevalue$\mu(z)$ = membership function

z^* = defuzzification value

The fuzzy rule composition provides the input for the defuzzification process, and the resulting output is a number in the fuzzy set's domain [6].

The following is the result of using the Matlab program to test the implementation of mamdani fuzzy logic to anticipate the number of passengers on the Pannakkukang Mall - Galesong Harbor line bus. The number of passengers is 1,500 when the day value = 0.5 and the weather temperature = 30 is provided. As a result, the number of passengers is classified as quiet. PT Borlindo Mandiri Jaya was able to lower the number of bus units in operation after obtaining the "quiet" category from the output of the Mamdani fuzzy system. PT Borlindo Jaya can increase the number of bus partners who will operate if the Mamdani fuzzy system output of the number of passengers is "crowded." **Figure 6** shows the test result of the fuzzy system.

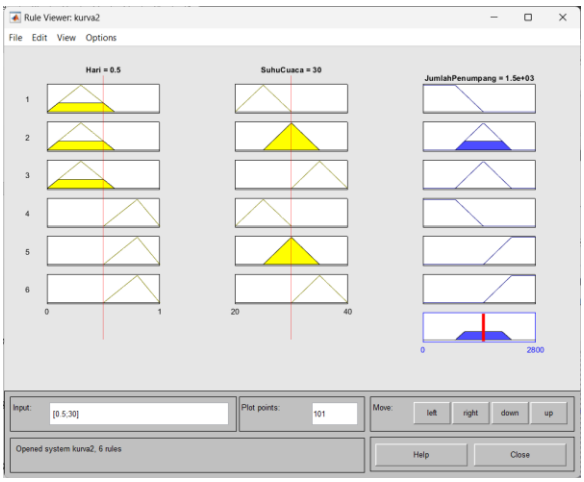

Figure 6. Fuzzy system test results

4. CONCLUSION

Based on the findings of the study, the following conclusions can be drawn:

1) The Mamdani approach can be utilized to anticipate the number of bus passengers on the Pannakkukang Mall route to Galesong Port using a fuzzy inference system (FIS).

2) Based on the input of the day value and weather temperature, the test results are 1,500, indicating that the number of passengers is low. In other words, when the "quiet" category is acquired from the Mamdani fuzzy system output, PT Borlindo Mandiri Jaya can reduce the number of bus units in operation, and vice versa.

5. ACKNOWLEDGEMENT

The authors would like to thank Makassar State University and PT Borlindo Mandiri Jaya for their assistance in conducting this study.

6. REFERENCES

[1] K. P. R. Indonesia, "TEMAN BUS Transportasi Ekonomis Mudah Andal dan Nyaman," 2020. https://temanbus.com/.
[2] E. F. Yogachi, V. M. Nasution, and G. Prakarsa, "Design and Development of Fuzzy Logic Application Mamdani Method in Predicting The Number of Covid-19 Positive Cases in West Java," IOP Conf. Ser. Mater. Sci. Eng., vol. 1115, no. 1, pp. 1–15, 2021, doi: 10.1088/1757-899x/1115/1/012031.
[3] E. F. Yogachi, V. M. Nasution, and G. Prakarsa, "Design and Development of Fuzzy Logic Application Mamdani Method in Predicting The Number of Covid-19 Positive Cases in West Java," IOP Conf. Ser. Mater. Sci. Eng., vol. 1115, no. 1, pp. 1–15, 2021, doi: 10.1088/1757-899x/1115/1/012031.
[4] S. Nurhayati, D. Supriadi, and T. H. M, "Sistem Prediksi Kebutuhan Vitamin A Menggunakan Metode Fuzzy Mamdani Vitamin A Need For Prediction System Using Mamdani Fuzzy Method," J. Manaj. Inform., vol. 13, no. 1, pp. 1–10, 2023.
[5] A. Ikhwan, M. Badri, M. Andriani, and N. Saragih, "Analisis Tingkat Kepuasan Pelanggan Menggunakan Fuzzy Mamdani (Studi Kasus: Busrain Bakery)," J. SAINTIKOM (Jurnal Sains Manaj. Inform. dan Komputer), vol. 18, no. 2, pp. 147–153, 2019, doi: 10.53513/jis.v18i2.153.
[6] D. L. Rahakbauw, F. J. Rianekuay, and Y. A. Lesnussa, "Penerapan Metode Fuzzy Mamdani Untuk Memprediksi Jumlah Produksi Karet (Studi Kasus: Data Persediaan Dan Permintaan Produksi Karet Pada Ptp Nusantara Xiv (Persero) Kebun Awaya, Teluk Elpaputih, Maluku-Indonesia)," J. Ilm. Mat. Dan Terap., vol. 16, no. 1, pp. 119–127, 2019, doi: 10.22487/2540766x.2019.v16.i1.12764
[7] O. Laia and P. Marpaung, "Penerapan Logika Fuzzy Mamdani Untuk Memprediksi Stok Persediaan Barang Proyek (Studi Kasus : Pt . Andhy Putra Medan)," JIKOMSI [Jurnal Ilmu Komput. dan Sist. Informasi], vol. 3, no. 3, pp. 48–59, 2021, [Online]. Available: http://ejournal.sisfokomtek.org/index.php/jikom/article/view/89/77.
[8] A. Burhanuddin, "Analisis Komparatif Inferensi Fuzzy Tsukamoto , mamdani dan Sugeno Terhadap Produktivitas Padi di Indonesia," LEDGER J. Inform. Inf. Technol. Anal., vol. 2, no. 1, pp. 48–57, 2023.
[9] G. Prakarsa and V. M. Nasution, "Penerapan Logika Fuzzy Menggunakan Metode Mamdani Pada Prediksi Jumlah Kasus Positif Covid-19," J. Media Inform. Budidarma, vol. 5, no. 4, p. 1660, 2021, doi: 10.30865/mib.v5i4.3282
[10] R. P. Prasetya, "Implementasi Fuzzy Mamdani Pada Lampu Lalu Lintas Secara Adaptif Untuk Meminimalkan Waktu Tunggu Pengguna Jalan," J. Mnemon., vol. 3, no. 1, pp. 24–29, 2020, doi: 10.36040/mnemonic.v3i1.2526.
[11] A. Dirgantara, A. Fauzi, and G. Ginabila, "Analysis of Air Pollution Levels in DKI Jakarta Province Using the Mamdani Fuzzy Inference System Method," J. Informatics Telecommun. Eng., vol. 4, no. 1, pp. 97–104, 2020, doi: 10.31289/jite.v4i1.3804.
[12] Román-Flores, Heriberto, Yurilev Chalco-Cano, and Juan Carlos Figueroa-García. "A note on defuzzification of type-2 fuzzy intervals." Fuzzy Sets and Systems 399, pp 133-145. 2020.
[13] Román-Flores, Heriberto, Yurilev Chalco-Cano, and Juan Carlos Figueroa-García. "A note on defuzzification of type-2 fuzzy intervals." Fuzzy Sets and Systems 399, pp. 133-145. 2021.
[14] Sridharan, M. "Application of Mamdani fuzzy inference system in predicting the thermal performance of solar distillation still." Journal of Ambient Intelligence and Humanized Computing 12, no. 11, pp. 10305-10319. 2021
[15] Chen, Yong, Feiyu Long, Wei Kuang, and Tianbao Zhang. "A method for predicting blast-induced ground vibration based on Mamdani Fuzzy Inference System." Journal of Intelligent & Fuzzy Systems Preprint, pp. 1-10. 2023
[16] Damayanti, Dela Rista, Suntoro Wicaksono, M. Faris Al Hakim, Jumanto Jumanto, Subhan Subhan, and Yahya Nur Ifriza. "Rainfall prediction in Blora regency using Mamdani's fuzzy inference system." Journal of Soft Computing Exploration 3, no. 1, pp. 62-69. 2022.

LOGIC
Journal of Engineering Design and Technology
Vol. 23 No.3 November 2023; p. 194 - 202

p-ISSN : 1412-114X
e-ISSN : 2580-5649
http://ojs2.pnb.ac.id/index.php/LOGIC

Effect of Current Strength and Flow Rate of Shielding Gas on the Impact and Tensile Strength of Gas Metal Arc Welding Result on Steel Plate Hot Rolled Coiled Materials

Radhi Nurvian Amrullah[1]* , Subagiyo[1]

1)Mechanical Engineering Department, State Polytechnic of Malang, Soekarno Hatta Street No. 09, Malang, Indonesia

Correponding email [1)] : radhinurvian.rn@gmail.com

Abstract. Gas metal arc welding **(**GMAW) is one of the welding techniques that is easy to use, especially to weld low-carbon steel. Low-carbon steel In general, low-carbon steel is widely used in the process of making frame structures, an example is a car frame. Car frames are generally made using materials that are strong, ductile, lightweight, and able to withstand impact and tensile loads when the car is used, one example of the material is steel plate hot rolled coiled (SPHC). The problem is that GMAW results are affected by welding parameters. In this study, the parameter chosen was the strong variation of the welding current and the flow rate of protective gases CO_2. The purpose of this study is to determine the strong influence of the current and flow rate of protective gases as well as the interaction on the impact and tensile strength of GMAW results on SPHC materials. This research uses an experimental method with current strength parameters of 120 A, 130 A, and 140 A, as well as variations in the flow rate of protective gases, namely 15 L/min, 20 L/min, and 25 L/min. In general, the results of the research show that the impact strength of the weld metal is lower than the raw material and the tensile strength of the weld metal is higher than the raw material. From the study, it can be seen that the optimal current strength and flow rate of protective gas is a current strength of 140 A and a flow rate of protective gas worth 25 L /minute with an impact strength of 2.91 J/mm2 and a tensile strength of 431.72 MPa.

Keywords: GMAW SPHC Material, Impact Strength, Tensile Strength.

1. INTRODUCTION

Along with the development of technology, the field of welding also develops. There are also many types of welding, including gas metal arc welding (GMAW). GMAW is one of the easy-to-use detectors, especially to weld low-carbon steels. Low-carbon steel is generally widely used in the process of making frame structures, an example is a car frame. Car frames are generally made using materials that are hard, ductile, lightweight, and can withstand impact and tensile loads when the car is used, one example of the material is steel plate hot rolled coiled (SPHC).

SPHC material is steel plate produced through a hot rolled process with commercial quality. SPHC plates are often also called black plates because these plates are blackish. SPHC in Japanese industry standards is encoded with JIS G3131 (Steel. B, 2011). SPHC material is often used as a material for making industrial workpieces that require easy maintenance and affordable prices such as making car frames. the welding process itself can be done using a variety of types of welding, one of which is GMAW.

GMAW welding is the process of welding or joining metal materials that use a heat source from electrical energy which is converted into heat energy. In the welding process, GMAW uses welding wire rolled in a roll and uses gas as a protector of the welding metal that melts during the welding process, so that the welded metal can be permanently fused [1]. Some GMAW welding parameters such as current strength and torch distance to the workpiece, influence the mechanical properties of the material such as strong and ductile properties. Strong and ductile properties of the material are very important, especially in the car frame, to ensure the connection in the

car frame remains strong when the car is used. Therefore, research is needed to analyze the nature of the material connection. From this description, the author took the initiative to make a research title entitled "The Strong Effect of Current and Flow Rate of Protective Gas on the Impact and Tensile Strength of GMAW Welding Results on SPHC Materials".

The purpose of this study is to determine the strong influence of current on the impact and tensile strength of GMAW welding results of SPHC material, the effect of protective gas flow rate on the impact and tensile strength of GMAW welding results of SPHC material, the effect of strong interaction of current and flow rate of protective gas on the impact and tensile strength of GMAW welding results of SPHC material.

2. METHODS

2.1 Research Concept Framework

This is a research concept framework, the independent variable is the current strength and flow rate of the protective gas, The controlled variable is gas the shield used is CO^2, the material is SPHC, the electrode is ER 70S-6 and the welding position is 1 G, the dependent variable is the result of the impact test and GMAW tensile allocation on the SPHC material.

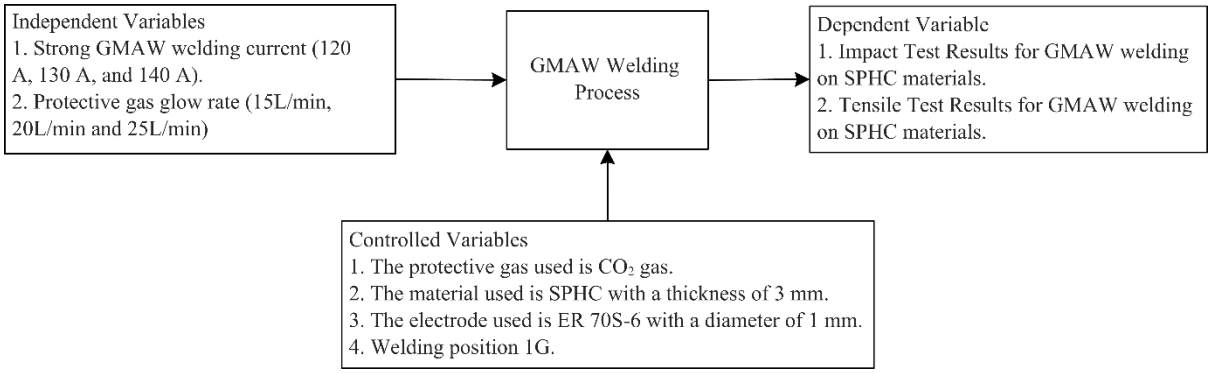

Figure 1. Research Concept Framework

2.2 Tools and Materials

Some of the tools and materials used in this research are the GMAW welding machine, CO_2 protective gas, material SPHC, hand grinding, drilling machine, and caliper.

2.3 Research Flowchart

The steps in conducting research follow the sequence of work as follows:

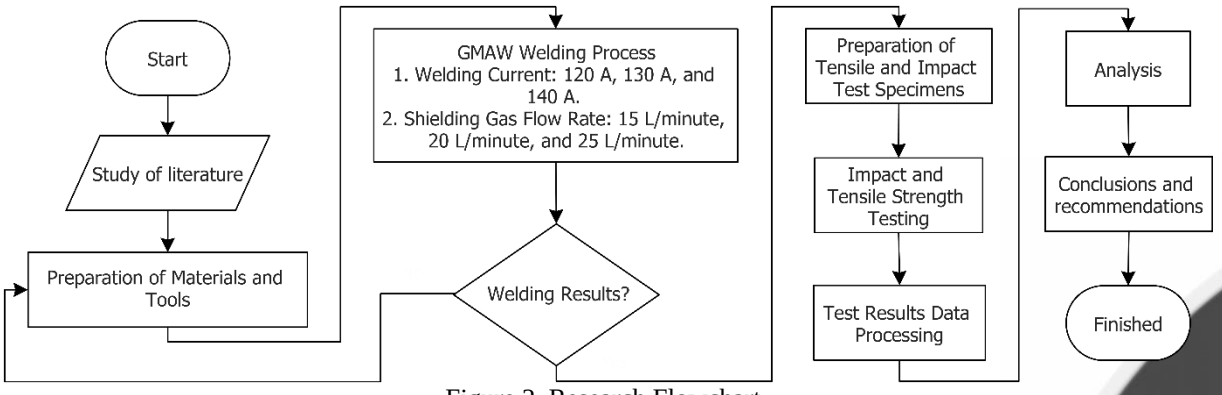

Figure 2. Research Flowchart

The welding process is carried out using strong variations of currents of 120 A, 130 A, and 140A, as well as the flow rate of protective gas used during welding of 15 L/min, 20 L/min, and 25 L/min. The manufacture of tensile test specimens is carried out using BS 709 (British *Standardtd*) standards, and charpy impact test specimens using ASTM E 23 – 02a standards. Tensile and impact strength tests are performed to determine the strength value resulting from GMAW welding using variations in the protective gas mixture and protective gas flow rate. Data processing of test results is carried out using the help of Excel and Minitab 2020 software with the DOE *Factorial* method. Then after obtaining the test data, data analysis will continue.

3. RESULTS AND DISCUSSION

3.1. Research Results

The results of the study were obtained from data collection from the GMAW welding process on SPHC material with a thickness of 3 mm with variations in current strength and protective gas flow rate, and each variable was replicated three times. The material tests used on these specimens are tensile and impact tests. The specification of SPHC material before welding is shown in Table 1.

Table 1 SPHC Material Specifications

Spec.	Chemical Composition (%)				Mechanical Properties		
	C	Mn	P	S	YS (MPa)	TS (MPa)	Elongation (%)
(*) SPHC	0,12 max	0,60 max	0,045 max	0,035 max	-	270 min	1,80≤T<3,20 : 29 min T<4,00 : 31 min

Table 2 Impact Strength Reference on Low-carbon Steel Material Raw

	Impact Strength (J/mm^2)
Raw Material 1	4,65
Raw Material 2	5,61
Raw Material 3	5,97
Average	5,41

3.2. Research Results of Tensile Testing Before Welding

Table 3 Tensile Strength Value in *Raw Material*

	Rated Tensile Strength (MPa)
Raw Material 1	433,38
Raw Material 2	406,98
Raw Material 3	415,94
Average	418,77

3.3. Results of Impact Testing Research Before Welding

Table 4 Value of Impact Strength in *Raw Material*

	Impact Strength (J/mm^2)
Raw Material 1	5,54
Raw Material 2	5,54
Raw Material 3	6,69
Average	5,92

3.4. Research Results of Tensile Testing After Welding

After the welding process and tensile testing of the specimen, the data used to determine the tensile strength is obtained using the calculation example formula as follows.

Figure 3 Welding specimen before the test

Of the twenty-seven specimens, tensile testing has been carried out, then calculations are carried out with formulas so that data is obtained and entered into the table as follows.

Table 5 Tensile Strength Value Data

Strong Current (A)	Protective Gas Flow Rate (L/min)	Rated Tensile Strength (MPa)			
		I	II	III	Average
120	15	460,54	432,9	347,36	413,60
	20	329,3	408,87	366,1	368,09
	25	420,7	418,32	463,33	434,12
130	15	373,6	324,6	417,8	372,00
	20	421,65	572,48	409,23	467,79

	25	359,18	387,38	457,4	401,32
140	15	438,32	434,42	480,78	451,17
	20	553,29	398,93	412,28	454,83
	25	437,51	436,31	422,23	432,02

3.5. Results of Impact Testing Research After Welding

Figure 4 Welding specimen before impact test

Of the twenty-seven specimens, impact testing has been carried out, then calculations are carried out with formulas so that data is obtained and entered into the table as follows.

Table 6 Impact Value Data

Strong Current (A)	Protective Gas Flow Rate (L/min)	Impact Test Value (J/mm^2)			
		I	II	III	Average
120	15	1,01	0,9	0,13	0,68
	20	1,33	1,09	1,91	1,44
	25	1,89	1,41	1,59	1,63
130	15	0,64	1,01	0,59	0,75
	20	0,14	0,34	0,59	0,36
	25	1,01	0,86	0,48	0,78
140	15	2,33	3,28	3,28	2,96
	20	1,15	1,19	1,36	1,23
	25	2,62	2,41	3,69	2,91

3.6. Tensile Test Data Processing

From the results of data collection, tensile test data processing was carried out *using* Minitab 2021 software using the DOE *Factorial method* to determine the influence of variables on specimens.

Analysis of Variance

Source	DF	Adj SS	Adj MS	F-Value	P-Value
Model	8	30515	3814,4	1,28	0,312
Linear	4	9781	2445,3	0,82	0,528
KUAT ARUS	2	8320	4159,8	1,40	0,272
LAJU ALIRAN GAS PELINDUNG	2	1462	730,8	0,25	0,785
2-Way Interactions	4	20734	5183,5	1,74	0,184
KUAT ARUS*LAJU ALIRAN GAS PELINDUNG	4	20734	5183,5	1,74	0,184
Error	18	53504	2972,5		
Total	26	84020			

Model Summary

S	R-sq	R-sq(adj)	R-sq(pred)
54,5204	36,32%	8,02%	0,00%

Figure 5 *Analysis of Variance* and *Model Summary of* Tensile Strength

To find out whether the research hypothesis is accepted or not, namely by looking at the results *of the P-Value* in the *Analysis of Variance.* The alpha value used is, at 5% or 0.05, the alpha value is the maximum limit of the *P-Value* error for the alternative hypothesis to be accepted. Based on the data of this study, the current strong variable has a P-Value of 0.272, so it can be stated that the current strong variable, does not have a significant influence on the tensile strength variable, and because the P-Value of the current strong variable exceeds the alpha limit, the null hypothesis is accepted and the alternative hypothesis is rejected. The protective gas flow rate variable has a P-value of 0.785, so it can be stated that the protective gas flow rate variable, does not have a significant effect on the tensile strength variable, and because the P-value of the protective gas flow rate variable exceeds the alpha limit, the null hypothesis is accepted and the alternative hypothesis is rejected. The variable of strong current interaction and flow rate of protective gas has a P-Value of 0.184, so it can be stated that the variable of strong interaction of current and flow rate of protective gas, does not have a significant effect on the variable of tensile

strength, and because the P-Value of the variable of strong current interaction and flow rate of protective gas exceeds the alpha limit, the null hypothesis is accepted and the alternative hypothesis is rejected.

In the R-sq coefficient, if the value is closer to 100%, it can be interpreted that the independent variable has a significant influence on the dependent variable. In the results of the data processing above, it can be seen that the R-sq coefficient has a value of 36.32%, so it can be interpreted that the independent variable has an influence of 36.32% on the tensile strength of the specimen.

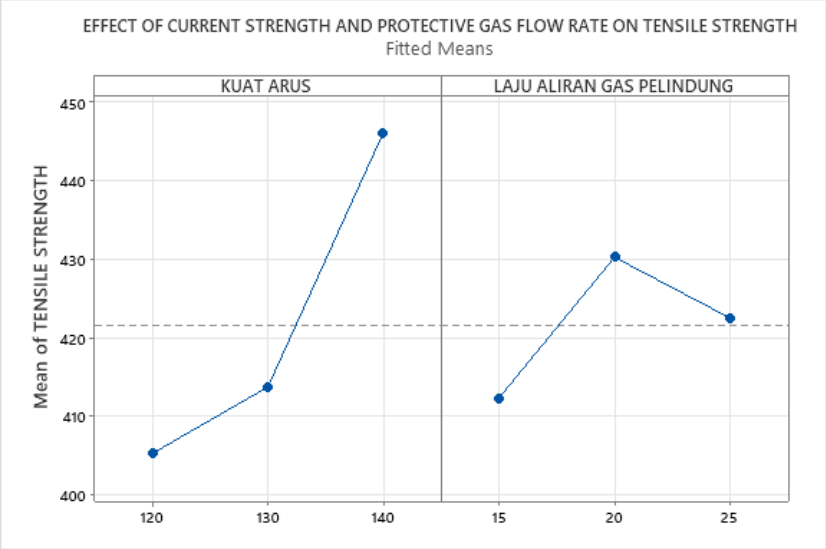

Figure 6 Effect of Current Strength Variation and Protective Gas Flow Rate on Tensile Strength

Figure 6 shows two lines, namely vertical and horizontal, the vertical line is a bound variable and the horizontal line is an independent variable. Based on the graph above, it can be seen that the current strength of 120 A and the flow rate of protective gas of 15 L/min produce the lowest tensile strength, and the current strength of 140 A and the flow rate of protective gas of 20 L/min produces the highest tensile strength.

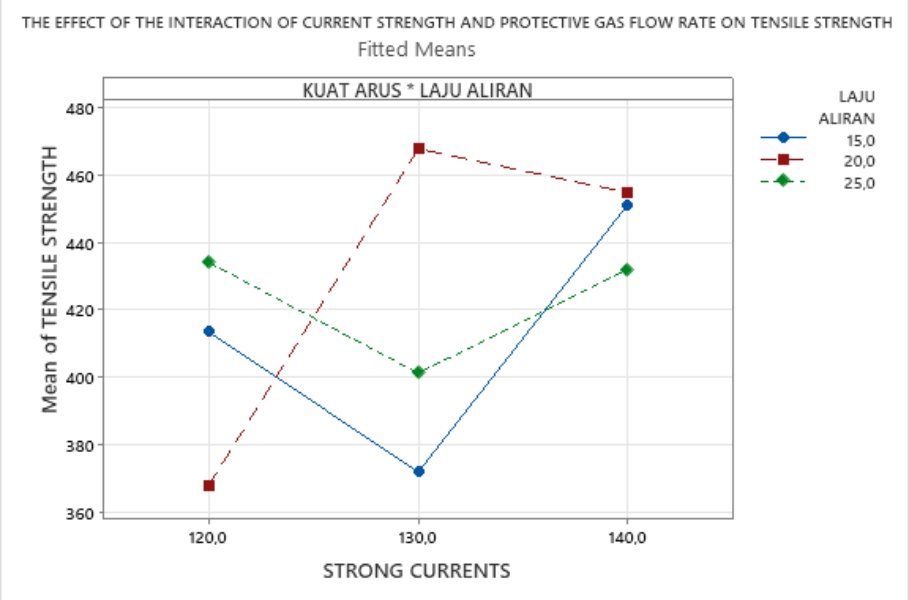

Figure 7 Effect of Interaction Current Strength and Flow Rate of Protective Gas on Tensile Strength

Figure 7 shows the influence of interaction variations in current strength and flow rate of protective gases on tensile strength. At a current strength of 120 A with a protective gas flow rate of 15 L/min has an average tensile strength of 413.6 MPa, then at a current strength of 120 A with a protective gas flow rate of 20 L/min there is a decrease in tensile strength with an average of 368.1 MPa, then there is an increase in tensile strength at a current strength of 120 A with a protective gas flow rate of 25 L/min with an average of 434.12 MPa. At a current strength of 130 A with a protective gas flow rate of 15 L/min has an average tensile strength of 372.04 MPa, then at a current strength of 130 A with a protective gas flow rate of 20 L/min there is an increase in tensile strength with an average of 467.79 MPa, then there is a decrease in tensile strength at an average current strength of 130 A with a protective gas flow rate of 25 L/min of 401.32 MPa. At a current strength of 140 A with a protective gas flow rate of 15 L/min has an average tensile strength of 451.17 MPa, then at a current strength of 140 A with a protective

gas flow rate of 20 L/min there is an increase in tensile strength with an average of 454.8 MPa, then there is a decrease in tensile strength at a current strength of 140 A with a protective gas flow rate of 25 L/min with an average of 432.01 MPa. From the graph above, it can also be seen that there is an interaction between the current strength and the flow rate of protective gas against the tensile strength, this can be seen from the lines on the graph that intersect each other.

3.7. Impact Test Data Processing

Dari hasil pengambilan data, selanjutnya dilakukan pengolahan data uji tarik menggunakan *software* minitab 2021 menggunakan metode DOE *Factorial* untuk mengatahui pengaruh variable terhadap spesimen.

Analysis of Variance

Source	DF	Adj SS	Adj MS	F-Value	P-Value
Model	8	21,625	2,7031	17,02	0,000
Linear	4	16,618	4,1546	26,17	0,000
KUAT ARUS	2	13,974	6,9868	44,00	0,000
LAJU ALIRAN GAS PELINDUNG	2	2,645	1,3224	8,33	0,003
2-Way Interactions	4	5,007	1,2517	7,88	0,001
KUAT ARUS*LAJU ALIRAN GAS PELINDUNG	4	5,007	1,2517	7,88	0,001
Error	18	2,858	0,1588		
Total	26	24,483			

Model Summary

S	R-sq	R-sq(adj)	R-sq(pred)
0,398474	88,33%	83,14%	73,73%

Figure 8 *Analysis of Variance* and *Model Summary* of Impact Test

To find out whether the research hypothesis is accepted or not, namely by looking at the results *of the P-Value* in the *Analysis of Variance.* The alpha value used is, at 5% or 0.05, the alpha value is the maximum limit of the *P-Value* error for the alternative hypothesis to be accepted. Based on the data of this study, the current strong variable has a P-Value of 0.000, so it can be stated that the current strong variable, has a significant influence on the impact strong variable, and because the P-Value of the current strong variable does not exceed the alpha limit, the null hypothesis is rejected and the alternative hypothesis is accepted. The protective gas flow rate variable has a P-value of 0.003, so it can be stated that the protective gas flow rate variable, has a significant influence on the impact strong variable, and because the P-value of the protective gas flow rate variable is less alpha limit, the null hypothesis is rejected and the alternative hypothesis is accepted. The variable of strong current interaction and flow rate of protective gas has a P-Value of 0.001, so it can be stated that the variable of strong interaction of current and flow rate of protective gas, has a significant influence on the strength of impact, and because the P-Value of the variable of strong interaction of current and flow rate of protective gas exceeds the alpha limit, the null hypothesis is rejected and the alternative hypothesis is accepted.

In the R-sq coefficient, if the value is closer to 100%, it can be interpreted that the independent variable has a significant influence on the dependent variable. In the results of the data processing above, it can be seen that the R-sq coefficient has a value of 88.33%, so it can be interpreted that the independent variable has an influence of 88.33% on the impact strength of the specimen.

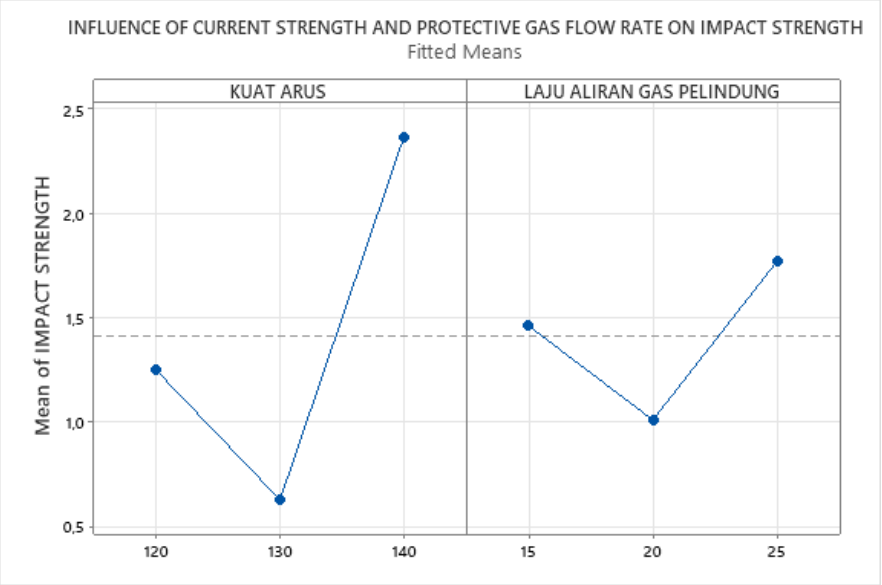

Figure 9 Effect of Current Strength Variation and Protective Gas Flow Rate on Impact Strength

The graph above has two lines, namely vertical and horizontal, the vertical line is a bound variable and the horizontal line is an independent variable. Based on the graph above, it can be seen that the current strength of 130 A and the protective gas flow rate of 20 L/minute produce the lowest impact strength, and the current strength of 140 A and the protective gas flow rate of 25 L/minute produces the highest impact strength.

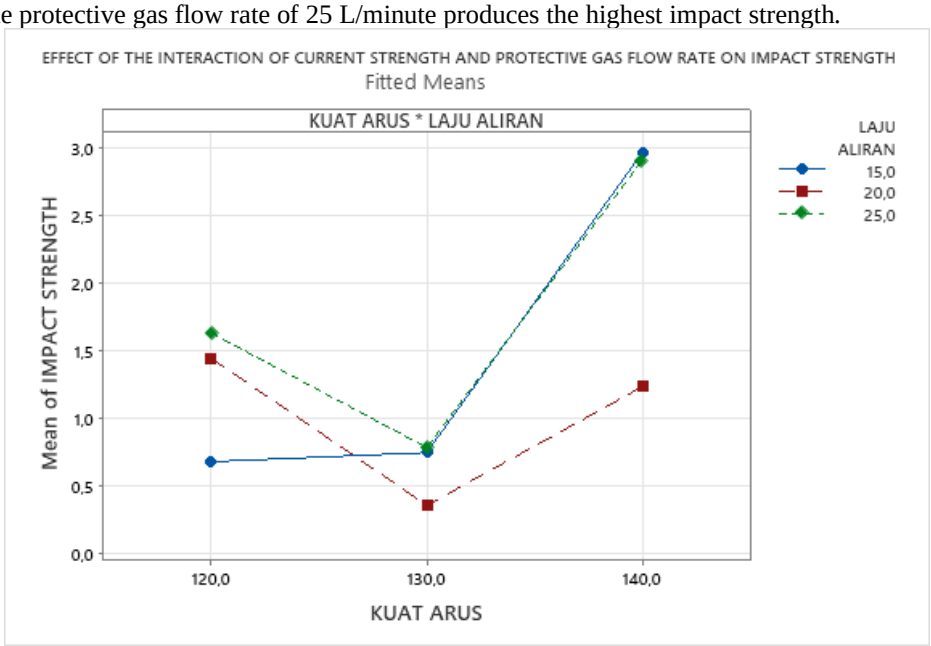

Figure 10 Effect of Current Strength Variation and Protective Gas Flow Rate on Impact Strength

The graph above shows the effect of interaction variations in current strength and flow rate of protective gases on impact strength. At a current strength of 120 A with a protective gas flow rate of 15 L/min has an average impact strength of 0.68 J/mm^2, then at a current strength of 120 A with a protective gas flow rate of 20 L/min an increase in impact strength with an average of 1.44 J/mm^2, there is an increase in impact strength at a current strength of 120 with a protective gas flow rate of 25 L/min with an average of 1.63 J / mm2. At a current strength of 130 A with a protective gas flow rate of 15 L/min has an average impact strength of 0.75 J/mm^2, then at a current strength of 130 A with a protective gas flow rate of 20 L/min an increase in impact strength with an average of 0.36 J/mm^2, there is a decrease in impact strength at a current strength of 130 A with a protective gas flow rate of 25 L/min with an average of 0.78 J/mm^2. At a current strength of 140 A with a protective gas flow rate of 15 L/min has an impact strength with an average of 2.96 J/mm^2, then at a current strength of 140 A with a protective gas flow rate of 20 L/min an increase in impact strength with an average of 1.23 J/mm^2, there is an increase in impact strength at a current strength of 140 A with a protective gas flow rate of 25 L/min with an average of 2.91 J / mm^2. From the graph above, it can also be seen that there is an interaction between the variation in current strength and

the flow rate of protective gas against the impact strength, this can be seen from the lines on the graph that intersect each other.

3.8 Discussion

Based on research that has been done, generally, the tensile strength of the weld is higher than the tensile strength of the parent material, based on the catalog table above, the parent material SPHC has a minimum tensile strength of 270 MPa, the following is the discussion.

In the figure below is a graph showing the average tensile strength in the SPHC material from the process.

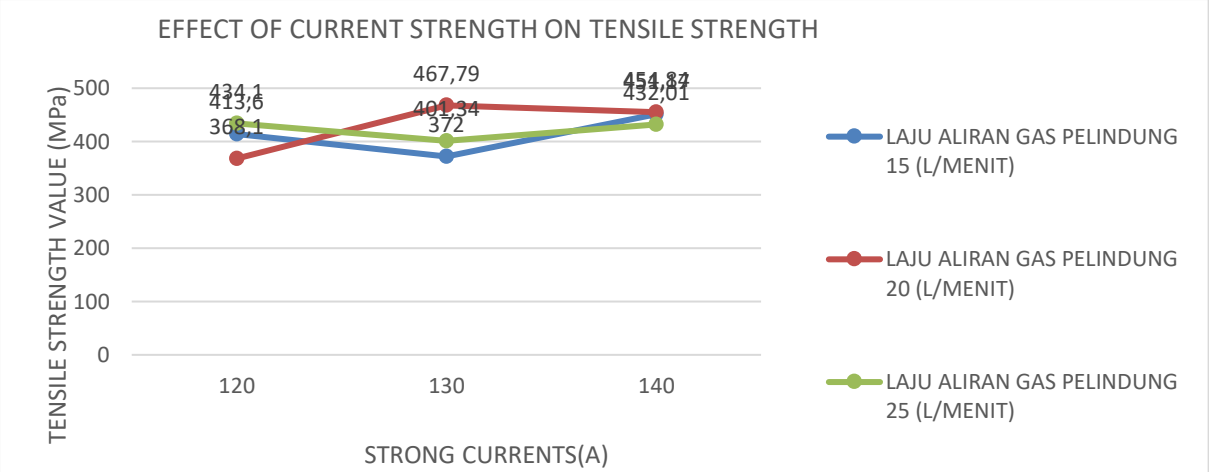

Figure 11 Effect of Current Strength Variation and Protective Gas Flow Rate on Tensile Strength

From the results of the graph above, it can be seen that the value of tensile strength after welding on average, has a higher value than the value of tensile strength before welding. The highest average tensile strength value of 467.79 MPa occurred at a current strength of 130 A and a protective gas flow rate of 20 L/mins, while the average value of a fixed tensile strength of 368.1 MPa occurred at a current strength of 120 A and a protective gas flow rate of 20 L/min. The increase in tensile strength is thought to be due to an increase in the strength of the current used to allow residual voltage not to occur. This decrease in tensile strength occurs allegedly because of the small strength of the current used it allows residual stress to occur in the weld area.

The figure below is a graph showing the average impact strength of SPHC material from the welding process with variations in current strength and a protective gas flow rate of 15 L/min.

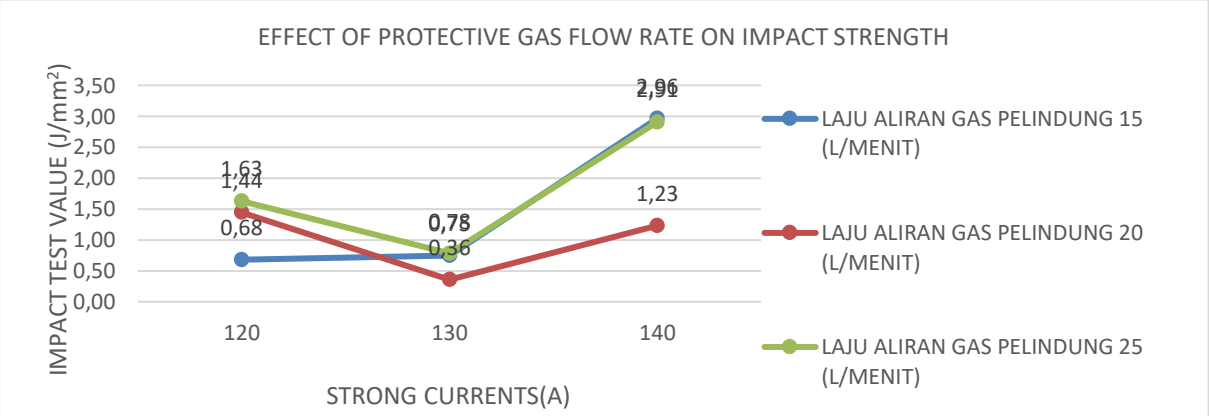

Figure 12 Effect of Current Strength Variation and Protective Gas Flow Rate on Impact Strength

From the results of the graph above, it can be seen that the value of impact strength after welding on average, has a lower value than the value of impact strength before welding. The highest average impact strength value of 2.96 J/mm^2 occurred at a current strength of 140 A and a protective gas flow rate of 15 L/min, while the lowest average impact strength value of 0.36 J/mm^2 occurred at a current strength of 130 A and a protective gas flow rate of 20 L/min. The increase in impact strength is thought to be due to the large amount of current used so that the residual voltage does not occur. This decrease in impact strength occurs allegedly because of the small strength of the current used so it allows residual voltage to occur in the weld area.

4. CONCLUSION

Based on the processing of analysis and discussion data, generally, the tensile strength of the weld metal has higher test results than the raw material, and the impact strength of the weld metal has lower test results compared to the raw material. Here are some conclusions from this study, namely:

4.1 The effect of strong current variations on tensile strength and impact results in the following conclusions:

a. Judging from the Analysis of Variance and the graph of the effect of strong current variations on tensile strength, statistically there is no effect but there is an insignificant increase. The highest average tensile strength of 446.01 MPa occurs at a current strength of 140A and the lowest average of 405.27 MPa occurs at a current strength of 120 A.

b. Judging from the *Analysis of Variance* and the graph of the effect of current strength variation on impact strength, statistically there is an influence on impact strength. The average high impact force of 2.3 J/mm2 occurred at a current strength of 140A and an average low of 0.63 J/mm^2 occurred at a current strength of 130 A.

4.2 The effect of protective gas flow rate variations on tensile strength and impact results in the following conclusions :

a. Judging from the *Analysis of Variance* and graphs of the effect of variations in protective gas flow rates on tensile strength, statistically there is no effect, but there is an insignificant increase. The average highest tensile strength of 430.24 MPa occurs at a protective gas flow rate of 20 L/min and the lowest average of 412.26 MPa occurs at a protective gas flow rate of 15 L/min.

b. Judging from the *Analysis of* Variance and the graph of the effect of current strength variation on impact strength, statistically there is an influence on impact strength. the highest average impact force of 1.78 J/mm^2 occurred at a protective gas flow rate of 25 L/min and an average low of 1.01 J/mm^2 occurred at a protective gas flow rate of 20 L/min.

4.3 The effect of the interaction of variations in current strength and flow rate of protective gases on tensile strength and impact results in the following conclusions:

a. Judging from the *Analysis of Variance* and the graph of the effect of the interaction of strong variations in current and flow rate of protective gases on tensile strength, statistics have no effect but there is an insignificant increase. From the influence of the interaction of variations in current strength and protective gas flow rate, the highest average tensile strength value of 467.79 MPa occurs at a current strength of 130 A and a protective gas flow rate of 20 L/min, while the average value of a fixed tensile strength of 368.1 MPa occurs at a current strength of 120 A and a protective gas flow rate of 20 L/min.

b. Judging from the *Analysis of Variance* and graphs, the effect of the interaction of variations in current strength and flow rate of protective gases on impact strength statistically there is an influence on impact strength. From the influence of the interaction of variations in current strength and protective gas flow rate on impact strength, the highest average impact strength value of 2.96 J/mm^2 occurred at a current strength of 140 A and a protective gas flow rate of 15 L/min, while the lowest average impact strength value of 0.36 J/mm^2 occurred at a current strength of 130 A and a protective gas flow rate of 20 L/min.

5. REFERENCES

[1] Novianto,Adi, Teknik Pengelasan Gas Metal (Mig/Mag). Yogyakarta: Universitas Negeri Yogyakarta. 2018

[2] Fakri.Zainal.,Bukhari.,Juhan.B. Analisa Pengaruh Kuat Arus Pengelasan GMAW Terhadap Ketangguhan Sambungan Baja AISI 1050. Journal of Welding Technology. 2019

[3] Suarsana, *DIKTAT PENGETAHUAN MATERIAL TEKNIK*. DENPASAR : UNIVERSITAS UDAYANA. 2014

[4] Prasetya, A.W., Rusiyanto., Pramono, *Pengaruh debit gas pelindung dan tegangan listrik terhadap tingkat kekerasan dan struktur mikro sambungan las GMAW pada baja karbon sedang EMS-45.* Jurnal Kompetensi Teknik 42 Vol. 8. 2017.

LOGIC
Journal of Engineering Design and Technology
Vol. 23 No.3 November 2023; p. 203 - 211

p-ISSN : 1412-114X
e-ISSN : 2580-5649
http://ojs2.pnb.ac.id/index.php/LOGIC

DESIGN OF CLEAN WATER BOOSTER PUMP FOR HIGH-RISE BUILDINGS

Luh Putu Ike Midiani[1)], I Made Duta Irawan[1)], I Ketut Bangse[1)], I Nyoman Gunung[1)]

1) Mechanical Engineering Department,Politeknik Negeri Bali, Badung Indonesia

Correponding email [1)] : putuikemidiani@pnb.ac.id

Abstract. A sanitary system is a supporting component designed to meet the clean water requirements of a building, primarily for sanitation activities. The average sanitary equipment used typically requires a shower pressure of ±1 Bar. However, the shower pressure can be significantly affected by factors such as the distance from the top tank and the building's layout, considering only the pressure due to gravity. To address inadequate shower pressure, an auxiliary pump known as a booster pump is necessary. The need for a booster pump is determined by the cumulative demand from plumbing equipment, where the total capacity required is 6057 liters/hour. To address this demand, the system employs two pump units, each with a capacity of 3 m^3/hour. The distribution pipes utilized in the system adhere to established standards and are made of random polypropylene with a diameter of 2 inches and a flow rate of 0.005889 m^3/second. The overall head loss resulting from this installation amounts to 31.62 meters. To accommodate the booster system, a pressure tank with a capacity of 67 liters is employed. The minimum working pressure required for the pumps is 1.8 Bar

Keywords: clean water, booster pump, high-rise building.

1. INTRODUCTION

As the population grows, the pattern of building construction shifts, namely the pattern of horizontal development which slowly begins to shift with vertical development. This is due to the limited land available for residential areas, where population growth in recent years has continued to increase, so a solution to the problem of providing residential areas is needed without having to take up a lot of land, namely through the construction of high-rise buildings [1][2].

The impact of this shift in development patterns is on the use of clean water, where in the past the clean water supply system was very inefficient because it provided too much water. But at present there are limitations in the use of the amount of water, which is highly considered due to energy savings and limited water resources for the long term [3]. Supporting facilities, especially the factor of using clean water is very crucial, as clean water is a basic need that is needed by humans in carrying out their daily lives.

In a clean water distribution system, especially in a high-rise building, a method is needed to provide proper clean water. In the field of clean water plumbing installations, obstacles are often found, namely the lack of water pressure in each sanitary ware, which has an impact on the flow rate for sanitary equipment. So clean water plumbing installations must be designed so that they can provide a minimum pressure of 1 kg/cm^2 ($\pm$1 Bar) on each sanitary device when used during peak hours and be efficient and economical [4][5].

Planning a clean water plumbing installation system uses SNI references for calculating clean water needs and determining the dimensions of clean water pipes, as in previous [1][6][7][8][9].

To achieve this goal, clean water plumbing systems in high-rise buildings must be designed by the technical terms and conditions that have been legalized or stipulated in Indonesia. The results of designing a clean water booster pump for high-rise buildings will increase the convenience of using water in this building.

The novelty is the building is very large and the water flow is very small, so this building cannot apply the direct connection method or use a pressure tank, so water distribution is implemented using a roof tank.

2. METHODS

The design of a clean water booster pump for high-rise buildings, according to Nayono [10] can use two methods, i.e. basic plan and preliminary plan. The high-rise buildings have two floors where the area of the first floor is 1500 m^2, so the total area of this building is 3000 m^2. The occupant capacity of this building is 120 people and water usage activities here tend to be moderate. The problem faced is a large building with a small water supply, so this building cannot apply the direct connection method or use a pressure tank. A suitable method for this problem is implementing water distribution with a roof tank [11][12].

The basic plan method is a method of calculating water requirements based on sanitary estimates, main pipe networks, or plumbing system diagrams, determining the pump plan and other components used which refer to SNI standards which can be seen in Figure 1 [5]. After the basic planning method is carried out, it is followed by a preliminary plan, where this plan contains calculations to determine the specifications of the material to be used [13].

The booster pump is an auxiliary pump that functions as a pressure booster in the water distribution installation. This pump works to overcome water discharge due to insufficient static pressure in the installation if only utilizing gravity [5][7]. The use of highly fluctuating water is also the reason for choosing this booster pump so the determination of the capacity of this booster pump is based on the method of the type and number of plumbing equipment with several parameters as listed. The types of plumbing tools are shown in Table 1, and the number of plumbing tools is shown in Table 2. The pressure required for each sanitary ware is shown in Table 3.

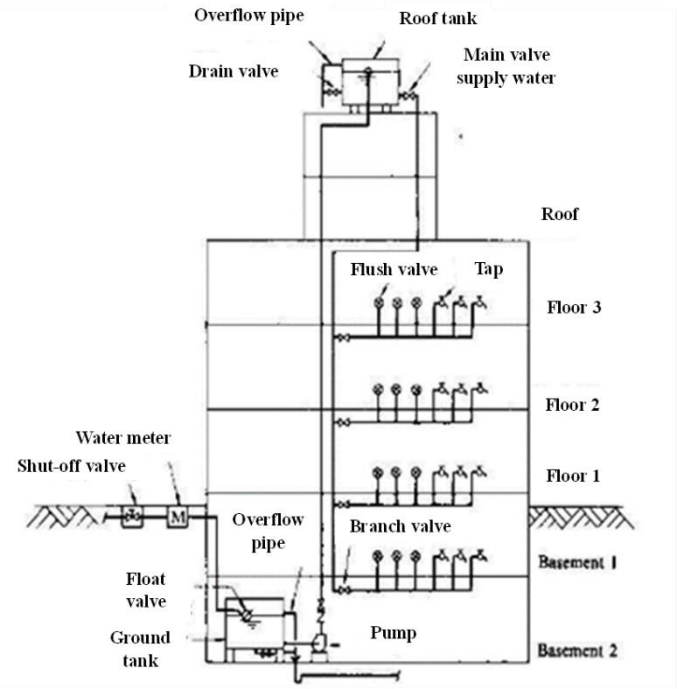

Figure 1. A system with a roof tank
Source: SNI 03-7065-2005F

The design of the booster pump needs to know the sanitary amount and the building's elevation. After the data has been obtained, the next step is to calculate the water needs by combining additional data from SNI standards. This water requirement is not only about the flow rate but also the head or pressure in the system. Where the minimum pressure at each point of the plumbing tool is on average 0.7 kg/cm^2 [13]. In general, it can be said that the standard pressure is 1 kg/cm^2. For static pressure, it is better to try between 4 kg/cm^2 to 5 kg/cm^2 [2]. The pressure on the pipe will affect the speed of the water flow, where the speed of the pipe in general in Indonesia is 0.9 to 2 m/secound [5][14]. The difference between the pipe diameter and the pump outlet diameter must be adjusted using a reducer.

Table 1. Water use in every sanitary

Name of plumbing unit	One time use (Liters)	Water filling time (second)
Toilets with flush valves	15	10
Toilets, flush tanks	14	60
Peturasan, flush valve	5	10
Peturasan, flush tank	14	300
Small hand sink	10	18
Normal hand wash	10	40
Kitchen sink, with 13mm faucet	15	
Kitchen sink, with 20 mm faucet	25	60
Bathtub	125	250
Shower	42	210

Source: SNI 03-7065-2005

Table 2. Percentage of usage on plumbing tools

Number of plumbing tools	1	2	4	8	12	16	24	32	40	50	70	100
Toilet with flush valve	1	50% One	50% 2	40% 3	30% 4	27% 5	23% 6	19% 7	17% 7	15% 8	12% 9	10% 10
Ordinary plumbing tool	1	100% Two	75% 3	55% 5	48% 6	45% 7	42% 10	40% 13	39% 16	38% 19	35% 25	33% 33

Source: Noerbambang & Morimura, 2005

Table 3. The pressure required for each sanitary

Name of plumbing tool	Minimum pressure (kg/cm^2)
Toilet with flush valve	0,7
Interlocking flush valve	0,4
Automatic faucet	0,7
Shower	0,7
Faucet	0,3
Water heater	0,3-0,7

Source: SNI 03-7065-2005

This preliminary plan determines the specifications of the booster pump and calculates the clean water required pipe, and pump sizes.

1) Capacity of booster pump (Q_{pu})

Booster pump capacity can be calculated based on the unit load factor of the plumbing equipment [4][11]. Because this is a pressure pump system, the number of pumps must be more than 1 unit with installations arranged in parallel, this aims to meet the demand during peak hours and meet the needs for water discharge in fluctuating usage [5][15].

$$Q\_booster = L \times t \times a \times n \quad (1)$$

where :

$Q_{booster}$ = Capacity of booster pump (m^3/hour)
L = Water use capacity of sanitary (liters)
t = Estimates of sanitary usage (hour)
a = Presentase penggunaan saniter (%)
n = number of sanitary

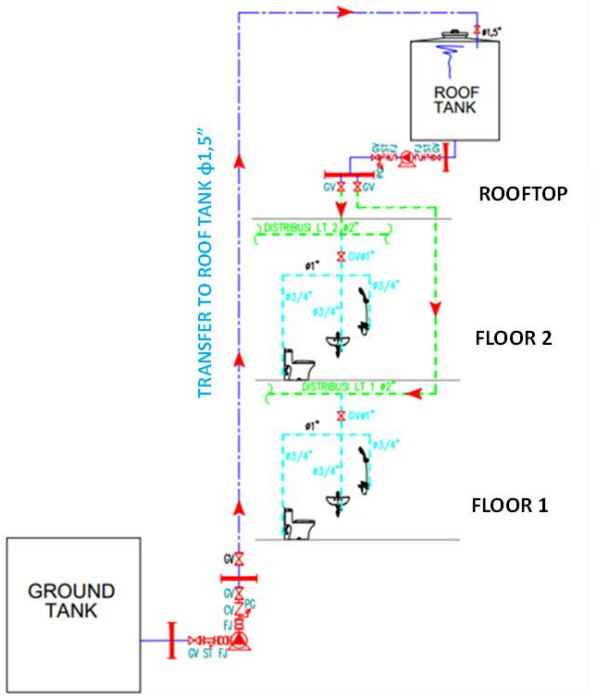

Figure 2. Schematic drawing for clean water installation in buildings

2) Pump discharge (Q_{pu})

The flow rate of the pump is known based on the formula according to Sularso [11].

$$Q\_pu = \frac{Q_{booster}}{3600} \times 3{,}5 \quad (2)$$

where :

Q_{pu} = Pump discharge (m^3/second)

3) Pipe distribution (D)

$$D = \sqrt{\frac{4 \times Q_{pu}}{v \times \pi}} \quad (3)$$

where :

D = Diameter of pipe (m)

v = Velocity of water (m/secound)

4) Pump head (H)

The total pump head can be determined based on the formula according to Sularso [11].

$$H = H_a + \Delta H_p + H_i + \frac{v^2}{2g} \quad (4)$$

where :

H = Head total of pump (m)

H_a = Potential height (m)

ΔH_p = The difference in pressure head at the water surface (m)

H_i = Total major losses and minor losses (m)

$\frac{v^2}{2g}$ = Head velocity of water in the pipeline (m)

g = Gravitation acceleration (9,8 m/s^2)

The total head is obtained by the parameters that cause losses to the system. The losses are called major losses, minor losses, and static heads, which determine losses using the following formulas[6].

Major losses caplosses (5)

$$H_f = \frac{10{,}66 \times {Q_{pu}}^{15}}{C^{1{,}85} \times D^{4{,}85}} \times L$$

where :

H_f = Pipe losses (m)

C = Pipe coefficient
D = Diameter of pipe (m)
L = Distance of pipe (m)

a) Minor losses
Effect head losses of pipe bends

$$h_n = n \quad (6)$$

where :
h_n = Friction loss in fittings (m)
n = Total fitting (unit)
v = Velocity of water (m/secound)
f = Friction loss each fittings unit

equal head losse f overlap $h_o = f \frac{(v^1 - v^2)^2}{2g}$ (7)

where :
h_o = Friction loss in reducer (m)
f = Friction loss each overloop unit
v_1 = Velocity of water inlet (m/second)
v_2 = Velocity of water outlet (m/second)

Effect head losses of reducer $h_o = f \frac{v_2^2}{2g}$ (8)

where :
h_o = Friction loss in overlook (m)
f = Friction loss of each reducer
v_2 = Velocity of water outlet (m/second)
g = Gravitation acceleration (9,8 m/s^2)

5) Minimum pump pressure (P) [16]

$$P_{booster} = (P]\!]_h + P\_min) \times 1.5 \quad (9)$$

$$P = \rho \times g \times h \quad (10)$$

where :
$P_{booster}$ = Minimum pressure of booster pump (Kg/cm^2)
P = Static pressure of booster pump (Kg/cm^2)
P_{min} = Minimum pressure on sanitary unit (Kg/cm^2)
ρ = Density of water (998,2 Kg/m^3)
h = Potential height (m)

6) Capacity of pressure tank (V) [1]

$$V_{tank} = \frac{Q_{booster} \times n}{3} \quad (11)$$

where :
V_{tank} = Capacity of pressure tank (liters)
n = Total pompa

3. RESULTS AND DISCUSSION

3.1. Basic plan results

With the calculation data that has been done, it is found that this building has 2 floors with a total of 71 rooms and a total occupant density in the building of 120 people. The number of sanitary equipment used in this building is shown in Table 4.:

Table 4. Total sanitary need

Name of sanitary	Total
For cold water	
Shower	36
Toilet with flush valve	46

Sink		47
Faucet 20mm		3
Laundry sink		3
Faucet 13mm		6
For hot water		
Shower		36
Kitchen sink		2
Laundry sink		3
	Total	182

3.2. Preliminary plan results

1) Capacity of the booster pump

The results from the initial data using formula (1) and a combination of tables 1 and 2 are presented in Figure 3 and Table 5,

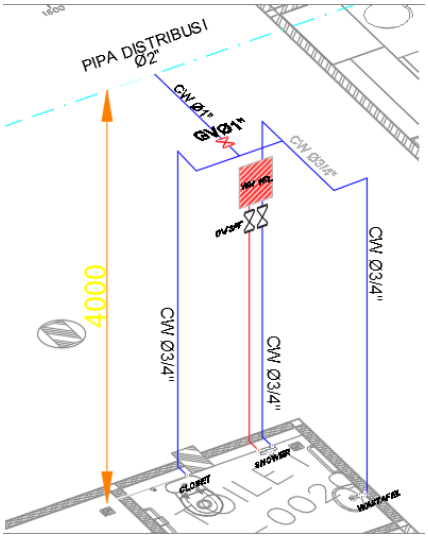

Figure 1. Isometric clean water installation in the bathroom

Table 5. The result of determining the pump capacity

NO	Sanitary	Water usage in sanitary (liters)	Sanitary quantity (units)	Usage percentage (%)	Hourly usage (hours)	Water usage (liters/hours)
COLD WATER						
1	Shower	42	36	39%	3	1769,04
2	Toilet with flush valve	14	46	16%	6	618,24
3	Sink	10	47	38%	6	1071,6
4	Kitchen sink with faucet 20mm	25	3	75%	6	337,5
5	Laundry sink	15	3	75%	5	168,75
6	Faucet 13mm	15	6	65%	6	351
AIR PANAS						
7	Shower	50	36	30%	3	1620
8	Kitchen sink	15	2	30%	6	54
9	Laundry sink	15	3	30%	5	67,5
					Total used water	6057,63

The total capacity of the booster pump is a system with more than one pump, so the total capacity will be divided by 2 so that each pump is 3000 liters/hour or 3 m^3/hour. After the pump capacity is obtained, determine the irrigation capacity using formula (2) so that:

$$Q_{pu} = \frac{\left(6{,}05\frac{m^3}{hour}\right)}{3600} \times 3{,}5$$

$$Q_{pu} = 0{,}005889\frac{m^3}{second}$$

So the irrigation discharge for this booster pump is 0,005889 m^3/second.

2) The diameter of the pipe distribution

The diameter of pipe distribution for the first floor and second floor can use formula (3) and for water flow rates follow the standards specified in the planned method, so when:

$$the\ D = \sqrt{\frac{4 \times 0{,}005889}{2 \times 3{,}14}}$$

$$D = \sqrt{0{,}003749}$$

$$D = 0{,}06122\ m \times 1000 = 61{,}2mm$$

So that the diameter of the pipe used is 61.2 mm. To make it easier to select pipes, the diameter size is 63 mm. Because the selection of pipe material refers to PPR, rounding the pipe diameter is equivalent to 2 inches. This pipe has a Hazen-William coefficient (C) of 150 [11][17].

3) Pump head

In the installation drawings it is known that the elevation of the 1st floor distribution pipe to the pump discharge is 6 m and the 2nd floor distribution pipe elevation to the pump discharge is 1.5 m. So the head required for the booster pump is as follows:

a) Major losses

It is known that the length of the distribution pipe from the roof tank to serve water on the 1st floor is 97 m and for the 2nd floor is 105 m. So that the head due to the surface of the distribution pipe and the length of the pipe is obtained using formula (5) as follows:

- For distribution pipe floor 1

$$Hf = \frac{\left(10{,}666 \times 0{,}005889^{1{,}85}\right)}{150^{1{,}85}\ 0{,}063^{4{,}85}} \times 97$$

$$Hf = 4{,}86\ m$$

- For distribution pipe floor 2

$$Hf = \frac{10{,}666 \times 0{,}005889^{1{,}85}}{150^{1{,}85}\ 0{,}063^{4{,}85}} \times 105$$

$$Hf = 5{,}26\ m$$

b) Minor losses

At the analysis stage using software to find out the basic plan drawings for this plumbing system, it was found that the distribution pipes for the 1st and 2nd floors obtained various types of fittings as shown in Table 6.

Table 6. Fittings needed on distribution pipes

Materials	Total fitting	
	1nd floor	2nd floor
El-bow 2”	10	9
Tee reducer 2” x 1”	19	30
Reducer 2” x 1”	0	1

For each fitting has a friction coefficient value (f) which refers to the determination of a source [11]. The results are given in Table 7.

Table 7. Minor loss calculation results

Explanation	1nd floor [m]	2nd floor [m]
Friction loss due el-bow (hn)	1,84	1,65
Friction loss due tee (ht)	3,88	6,12

Friction loss due to reducer (ho)	0	0,10
Total	5,72	7,87

c) Total losses

The total of this head will be used as a reference to determine the booster pump head used. So that the total loss due to head on the distribution pipe for floors 1 and 2 can be found using formula (4):

- Distribution pipe in 1st floor

$$H = 6\ m + 0 + (4{,}86m + 5{,}72) + \frac{2^2 \frac{m}{second}}{2\times 9{,}8\frac{m}{second}}$$

$$H = 16{,}784\ m$$

- Distribution pipe in 2nd floor

$$H = 1{,}5\ m + 0 + (5{,}26m + 7{,}87) + \frac{2^2 \frac{m}{detik}}{2\times 9{,}8\frac{m}{detik}}$$

$$H = 14{,}844\ m$$

So the total head required to select a pump is 31,628 m

4) Minimum pump pressure

To determine the minimum pressure specs that must be provided for this booster pump, it is assumed to have the minimum pressure required in Table 3. So that the minimum pressure for using a booster pump for the distribution of clean water on floors 1 and 2 can be determined if gravity is not used using the formula (9) to get:

$$P_{booster} = \left(0{,}5\frac{kg}{cm^2} + 0{,}7\ \frac{kg}{cm}\right]^2) \times 1.5$$

$$P_{booster} = 1{,}8\frac{kg}{cm^2}\ \times 0{,}98 = 1{,}76\ Bar$$

So the minimum working pressure for this booster pump is 1,8 Bar.

5) Compressive capacity

The pressure tank is a component used to control the pump so that it does not run continuously. To determine the capacity of the pressure tank can use the formula (11). Judging from the previously known pump capacity, this booster pump is sufficient to only use 2 pumps. So obtained for the pressure tank capacity:

$$Q = \frac{6057\frac{\ell}{hour}}{60\ minute} = 100{,}97\frac{\ell}{minute}$$

Where :

$$V = \frac{100{,}97\frac{\ell}{minute} \times 2\ unit}{3} = 67{,}3\ liter$$

Obtained for the pressure tank capacity is 67 liters. Because there is no pressure tank with this capacity in the market, we are looking for one with a capacity close to 80 liters.

4. CONCLUSION

Based on the results of the calculations that have been discussed, it can be concluded as follows:

1) The design of a clean water booster pump for high-rise buildings with a building area of 3000 m^2 and a capacity of 120 people has been carried out. There are two types of water used, namely cold water and hot water which will serve 142 units of sanitary equipment using a pump called a booster pump. To service all of these sanitary devices, two booster pump units are needed, each having a capacity of 3 m^3/hour. This pump must be able to meet the predetermined head of 31.62 m. This system uses a pressure tank with a capacity that must be met, namely 67.3 liters. This pressure tank will be set with a pump control (pressure switch) to regulate the work of pumps one and two. The minimum pressure for the booster pump is 1.76 Bar. The type of pipe used is PPR (Polypropylene Random) with a diameter of 2 inches.
2) From the specifications above, the pump that is suitable for use as a booster pump is a vertical multistage centrifugal pump. The placement of this booster pump will be designed with positive suction line conditions.

5. REFERENCES

[1] Suhardiyanto, "Perancangan Sistem Plambing Instalasi Air Bersih dan Air Buangan Pada Pembangunan Gedung Perkantoran Bertingkat Tujuh Lantai," *J. Tek. Mesin*, vol. 05, pp. 2–9, 2016.
[2] F. Muhamad and E. Wardhani, "Studi Penghematan Air pada Sistem Plambing Air Bersih di Apartemen

Menara Cibinong Tower Mahoni," vol. VI, no. 4, pp. 2303–2309, 2021.
[3] K. C. B. Artayana and G. Indra, "Perencanaan Instalasi Air Bersih dan Air Kotor Pada Bangunan Gedung dengan Menggunakan Sistem Pompa," vol. 4, no. 1, pp. 51–56, 2010.
[4] I. P. Lilipaly, R. E. Badriani, U. Jember, and J. Timur, "Perencanaan Sistem Plambing Dan Hidran Kebakaran Pada Proyek Pembangunan Hotel Pesona Alam," vol. 10, pp. 266–279, 2021, doi: 10.22225/pd.10.2.2818.266-279.
[5] S. 03-7065-2005, "Tata cara perencanaan sistem plambing," 2005.
[6] P. Wirasakti and L. Apriyanti, "Perencanaan Sistem Instalasi Plambing Air Bersih Apartemen Royal Paradise Bandung," vol. 7, no. 1, pp. 1–12, 2019.
[7] Ubaedilah, "ANALISA KEBUTUHAN JENIS DAN SPESIFIKASI POMPA UNTUK SUPLAI AIR BERSIH DI GEDUNG KANTIN BERLANTAI 3 PT ASTRA DAIHATSU MOTOR," vol. 05, no. 3, pp. 119–127, 2016.
[8] A. Gofar, "Perancangan sistem plambing di gedung asrama 6 institut teknologi sumatera," pp. 1–10.
[9] R. D. Riyadi, "PERENCANAAN SISTEM PLAMBING PADA GEDUNG LABORATORIUM TEKNIK 5 INSTITUT TEKNOLOGI SUMATERA," vol. 3, no. 1, pp. 1–9, 2005.
[10] R. N. Syamsudin, "Pengembangan Modul Pembelajaran Mata Kuliah Praktik Kerja Plambing dan Sanitasi di Prodi Pendidikan Teknik Sipil dan Perencanaan FT UNY," pp. 83–93, 2020.
[11] Sularso, "Pompa dan Kompresor".
[12] A. S. of P. Engineers, "Plumbing Engineering Design Handbook Volume 1," vol. 1, 2004.
[13] E. S. Menon, "Piping Calculations Manual".
[14] D. W. Widihasta, "PERENCANAAN SISTEM AIR BERSIH PADA PEMBANGUNAN APARTEMEN SUNCITY SIDOARJO," *JOS MRK*, vol. 2, pp. 66–71, 2021.
[15] A. Agung, A. Suryawan, M. Suarda, and I. G. K. Sukadana, "Penentuan dimensi perpipaan sistem pompa paralel," vol. 9, no. 1, pp. 84–90, 2016.
[16] J. J. Susilo, "Studi Perencanaan Penyediaan Air Bersih Pada gedung Bertingkat Tunjungan Plasa VI Kota Surabaya.pdf." 2014.
[17] P. P. Association, "Handbook of PVC Pipe Design and Construction".

LOGIC
Journal of Engineering Design and Technology
Vol. 23 No.3 November 2023 ; p. 212 - 218

p-ISSN : 1412-114X
e-ISSN : 2580-5649
http://ojs2.pnb.ac.id/index.php/LOGIC

Analysis of the Use of 12 kg LPG (Liquified Petroleum Gas) Conveyance to Complaints of Household Workers

I Nyoman Sutarna[1], I Nengah Ludra Antara[1], Kadek Agus Mahabojana DP[1]

1) Department of Mechanical Engineering, Politeknik Negeri Bali, Badung, Indonesia

Correponding email [1)]: sutarnanyoman@yahoo.co.id

Abstract. Manual conveyance is the work of transporting material carried out by workers to move material from an origin location to a destination location. The purpose of the study was to overcome the complaints experienced by housewives in the process of transporting 12kg LPG. The research was conducted using a two-period cross over design method. Musculoskeletal complaints experienced by housewives on the back, waist, knees, and calves. Musculoskeletal complaints were measured using a Nordic Body Map questionnaire with a Likert scale, and the data obtained were tested with independent t-test and t-pair. The results of the analysis showed that the use of 12 kg LPG conveyance could reduce musculoskeletal complaints from an average of 80.1 to 70 or decreased by 12.6%. It was concluded that the use of 12 kg LPG conveyance could reduce musculoskeletal complaints in housewives. It is recommended for those over 30 years of age to lift and carry heavy loads to use assistive devices.

Keywords: 12 kg LPG conveyance. musculoskeletal complaint, household worker

1. INTRODUCTION

There are many routine activities carried out in the household in daily life. One of these activities is transporting 12 kg LPG which is used for cooking. This work is carried out with a non-physiological attitude, so it has the potential to cause musculoskeletal complaints and injuries if not managed ergonomically.

Work positions that are not ergonomic or work attitudes are not physiological, which can cause bone abnormalities in workers [1], [2]. Work positions that are not physiological due to the demands of tasks, work tools, and work positions that are not by the ability of the worker result in increased musculoskeletal complaints [3]–[5]. The implementation of routine activities in a family is usually arranged through the division of tasks to complete them. Knowledge of ergonomic work positions has not been possessed by workers and it is proven that problems are still found related to non-ergonomic work postures in households.

From the survey and initial measurements of 16 housewives in Pupuan District, Tabanan Regency, 75% of respondents stated that the work process that housewives complain about the most when their husband is not at home is the process of transporting 12 kg LPG, so they need to get priority to find a solution immediately.

The musculoskeletal complaints felt in the process of transporting 12 kg LPG contents were on the back, waist, both knees, and calves. Complaints that arise in the process of transporting 12 kg LPG are caused, among other things, because transporting 12 kg LPG is carried out in a work position that is not physiological or with a forced labor attitude, this can result in increased musculoskeletal complaints. Working with a posture that is not physiological will cause many complaints, especially fatigue and musculoskeletal complaints, and will ultimately reduce work productivity [6]–[8].

In overcoming this problem, it is necessary to change the work position and use manual tools such as a 12 kg LPG transporter, in the hope of alleviating the musculoskeletal complaints of housewives.

The objectives to be achieved in this research are to (a) identify the complaints experienced by

housewives in the process of transporting 12 kg LPG, and (b) how to deal with complaints experienced by housewives in the process of transporting 12kg LPG.

The benefits to be achieved in this research are as follows (a) provide information regarding problems in the process of transporting 12 kg LPG, (c) provide information on actions that need to be taken to overcome problems in the process of transporting 12 kg LPG, (c) for scientific treasures, the results of this study are expected to inspire for other researchers to conduct more comprehensive studies.

2. METHODS

2.1 Description of conveyance

This conveyance is used to transport 12 kg LPG contents. In the process of transporting LPG, there are two ways as follows: (1) the manual (human) method without the help of conveyance, (2) the manual (human) method with the help of the conveyance. Of these two ways in the analysis of musculoskeletal complaints.

2.2 Research Design

The method in this research is experimental. The experimental method is to experiment directly on the object, where the researcher wants to know the causal effect between the independent and dependent variables. So the experimental method is a quantitative research method used to determine the effect of the independent variable (treatment) on the dependent variable (outcome) under controlled conditions [9]. The experimental method applied in this study is a treatment-by-subject design which was developed in the form of a two-period cross-over design. A cross-design between periods required washing out, to eliminate the effect of the first treatment on the next treatment [2]. The research design is shown in Figure 1.

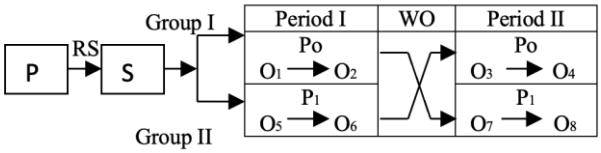

Figure. 1 Two Period Cross Over Design

Description:
P : Population
S : Sample
RS : Random Sampling
Po : Before using the conveyance
P1 : After using the conveyance
Group I : The group that worked before using the conveyance, continued to work to group II who already used the means of conveyance
Group II : The working group is already using the conveyance, proceed to group I before using the conveyance
O1, O3, O5, O7: Initial data collection before work begins on resting pulse and musculoskeletal complaints
O2, O4, O6, O8 : Final data collection after completion of work on musculoskeletal complaints
Wo : Washing Out to remove the effects of previous work, given 2 hours

2.3 Population and Sample

The population in this study was housewives transporting 12 kg LPG in Pupuan, Tabanan, Bali. The target population was 20 housewives, while the reachable population was 16. The number of samples in this study were 16 housewives, who would look for musculoskeletal complaints before and after using the means of transportation.

2.4 Variable classification

The variables in the study can be divided into three as follows:

1. The independent variable is the use of 12 kg LPG conveyance, before and after using the conveyance.
2. The dependent variable was musculoskeletal complaints in 16 housewives, before and after using the conveyance.
3. Control variables are gender, education level, work experience, health.

2.5 Variable operational definition

The definitions of variables related to this research are as follows:

1. Manual transportation means the work of transporting materials carried out by workers to move materials from an origin location to a destination location [8]. The reason for using manual work with human labor in this material moving activity is because there are several advantages that can be obtained, namely more flexibility, in moving materials in irregular work locations, cheaper, and easy to do for light loads [4].
2. Ergonomics is the science, technology and art to harmonize tools, how work is carried out on human abilities, abilities and limitations so that healthy, safe, comfortable and efficient working conditions and environments are obtained so that the highest productivity is achieved [10].
3. Musculoskeletal complaints are complaints in the parts of the skeletal muscles experienced by subjects both before work and after work that are subjective, musculoskeletal complaints are measured using a Nordic Body Map questionnaire with a Likert scale [9].

2.6 Research procedure

To avoid errors in data collection, the following research procedures were made:

1. Preparation stage

The stages of preparation in carrying out research are as follows:

a. Library studies, books that are appropriate and relevant to the research topic.
b. Determine the place of research.
c. Determine the number of samples of 16 housewives transporting 12 kg LPG
d. Preparing data collectors and tools for research purposes

2.7 Research implementation stage

The stages in the implementation of the research are as follows:

a. Before starting work, each subject was given a Nordic Body Map questionnaire with four Likert scales and the subjects were asked to fill in themselves by marking grass (√), on the items according to the complaints they felt, then the results were collected.
b. After completing the work, each subject was given another Nordic Body Map questionnaire with four Likert scales and the subject was asked to fill it out himself by marking grass (√), on the items according to the complaints they felt, then the results were collected.
c. Record the value of musculoskeletal complaints before work and after work, namely the number of scores of musculoskeletal complaints according to the level of complaints felt by using four Likert scales.
d. The score of musculoskeletal complaints is calculated based on the difference in the score of musculoskeletal complaints after the 12 kg LPG transfer process minus the musculoskeletal complaint score before the 12 kg LPG transfer process.
e. The data obtained is then processed and analyzed with the help of a computer program SPSS (Statistical Package for The Social Science) version 22.0.

3. RESULTS AND DISCUSSION

3.1 Musculoskeletal complaints data

The mean value of musculoskeletal complaints was calculated based on the value of complaints after transporting LPG minus the value of complaints before transporting LPG for each treatment. The analysis of significance in this study was carried out in stages which included analysis of comparability, period effects, residual effects, and treatment effects.

Figure 2. Lift and transport 12 kg LPG without conveyance

Figure 3. Lift and transport 12 kg LPG with conveyance

Comparability analysis

The mean difference between musculoskeletal complaints before transporting LPG between treatments in period I was analyzed by independent t-test. The results of the analysis can be shown in table 1.

Table1. Independent t-test data on musculoskeletal complaints before transporting LPG between treatment period I

Subject Groups	N	Mean Score of Musculoskeletal Complaints	Standard Deviation	Average Difference	t	p
Treatment 1	8	37,27	0,98	-0,075	-0,114	0,911
Treatment 2	8	37,25	1,58			

In table 1, the results of the analysis using the independent t-test obtained that the mean between treatment 1 and treatment 2 in period I was not different ($p>0.05$) with $t = -0.114$ and $p = 0.911$. This situation shows that musculoskeletal complaints carrying LPG groups PO and P1 in the treatment period I can be considered the same.

Analysis of the period effect

The period effect is calculated based on the difference in musculoskeletal complaints in period I PO minus the difference in musculoskeletal complaints in period II for group I compared to the difference in musculoskeletal complaints in period I minus the difference in musculoskeletal complaints in period II for group II. The data from the analysis using the Independent t-test can be seen in Table 2.

Table 2 shows that the results of the analysis using the independent t-test were not different ($p>0.05$) with $t = -0.154$ and $p = 0.880$. This shows that the treatment period does not affect the subject's musculoskeletal complaints in period I and period II.

Table2. Independent t-test of the difference between musculoskeletal complaints between group I and group II

Subject Group	N	Mean Score of Musculoskeletal Complaints	Standard Deviation	Average Difference	t	p
Treatment 1	8	10,46	2,47			
				-0,300	-0,154	0,880
Treatment 2	8	10,16	2,92			

Carry-over effect

Table 2 shows that the results of the analysis using the independent t-test were not different ($p>0.05$) with $t = -0.154$ and $p = 0.880$. This shows that the treatment period does not affect the subject's musculoskeletal complaints in period I and period II.

Table 3. Independent test t-test mean difference in musculoskeletal complaints between group I and group II

Subject Group	N	Mean Score of Musculoskeletal Complaints	Standard Deviation	Average Difference	t	p
Treatment 1	8	9,97	2,08			
				-0,68	-0,592	0,563
Treatment 2	8	10,65	2,45			

Table 3 shows that the results of the analysis using the Independent t-test were not different (p>0.05) with t= -0592 and p = 0.563. This means that there is no effect of the rest of the treatment on the next treatment.

Treatment effect analysis

In this study, the treatment effect was evaluated from the mean difference between musculoskeletal complaints after transporting 12 kg LPG contents minus musculoskeletal complaints before transporting 12 kg LPG at PO, compared to the mean difference between musculoskeletal complaints after transporting 12 kg LPG contents minus musculoskeletal complaints before transporting. LPG content of 12 kg on P1. The results of the analysis of significance with the t-pair test can be seen in Table 4.

Table 4. T-pair test of different mean musculoskeletal complaints before and after transporting 12 kg LPG.

Subject Group	N	Mean Score of Musculoskeletal Complaints	Standard Deviation	Average Difference	t	p
Treatment PO	16	80,09	1,74			
				-10,08	-15,428	0,000
Treatment P1	16	70,01	1,99			

Table 4 shows that with t-pair analysis the results are different (p>0.05) with t = -15.428 and p = 0.000. This shows that there is a difference between PO and P1. Therefore, it can be stated that the use of a 12 kg LPG conveyance can reduce musculoskeletal complaints in housewives.

A comparison of musculoskeletal complaints after and before transporting 12 kg LPG contents between PO and P1 can be seen in Table 5.

Table 5 Data analysis of mean musculoskeletal complaints between Group I and Group II

		Period I				Period II			
		PO				P1			
		Pre	Post	Average Difference	SD	Pre	Post	Average Difference	DS
Mean musculoskeletal complaints group I	8	37,3	80,2	42,9	1,,8	37,2	70,3	33,1	2,6
		Period I				Period II			
		P1				PO			
		Pre	Post	Average Difference	SD	Pre	Post	Average Difference	SD
Mean Musculoskeletal Complaints Group II	8	37,2	69,7	32,5	1,7	36,9	80,0	43,1	3,2

Table 5 shows that musculoskeletal complaints before transporting 12 kg LPG, PO in group I, and PO in group II between period I and period II can be considered the same, after treatment there is a difference between PO and P1. Therefore, it can be stated that the use of a 12 kg LPG conveyance can reduce musculoskeletal complaints in housewives, for more details it can be shown in Figure 4.

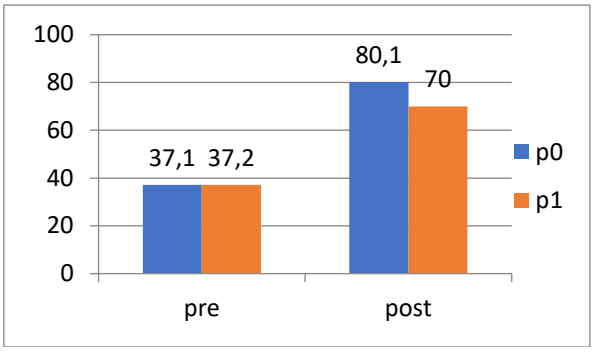

Figure 4. Musculoskeletal complaints before (P0) and after treatment (P1)

The subjects in this study were housewives, the average age of the subjects was 57 years. According to Manuaba [10], a person's physical capacity is directly related to age and reaches its peak at the age of 25 years. The effect of the physiological ability of muscles is in the age range of 20 to 30 years, over the age of 30 years the physiological ability of muscles decreases [2], [11].

The results of the analysis after using the 12 kg LPG conveyance showed a difference ($p>0.05$) and a decrease in musculoskeletal complaints from the average score of 80.1 to 70, or a decrease of 12.6%. In line with what was stated by Lilik [12], Santosa [13], and Yusuf [14], they stated that the practice position of standing and bending is the wrong position in working especially when using equipment will cause musculoskeletal disorders. Musculoskeletal complaints experienced by housewives are on the back, waist, both knees, and calves. Musculoskeletal disorders experienced by housewives are caused by the accumulation of lactic acid which ultimately causes fatigue or pain in musculoskeletal [15], [16].

4. CONCLUSION

Based on the results of the analysis and discussion, it can be concluded that the use of a 12 kg LPG conveyance can reduce musculoskeletal complaints from an average of 80.1 to 70 or a decrease of 12.6%. At the age of over 30 years to transport and lift heavy loads are advised to be careful, you should use a conveyance or material handling to avoid the occurrence of disturbances in the skeletal muscles.

5. ACKNOWLEDGEMENT

We would like to thank the head of the Bali State Polytechnic research center and our fellow Bali State Polytechnic lecturers who have helped a lot in completing this research until it was published in this journal.

6. REFERENCES

[1] J. Dul and B. Weerdmeester, *Ergonomics For Beginners A Quick Reference Guide, Second Edition*, 3rd ed. London: Taylor & Francis, 2008.
[2] K. H. E. Kroemer and E. Grandjean, *Fitting The Task To The Human, Fifth Edition A Textbook Of Occupational Ergonomics*. London: CRC Press, 2009.
[3] A. A. N. B. Mulawarman, I. K. G. J. Suarbawa, and M. Yusuf, "Slice Tool Model Design Dynamo Drive Tempeh to Increase Work Productivity of Tempeh Chip Craperers," *Am. J. Appl. Sci. Res.*, vol. 8, no. 4, pp. 88–92, 2022.
[4] I. G. Santosa and M. Yusuf, "The Application of a Dryer Solar Energy Hybrid to Decrease Workload and Increase Dodol Production in Bali," *Int. Res. J. Eng. IT Sci. Res.*, vol. 3, no. 6, Nov. 2017.
[5] B. Gajšek, A. Draghici, M. E. Boatca, A. Gaureanu, and D. Robescu, "Linking the Use of Ergonomics Methods to Workplace Social Sustainability: The Ovako Working Posture Assessment System and Rapid Entire Body Assessment Method," *Sustain.*, vol. 14, no. 7, 2022.
[6] M. Yusuf, "Design of Jewel Stone Sharpener to Increase Jewel Worker Work Productivity in Bali," in *International Conference on Engineering, Technology, and Industrial Application (ICETIA)*, 2014, pp. 353–357.
[7] W. Poochada, S. Chaiklieng, and S. Andajani, "Musculoskeletal Disorders among Agricultural Workers of Various Cultivation Activities in Upper Northeastern Thailand," *Safety*, vol. 8, no. 3, 2022.
[8] A. Manuaba, "Accelerating OHS-Ergonomics Program By Integrating 'Built-In" Within The Industry's Economic Development Scheme Is A Must-With Special Attention To Small And Medium Enterprises (SMEs)," in *Proceedings the 21st Annual Conference of The Asia Pasific Occupational Safety & Health*

Organization, 2005.
[9] E. A. Gehan and N. A. Lemak, *Statistics in Medical Research, Developments in Clinical Trials*. New York, USA: Springer US, 2012.
[10] A. Manuaba, "Total Approach is a Must for Small and Medium Enterprises to Attain Sustainable Working Conditions and Environment, with Special Reference to Bali, Indonesia," 2006.
[11] R. S. Bridger, *Introduction to Ergonomics, 3rd Edition*. London: Taylor & Francis, 2008.
[12] L. Sudiajeng, T. Tarwaka, K. Sutapa, M. Sudana, and M. Yusuf, "Ergonomic tetrapod reduces the MSDs risk and productivity of steel-bar assembly for reinforcement concrete beams," *Int. Res. J. Eng. IT Sci. Res.*, vol. 9, no. 1, pp. 1–13, Dec. 2022.
[13] I. G. Santosa, M. Yusuf, I. N. Gunung, and I. K. Rimpung, "Application of Forging Hammer to Increases Productivity of Balinesse Blacksmith BT - Proceedings of the International Conference on Innovation in Science and Technology (ICIST 2020)," in *Proceedings of the International Conference on Innovation in Science and Technology (ICIST 2020)*, 2021, pp. 195–199.
[14] M. Yusuf, M. Santiana, and W. D. Lokantara, "Improvement of work posture to decrease musculoskeletal disorder and increase work productivity jewelry worker in bali," in *Proceeding International Joint Conferenceon Science and Technology (IJCST) 2017*, 2017, pp. 242–247.
[15] S. Racinais *et al.*, "Consensus recommendations on training and competing in the heat," *Br. J. Sports Med.*, vol. 49, no. 18, pp. 1164 LP – 1173, Sep. 2015.
[16] M. Helander, *A Guide to Human Factors and Ergonomics*, vol. 51, no. 6. 2006.

LOGIC
Journal of Engineering Design and Technology
Vol. 23 No.3 November 2023 ; p. 219 - 224

p-ISSN : 1412-114X
e-ISSN : 2580-5649
http://ojs2.pnb.ac.id/index.php/LOGIC

EFFECT OF AC COMPRESSOR MODIFICATION ON FUEL CONSUMPTION IN CAR

Mokh Hairul Bahri [1)], Dudi Irawan [2)], Adi Pratama Putra [3)]

1) Mechanical Engineering Department, Universitas Muhammadiyah Jember, Karimata Street Number 49, Jember, East Java, Indonesia
2) Electrical Engineering Department, Universitas Muhammadiyah Jember, Jl. Karimata 49, Jember, Indonesia
3) Mechanical Engineering Department, Universitas PGRI Banyuwangi, Ikan Tongkol Street Number 22 Kertosari, Banyuwangi, East Java, Indonesia

Correponding email [1)] : mhairulbahri@unmuhjember.ac.id

Abstract. The cooling system is a refrigeration technology that is growing, especially regarding the cooling medium (refrigerant), new vehicles nowadays mostly use air conditioning to condition the air in the vehicle's cabin, but for now, there are still many aspects that have not been given much attention, especially the compressor. Compressor systems in vehicles still rely on the engine as a direct drive resulting in increasingly wasteful fuel consumption and reducing the performance of the vehicle. This study analyzes the results of modifying a conventional compressor into an electric compressor by utilizing a split AC compressor whose supply voltage is obtained from a DC to AC inverter on vehicle fuel consumption and the required electrical energy. Inverter modification is highly recommended in the application of car air conditioners, split AC compressors, and others. The results of this research show that AC compressors using split compressors affect fuel consumption.

Keywords: air conditioning, split ac, refrigeration, compressor,

1. INTRODUCTION

Comfort while driving, especially in a car is very necessary, so various ways are done to ensure a comfortable driving experience. An effective way at this time is to condition the air by installing an air conditioner [1]. An Air Conditioner (AC) is a tool used to regulate or condition air quality which includes air circulation, humidity adjustment, cleanliness regulation, and air purification. Air Conditioner has become a relatively important requirement for vehicle users, both for drivers of public transport cars and private cars [2]. The compressor which is the main component has an important role in circulating and compressing the refrigerant flow in the air conditioning system. Changes in engine speed will affect the work of the compressor, which affects the performance of the air conditioning system in vehicles [3]. Air conditioning in the room helps regulate air cooling in the room, this conditioning aims to provide comfort, to reduce fatigue [4]. The higher the temperature from outside and from the room, the higher the cooling capacity of the inverter AC and will cause the compressor motor rotation to change [5]. Refrigerants containing CFCs (Chloro Fluoro Carbon) and HCFCs (Hydro Chloro Fluoro Carbon) harm the environment which can reduce the ozone layer which can cause global warming. Based on the reason above, a regulation was made that prohibited the use of a compound containing CFCs and HCFCs. As an alternative, environmentally friendly refrigerant R-134a (without CFCs) is used [6]. Refrigerant coming out of the compressor will be in the form of high-pressure gas and high temperature. Refrigerant from the compressor will be pumped into the condenser

[7]. The condenser in the AC cooling system is cooled by an extra fan or additional fan so that the refrigerant that passes through the condenser changes from gas to liquid [8]. The refrigerant that passes through the expansion valve hole experiences a decrease in temperature and pressure. After the refrigerant passes through the expansion valve, it will enter the evaporator [9]. Air conditioning machine commonly called Air Conditioning (AC) Split is one of the air conditioning machines that work with a vapor compression cycle. The vapor compression cycle is one of the cycles used for mechanical refrigeration systems, where the refrigerant vapor will be compressed by the compressor as the main component in addition to other components such as the condenser, expansion valve, and evaporator [10]. Poor system performance can be caused by compressor performance that is not optimal, as one of the main components of the cooling system. As a result, the amount of refrigerant flowing through the system and through the evaporator and condenser also decreases [11].

From the description above, it can be seen that the use of an air conditioner is very necessary for thermal comfort in a vehicle environment. Since the fuel consumption coefficient is very influential on the vehicle, the addition of a load such as an air conditioner will burden the engine which will make fuel consumption even more wasteful. The efficiency of fuel consumption can be described by the specific fuel, which is a characteristic of fuel consumption in grams per power unit per hour of the engine [12]. Fuel consumption (mf) is directly proportional to engine speed (rpm) and Specific fuel consumption (Sfc) is inversely proportional to engine speed, meaning that fuel consumption is more efficient when the engine speed is higher, especially at low and medium rpm [13]. This research uses a split compressor which is rarely used in cars. Optimal fuel efficiency to maintain high-efficiency levels and low levels, is an important goal for power in the engine and fuel efficiency depending on the characteristics of the vehicle [14],[15]. Therefore, it is necessary to test and analyze the car AC compressor to the split AC compressor for fuel consumption.

2. METHODS

The method applied in this study uses experiments that aim to analyze the modification of a car AC compressor to a split AC compressor on fuel consumption. The framework of thought can be seen in the following figure:

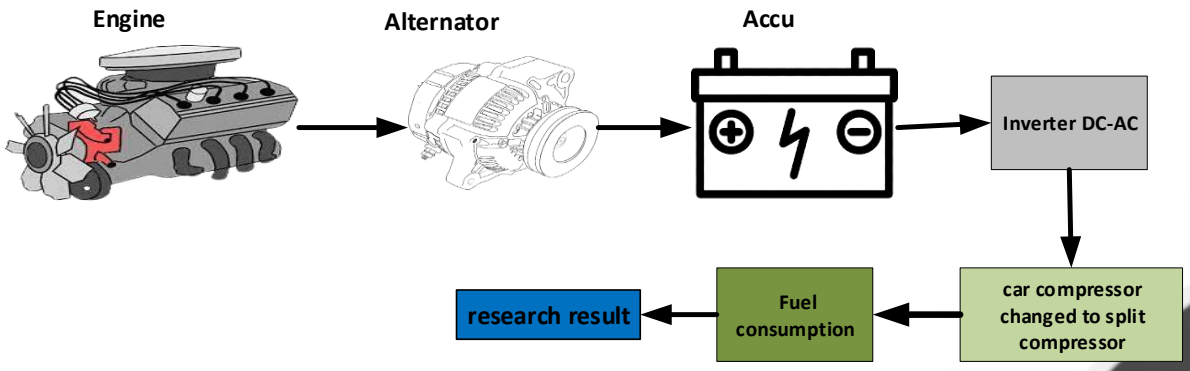

Figure 1. Research framework

The compressor is the main cooling system for cars that utilizes the drive on the engine. In this study, the compressor that should be driven by the engine will be driven by an electric compressor on the split. The difference between a car compressor and a split AC compressor is in the piston player inside to compress the freon, namely the engine is rotated on the car compressor, and the electric motor is driven on the split AC compressor. By changing the compressor which should be driven by the engine to be driven by an electric compressor on the split, it is expected that fuel consumption will be more efficient.

3. RESULTS AND DISCUSSION

The cooling system in this study has been modified by using a split compressor for fuel efficiency in vehicles. The refrigerant used for this study was R134a in 1 can of 390 grams. This test was carried out for 2 tests with different RPM variations. From these RPM variations, data will be generated regarding the effect of using a split AC compressor on fuel efficiency. Figures and tables can be seen as follows:

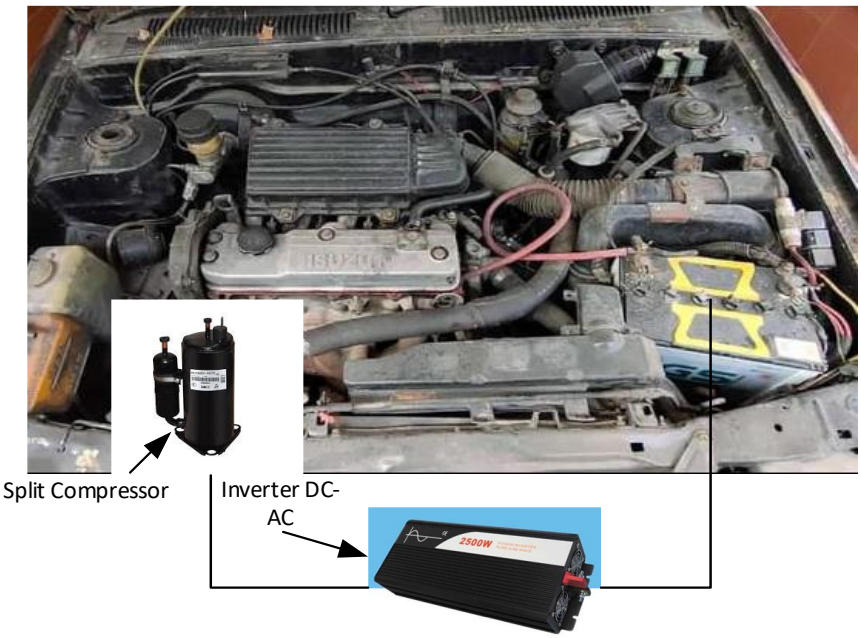

Figure 2. Modified split AC compressor

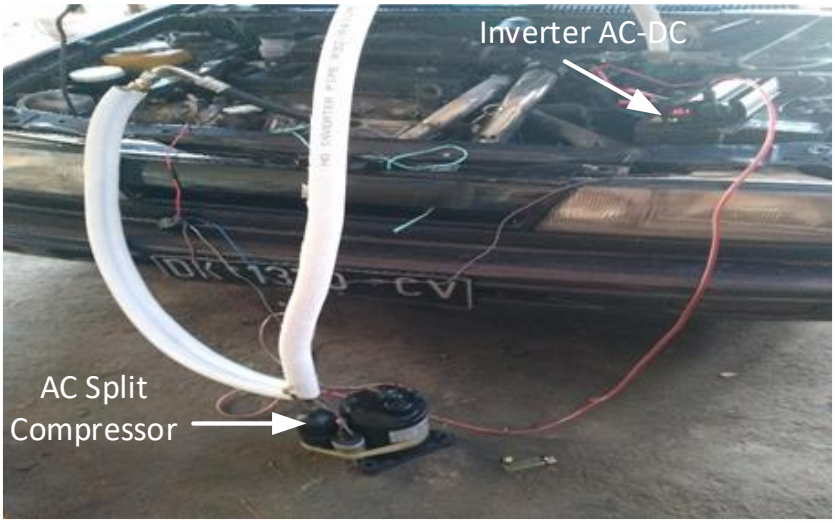

Figure 3. Split AC Testing in Vehicles

Figures 2 and 3 show the process of testing compressor modifications to car compressors and electric motors driven to split AC compressors. In the tests carried out, a table will be shown showing the fuel coefficient in the car by modifying the compressor using electricity on the split.

Table 1. Fuel Consumption (830 RPM)

Fuel Consumption (830 RPM)		
Minutes	Standard Compressor CC/Minutes	Split Compressor CC/Minutes
1	2,19	1,59
2	2,27	1,92
3	2,38	2,11
4	2,43	2,21
5	2,48	2,34
6	2,78	2,41
7	2,82	2,48
8	2,91	2,67
9	3,05	2,87
10	3,02	2,91
11	3,39	3,23
Average	2,70	2,43

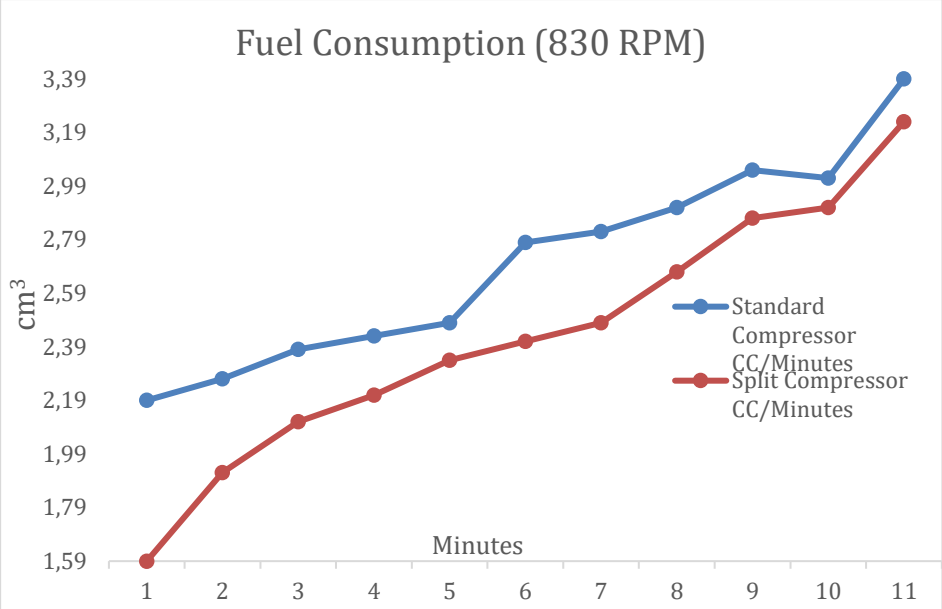

Figure 3. Fuel Consumption graph (830 RPM)

Table 2. Fuel Consumption (871 RPM)

Fuel Consumption (871 RPM)		
Minutes	Standard Compressor CC/Minutes	Split Compressor CC/Minutes
1	2,41	2,11
2	2,89	2,21
3	2,97	2,26
4	3,19	2,34
5	3,48	2,52
6	3,52	2,63
7	3,71	2,71

8	3,81	2,89
9	3,92	2,91
10	4,02	3,21
11	4,11	3,31
Average	3,46	2,65

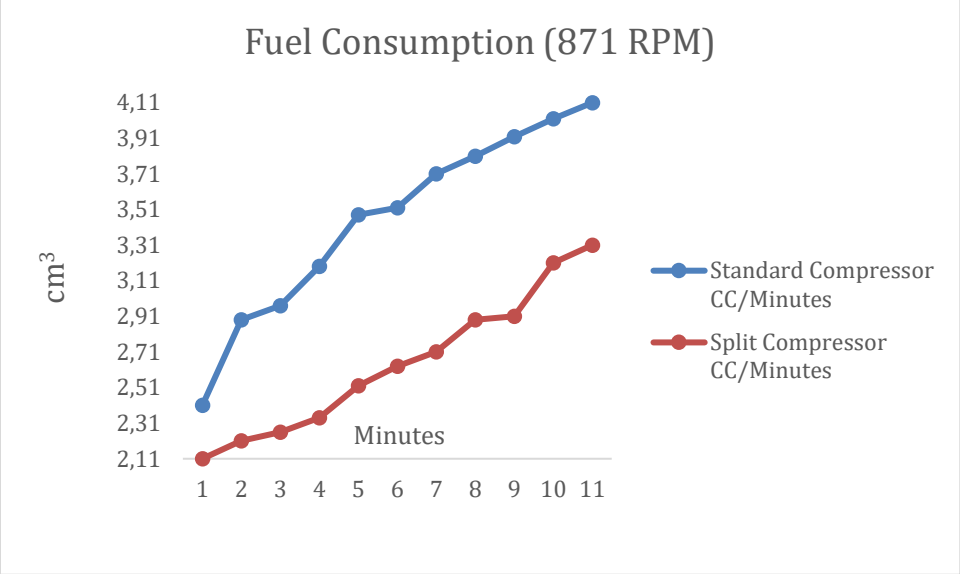

Figure 4. Fuel consumption graph (871 RPM)

Figures 3 and 4 show graphs of fuel consumption using a speed of 830 RPM, the results obtained using a split compressor fuel consumption is more efficient with an average value of 2.43 cc/minute while the average value using a standard compressor is 2.70 cc/minutes. The graph of fuel consumption in Figure 4 uses a speed of 871 RPM, the results obtained using an average split are 2.65 while with a standard compressor, the value obtains an average value of 3.46. The difference between these two data is that the standard AC compressor uses a larger rotation from the vehicle engine than the split-type compressor, the use of rotation on the standard vehicle compressor results in greater fuel consumption so the use of split AC in the vehicle is more efficient.

4. CONCLUSION

The results obtained from this study show that the AC compressor using a split compressor affects fuel consumption. This is attributed to the fact that the split AC compressor does not require engine power to move it. Based on the data obtained, the split compressor demonstrates an average fuel consumption that is lower than the AC compressor.

5. ACKNOWLEDGEMENT

We would like to say thank you very much to:
1. Rector Of Universitas Muhammadiyah Jember and all his staff.
2. Dean of Technical Faculty of Universitas Muhammadiyah Jember.
3. Head of LPPM Universitas Muhammadiyah Jember for financial support in research budget year of 2023.

6. REFERENCES

[1] Hairul. *et al.*, “Analysis of Modification of Car AC Compressor To Split Ac Compressor On,” vol. 22, no. 3, pp. 283–288, 2022.
[2] S. Hermawan and R. Novianto, “Trouble Shooting Sistem Air Conditioner (AC) Pada Trainer AC

Mobil," *Surya Tek.*, vol. 1, no. 1, pp. 26–33, 2017.
[3] S. Malo and R. Griñó, "Adaptive Feed-Forward Cancellation Control of a Full-Bridge DC-AC Voltage Inverter," *IFAC Proc. Vol.*, vol. 41, no. 2, pp. 4571–4576, 2008, doi: 10.3182/20080706-5-kr-1001.00769.
[4] R. Joto, "Studi Perbandingan Pemakaian Energi Air Conditioner Inverter Dengan Air Conditioner Konvensional," vol. 11, no. 01, pp. 111–121, 2013.
[5] A. Jaya Saputra, Atmam, and Zulfahri, "Studi Kecepatan Putaran Motor Compressor Air Conditioner Inverter Terhadap Perubahaan Suhu Ruangan," *SainETIn*, vol. 3, no. 1, pp. 17–24, 2018, doi: 10.31849/sainetin.v3i1.3027.
[6] M. P. Dr. Rosalina Kumalawati, M.Si. Dr. Ellyn Normelani, M.S. Dr. Norma Yuni Kartika, M.Sc. Dr. Isnasyauqiah, MT. Selamat Riadi, M.Pd. Desi Nurandini, M.Eng. Muhammad Efendi, *INVENTARISASI PERLINDUNGAN LAPISAN OZON (Studi di Kota Banjarmasin)*. 2020.
[7] S. Senoadi, A. A. Aliandi, and R. Permatasari, "Pengaruh Perbedaan Tegangan Pemanas terhadap Performa Refrigeran R12, R134a dan MC134 pada Refrigeration Laboratory Unit," *Mesin*, vol. 10, no. 1, pp. 8–13, 2019, doi: 10.25105/ms.v10i1.4128.
[8] R. S. Subagyo, F. Oktapiyanor, Fadliyanur, Muchsin, and H. Y. Nanlohy, "Analisis Kinerja Ac Mobil Dengan Variasi Freon R-134a, Hfc-134 Dan Mc-134," *Sci. J. Mech. Eng. Kinemat.*, vol. 6, no. 2, pp. 119–128, 2021, doi: 10.20527/sjmekinematika.v6i2.193.
[9] A. Tito Muliawan. dkk, "Analisis Performansi AC Split dengan Perbandingan Refrigerant R410a Dan R32 Berdasarkan Variasi Putaran Fan Evaporator," *J. Jur. Tek. Pendingin dan Tata Udar. Politek. Negeri Indramayu*, vol. 29, pp. 647–655, 2019.
[10]F. Konrad, S. Pradana, and S. P. Sari, "Pemanfaatan Energi Panas pada Mesin Pengkondisian Udara 2 PK Sebagai Media Pemanas Air Mandi," *Mechanical*, vol. 6, pp. 15–27, 2015, doi: 10.23960/mech.v6.i1.201503.
[11]A. F. Fauzan, "Studi Eksperimen Pengaruh Penambahan Nanofluids pada Pelumas Kompresor Terhadap Peningkatan Performa Mesin Pengkondisian Udara," 2018.
[12]J. D. Osorio and A. Rivera-Alvarez, "Efficiency enhancement of spark-ignition engines using a Continuous Variable Valve Timing system for load control," *Energy*, vol. 161, pp. 649–662, 2018, doi: 10.1016/j.energy.2018.07.009.
[13]E. Julianto and S. Sunaryo, "Analisis Pengaruh Putaran Mesin Pada Efisiensi Bahan Bakar Mesin Diesel 2Dg-Ftv," *J. Penelit. dan Pengabdi. Kpd. Masy. UNSIQ*, vol. 7, no. 3, pp. 225–231, 2020, doi: 10.32699/ppkm.v7i3.1282.
[14]M. Bidarvatan, M. Shahbakhti, S. A. Jazayeri, and C. R. Koch, "Cycle-to-cycle modeling and sliding mode control of blended-fuel HCCI engine," *Control Eng. Pract.*, vol. 24, no. 1, pp. 79–91, 2014, doi: 10.1016/j.conengprac.2013.11.008.
[15]K. Tampubolon and F. R. Koto, "Analisis Perbandingan Efisiensi Kerja Mesin Bensin Pada Mobil Tahun 2000 Sampai Tahun 2005 Dan Mobil Tahun 2018 Serta Pengaruh Terhadap Konsumsi Bahan Bakar Dan Cara Perawatannya Sebagai Rekomendasi Bagi Konsumen," *J. Mech. Eng. Manuf. Mater. Energy*, vol. 3, no. 2, p. 76, 2019, doi: 10.31289/jmemme.v3i2.2773.

LOGIC
Jurnal Rancang Bangun dan Teknologi
(Journal of Engineering Design and Technology)
Address : Gedung P3M, It.1 Politeknik Negeri Bali, Bukit Jimbaran
PO BOX 1064 Kuta Selatan, Badung, Bali - Indonesia
Telp. (+62)361 701981 Fax. (+62)361 701128
Email: logic@pnb.ac.id

1412-114X